UNIVERSITY OF Southampton

Centre for Biological Sciences

Hapten-mediated contact allergy: a proteomic and immunological approach

By

Pete Boyd BSc. (hons)

Thesis for the degree of Doctor of Philosophy

January 2014

Supervisors – Dr Neil Smyth, Dr Paul Skipp & Prof. Eugene Healy

UNIVERSITY OF SOUTHAMPTON

ABSTRACT

FACULTY OF NATURAL AND ENVIRONMENTAL SCIENCES

Biological science

Doctor of Philosophy

HAPTEN-MEDIATED CONTACT ALLERGY: A PROTEOMIC AND IMMUNOLOGICAL APPROACH

By Peter Stewart Boyd

Allergic contact dermatitis (ACD) is a prevalent skin condition caused by chemical haptens, which enter the epidermis, and by modifying self-proteins, render them immunogenic via the activation of hapten-specific T-cells. It is currently not known which specific protein modifications are responsible for sensitization.

This work investigates the extreme sensitizer DNCB, which confers a dinitrophenyl (DNP) protein modification. Immortalised keratinocytes (HaCaT), incubated with DNCB were compared to *ex vivo* human skin using immunofluorescence and western blot detection of DNP-proteins, showing widespread protein modification and similarities between tissue and cells when using a clinical dose. Proliferation assays using lymphocytes from DNCB-sensitive donors showed responses to DNP proteins isolated from DNCB-treated HaCaT cells and primary keratinocytes. While western blot analysis of pH gradient separated fractions identified a number of DNP-proteins in the DNP-HaCaT cell lysates, these were not immunogenic in lymphocyte assays. The model protein human serum albumin (HSA) was used to investigate the modification kinetics of DNCB by identifying which amino acid residues were changed more readily using a range of DNCB concentrations and incubation times. Cysteine residues, including those in disulphide bonds and particularly cysteine 34 are more readily modified than lysine in HSA, suggesting that DNCB is able to alter the structure of proteins. A novel process of hapten-reversal by a process termed 'thiolysis' was found to remove DNP groups from the cysteine residues of synthetic peptides derived from the sequence of HSA containing cysteine 34 using the reducing agent dithiothreitol. Identical peptides with C34→K34 showed no such hapten-reversal. This corresponds to the unexpected immunogenicity of the cysteinyl peptide and also the DNP modified tripeptide glutathione. Anti-DNP western blots show that the DNP group is transferred to other proteins during incubation with human monocytes in culture. This suggests a cellular process of removing DNP groups and GILT, a thiol reductase present in the endosomes is presented as a candidate for this process. This work demonstrates that DNCB can generate a wide variety of DNP protein adducts and that cysteinyl moieties are able to stimulate lymphocyte proliferation by way of hapten transfer. This highlights a potentially novel process involved in the mechanism of contact allergy.

Contents

Table of figures 11

Acknowledgements 15

Publications 17

Abbreviations 19

1. GENERAL INTRODUCTION 21

1.1 The public health and economic impact of ACD 21

1.2 Skin biology 22

1.2.1 Anatomy 22

1.2.2 Barrier function and basic skin immunology 24

1.3 Pathologies of the skin 27

1.3.1 Innate responses to chemicals and pathogens 27

1.3.2 Allergic contact dermatitis 28

1.4 The mechanisms of ACD 29

1.4.1 Penetration of a xenobiotic into the epidermis 29

1.4.2 Haptenation of proteins 29

1.4.3 Bioactivation: pro and pre-haptens 31

1.4.4 Antigen processing and MHC loading 32

1.4.5 Irritancy, innate immunity and DC migration 32

1.4.6 Antigen presentation and T-cell activation 33

1.4.7 The elicitation of ACD 35

1.5 2,4-dinitro-1-chlorobenzene (DNCB) as a model sensitizer 37

1.6 The proteomics approach 40

1.6.1 Sample fractionation 42

1.6.2 Mass spectrometry ion sources 46

1.6.3 Quadrupoles 48

1.6.4 Mass analysers 49
1.6.5 Tandem mass spectrometry 52
1.6.6 Analysis of MS data 54
1.7 Aims and objectives 57
2 MATERIALS AND METHODS 59
2.1 Cell culture 59
2.2 Treatment of HaCaT and primary keratinocyte cells with DNCB & [^{14}C]-DNCB 59
2.3 Culture of primary keratinocytes 59
2.4 Preparation and treatment of human skin 60
2.5 Sectioning and fixation of *ex vivo* human skin 60
2.6 Separation of epidermis from *ex vivo* human skin and lysis of epidermal cells 60
2.7 Culture of HaCaTs on microscope slides and fixation of adherent cells 61
2.8 Immunofluorescence detection of dinitrophenyl epitopes, dendritic cells and nuclei in sections of human skin and HaCaT cells 61
2.9 Fluorescent and laser confocal microscope analysis of immune-stained human skin and HaCaT cells 62
2.10 Cell lysis and protein extraction for SDS-PAGE 62
2.11 Determination of protein concentration by bicinchoninic acid (BCA) assay 63
2.12 SDS-PAGE separation of proteins from lysates of cell lines and epidermis from *ex vivo* skin 63
2.13 Detection of dinitrophenyl adducts using western blot 63
2.14 Densitometry analysis of anti-dinitrophenyl western blots: qualitative comparison of human skin with HaCaTs 64
2.15 Detection of dinitrophenyl adducts using autoradiography 64
2.16 Preparation of cell lysates for addition to lymphocyte assays 65
2.17 Isoelectric focussing fractionation of HaCaT proteins 65

2.18 Isolation of PBMCs from human blood 66
2.19 Lymphocyte proliferation assays (LPA) 66
2.20 Precipitation, non-reducing enzymatic digestion and peptide de-salting of protein lysates and fractions 67
2.21 De-salting of peptides 67
2.22 MS^E analysis of peptides from HaCaT lysates and fractions 68
2.23 Incubation of human serum albumin with DNCB 68
2.24 In-gel protein digestion 68
2.25 Nano-LC-MS^E data analysis of DNP-HSA 69
2.26 Isolation and culture of human monocytes from peripheral blood mononuclear cells 70
2.27 Incubation of human monocytes with DNP-modified synthetic peptides in culture 70
2.28 Thiolysis of DNP groups from synthetic peptides using dithiothreitol 70
2.29 Mass spectrometric analysis of synthetic peptides 71
3 DETECTION OF COVALENT PROTEIN MODIFICATION IN HUMAN SKIN AND HACAT CELLS USING IMMUNOFLUORESCENCE AND IMMUNOBLOTTING 73
3.1 Introduction 73
3.2 Experimental design 75
3.3 Results 77
3.3.1 High dose DNCB effects in *ex vivo* skin 77
3.3.2 Penetration of DNCB into *ex vivo* skin during a 16 hour incubation 78
3.3.3 Clinical dose analysis of dinitrophenyl proteins in skin 79
3.3.4 Immunofluorescence of dinitrophenylated proteins in HaCaT cells 82
3.3.5 Comparison of modification dose-response in HaCaT cells using western blot 84
3.3.6 Validation of western blots using [^{14}C]-DNCB radiolabelling 87

3.4 Discussion 89
3.4.1 Summary 92
4 ASSAYING THE IMMUNOGENICITY OF DNCB MODIFIED PROTEINS EXTRACTED FROM HACAT CELLS 95
4.1 Introduction 95
4.2 Experimental design 97
4.3 Results 99
4.3.1 Lymphocyte proliferation in response to DNCB 99
4.3.2 Lymphocyte proliferation in response to DNCB modified cell proteins 101
4.3.3 Lymphocyte proliferation responses to primary keratinocytes 106
4.4 Discussion 108
4.5 Summary 110
5 THE EFFECTS OF DNCB CONCENTRATION AND INCUBATION TIME ON THE MODIFICATION OF HUMAN SERUM ALBUMIN 113
5.1 Introduction 113
5.2 Experimental design 117
5.3 Results 119
5.4 Discussion 133
5.4.1 Summary 138
6 A NOVEL PROCESS OF HAPTEN TRANSFER IN MEDIATING IMMUNOGECITY TO DNCB 141
6.1 Introduction 141
6.2 Experimental design 147
6.3 Results 151
6.3.1 Differences in immunogenicity and antigen processing between DNP-Cys and DNP-Lys 151
6.3.2 The buffer pH has a pronounced effect on the reduction properties of dithiothreitol (DTT) 154

6.3.3 Exploring the removal of DNP groups from DNP-Cys using DTT and GILT 154

6.4 Discussion 162

6.4.1 Summary 168

7 GENERAL DISCUSSION AND FUTURE WORK 171

7.1 Summary of experimental work and results 171

7.2 Can models be used to determine sensitizers? 173

7.3 Is DNCB immunogenicity driven by specific or generic protein modifications? 174

7.4 Summary 177

7.5 Further work 178

8 Appendix 181

9 REFERENCES 183

Table of figures

Figure 1.1. Cross section of human skin 23

Figure 1.2. Cross section of human skin showing Langerhans cells 26

Figure 1.3. Cross section of human skin showing dermal dendritic cells 27

Figure 1.4. An example of how allergic contact dermatitis presents on skin. 28

Figure 1.6. Nucleophilic aromatic substitution 30

Figure 1.7. Michael addition reaction 31

Figure 1.8. Overview of the mechanism of sensitization. 36

Figure 1.9. Dinitrphenylation of amino acid side chains 37

Figure 1.10. DNCB dose response 38

Table 1.1. The effect of dose area on sensitization 39

Figure 1.11. Mass spectrometry based proteomics 41

Figure 1.12. 2-Dimensional gel electrophoresis 43

Figure 1.13. Liquid chromatography chromatogram 45

Figure 1.14. Matrix-assisted laser desorption ionisation 46

Figure 1.15. Electrospray ionisation 47

Figure 1.16. Quadrupoles 48

Figure 1.17. Mass spectra 49

Figure 1.18. Fourier transform ion cyclotron resonance 50

Figure 1.19. Orbitrap mass spectromter 51

Figure 1.20. Time of flight mass spectrometry 52

Figure 1.21. Tandem mass spectrometry fragment ions 53

Figure 3.1. High dose DNCB may rupture the basement membrane 77

Figure 3.2. DNCB penetration into human epidermis over time 78

Figure 3.3. Variable penetration of DNCB into epidermis between donors 80

Figure 3.8. Western blot comparison of the distribution of DNP-proteins in HaCaT cell lysate treated with different DNCB doses 85

Figure 3.9. Western blot comparison of DNP-proteins in different skin donors 86

Figure 3.11. Autoradiographic detection of DNP-proteins in HaCaT cells and skin 88

Figure 4.1. T-cell proliferation responses to positive control and DNCB 99

Figure 4.2. T-cell responses to direct treatment with DNCB..... 100

Figure 4.3. Dinitrophenylated proteins in whole cell lysates and lysate fractions from DNCB-treated HaCaTs 101

Figure 4.4. T-cell responses to dinitrophenyl HaCaT proteins 102

Figure 4.5. No lymphocyte proliferation responses to DNP-labelled HaCaT proteins with a repeat experiment 103

Figure 4.6. No proliferation in response to 12 DNP-HaCaT protein fractions 104

Figure 4.7. Lymphocyte responses to DNP-HSA 105

Figure 4.8. T-cell responses to dinitrophenyl primary keratinocyte proteins 106

Table 4.1. Low T-cell proliferation responses 107

Figure 5.1. An annotated structure of HSA 114

Figure 5.2. Mass spectrometric method of identifying DNP adducts in human serum using stable isotope labelled DNCB 118

Figure 5.3. Dinitrophenylation of human serum albumin..... 119

Figure 5.4. Mass spectrometric identification of amino acid residues modified by DNCB..... 121

Figure 5.5. An isotope triplet showing 2 DNP modifications..... 123

Figure 5.6. A heat map of DNP modifications to HSA 125

Figure 5.7. Modifications found at time zero are also influenced by incubation time 126

Figure 5.8. The distribution of HSA residues found modified by DNCB 127

Figure 5.9. Cysteines within HSA found to be modified..... 128

Figure 5.10. The total number of residues modified at 5 DNCB concentrations over time..... 129

Figure 5.11. Comparing the modification kinetics of cysteine and lysine..... 131

Figure 5.12. DNCB is not able to reduce disulphide bonds in bodipy-FL-cysteine..... 135

Figure 6.1. The reduction of disulphide bridges in proteins by GILT 143

Figure 6.2. Thiolysis of DNP from synthetic peptides 149

Figure 6.3. DNP-cysteine stimulates T-cell proliferation non-specifically 151

Figure 6.4. The transfer of haptens from DNP-Cys to proteins within monocytes in culture..... 152

Figure 6.5. DTT shows reduced activity at low pH 154

Figure 6.6. DTT removes the DNP group from the cysteinyl peptide..... 155

Figure 6.7. DTT does not affect the DNP group on the lysinyl peptide 156

Table 6.1. Peptide ions denoting the presence or absence of the DNP group..... 157

Figure 6.8. DTT thiolysis of DNP from a DNP-Cys peptide by DTT concentration, pH and incubation period..... 158

Figure 6.9. rM GILT is a powerful reducing agent at pH 4.5 159

Figure 6.10. GILT thiolysis of DNP-C at two time points 160

Figure 6.11. GILT reduction is dependent on DTT activation and is not affected by prior incubation with the DNP-peptides 161

Figure 6.12. A proposed reaction schema for DTT thiolysis of DNP groups from cysteine..... 164

Figure 6.13. Proposed reaction of DNP thiolysis leading to GILT inhibition 165

Figure 6.14. Proposed reaction of GILT thiolysis leading to a mixed disulphide GILT 166

Figure 8.1. Progressive modifications of disulphide bond cysteines within HSA..... 181

Acknowledgements

Firstly, I would like to thank greatly my PhD supervisors Dr Neil Smyth, Dr Paul Skipp and Professor Eugene Healy as well as my industrial supervisors at Unilever Dr Maja Aleksic and Dr Richard Cubberley for their guidance, support, intellectual input and patience. Their supervision has been indispensable in my training to become an independent researcher. I would also like to mention that Paul Skipp encouraged me to undertake the PhD during his supervision of my third year undergraduate project. This was a fantastic opportunity I will always be grateful to have been given.

I wish also to thank Professor David O'Connor and Dr Chris Pickard who were supervisors on the project when I started, but have since left the University of Southampton. David's guidance was critical during my first year and Chris's continual intellectual input during the entire PhD, largely delivered over a pint, has been crucial in shaping the direction of a lot of the work. While not formally my supervisor, Professor Peter Friedmann has lent me his considerable experience in the field of contact allergy and been very supportive of the work.

I would also like to thank all of my colleagues within the School of Medicine Clinical and Experimental Science division at Southampton General Hospital, as well as my colleagues within the Centre for Biological Sciences, for all of their support, guidance and good company throughout my PhD.

I will always be grateful to my family, who have given me comprehensive support since I made the career move to science 8 years ago; and the very many wonderful friends which I am lucky to know both in Southampton and further afield, who have constantly encouraged me during difficult times and been patient with not seeing me often while I've been carrying out this work. Special thanks go to Amy and Stefan who have been the prosthetic family I couldn't do without and Sean Bennett for his unfailing support and encouragement.

Last but not least, I would like to thank my fiancée Dr Christine Ayoub, who has been patient and understanding during the PhD and has kept me grounded, optimistic and happy during the busy times. Thank you all.

This work was funded by a BBSRC CASE studentship BB/G529832/1 with Unilever.

Publications

Boyd P., Pickard C., Parkinson E., Skipp P., Aleksic M., Friedmann P., O'Connor D., Healy E. (2011) Response of T cells from DNCB-sensitised individuals to dinitrophenylated proteins in HaCaT cells. Journal of Investigative Dermatology, 131:S92-S92

Newell L, Polak ME, Perera J, Owen C, Boyd P, Pickard C, Howarth PH, Healy E, Holloway JW, Friedmann PS, Ardern-Jones MR (2013) Sensitization via healthy skin programs Th2 responses in individuals with atopic dermatitis. Journal of Investigative Dermatology, 133(10) :2372-80

Abbreviations

ACD	Allergic contact dermatitis
APC	Antigen presenting cell
BFLC	Bodipy-FL-cysteine
CHS	Contact hyper-sensitivity
dDCs	Dermal dendritic cells
DMSO	Dimethyl sulphoxide
DNCB	2,4-dinitro-1-chlorobenzene
DNP	Dinitrophenyl
DTT	Dithiothreitol
ESI	Electropsray ionisation
GeLC	Gel electrophoresis liquid chromatography
GILT	Gamma interferon-inducible lysosomal thiol reductase
HPC	Hapten-protein complex
HSA	Human serum albumin
IEF	Isoelectric focussing
IFN-γ	Interferon gamma
IPG	Immobilised pH gradient
LC	Liquid chromatography
LCs	Langerhans cells
LLNA	Local lymph node assay
LPA	Lymphocyte proliferation assay
m/z	Mass to charge ratio
MHC	Major histocompatibility complex
MS	Mass spectrometry
MS/MS	Tandem mass spectrometry
PAGE	Polyacrylamide gel electrophoresis
PBMCs	Peripheral blood mononucleocytes
PHA	Phytohaemagglutinin
PLGS	ProteinLynx Global Server
RP	Reverse phase
S-S	Disulphide
SC	Stratum corneum
SDS	Sodium dodecyl sulphate
SNAr	Nucleophilic aromatic substitution
TCR	T-cell receptor
UPLC	Ultra performance liquid chromatography
UV	Ultraviolet

1. GENERAL INTRODUCTION

Allergic contact dermatitis (ACD) is a prevalent skin condition that is caused by chemical agents, known as sensitizers, which covalently modify proteins in the skin by a process called haptenation (Coenraads and Goncalo, 2007; Friedmann, 2006). Subsequent exposure to the sensitizer triggers an allergic response as the modified proteins are treated as foreign by the host immune system. The pathological effects of ACD can be serious with severe itching, inflammation, blisters and open sores. This can cause a major loss in the quality of life in sufferers, particularly if the effects are in visible areas such as the face and hands (Skoet et al., 2003).

1.1 The public health and economic impact of ACD

Skin sensitization is a public health issue (Peiser et al., 2012; Thyssen et al., 2007), as well as impacting industry costs. Allergic contact dermatitis can be caused by a wide variety of substances with varying degrees of potency. Each sensitizer will usually affect a percentage of people to varying degrees of severity and many chemicals potentially carry this risk. Severe ACD is painful, and can leave permanent skin damage and cause distress. Previous studies have estimated that, in the USA alone, the annual costs of ACD are between $200 M and $1000 M (Jacob and Steele, 2006).

ACD is also of importance to industry. Cosmetic and toiletry products are widely used and are in regular and direct contact with skin. It is therefore important to ensure that chemicals likely to cause ACD are not present in these products, or are used well below an established sensitizing threshold in order to reduce risk to the public. Animal testing has been the typical screening method for novel chemicals prior to their use in the manufacture of cosmetic and toiletry products. However, the 7th amendment to the European Union's Cosmetics Directive (76/768/EEC, 2003) outlaws the sale and marketing of cosmetics and toiletries tested on animals in countries within the European Union (EC, 2003). To reduce the risk of legal challenges and loss of sales, the industry must react to this change by developing accurate and reliable non-animal methods of modelling the biochemical mechanism underlying ACD, in order to confidently screen potential sensitizers.

It is therefore of vital importance that any chemicals added to a product that could come into contact with skin are thoroughly screened for their potential to sensitize humans or animals.

1.2 Skin biology

The skin is the largest organ of the human body and carries out a variety of functions including temperature regulation, fluid balance, waste excretion, pH equilibrium, and UV protection. It also serves as a physical barrier to the external environment and acts as a sensory organ (Harding, 2004). As well as the main tissue component, the skin contains hair follicles, sebaceous glands, sensory capsules and, in the case of the glabrous (i.e. devoid of hair follicles) skin of the hands and feet, eccrine glands and raised ridges, which form the "fingerprints".

1.2.1 Anatomy

The skin is generally considered as being composed of three layers: epidermis, dermis and a sub-cutaneous fat layer. The dermis is comprised primarily of extracellular matrix components, mostly collagen. The dermis also receives most of the skin's blood supply and contains lymphatic vessels. Separating the dermis and epidermis is a basement membrane, the dermal-epidermal junction.

The cells in the epidermis are responsible for the structural integrity of the skin facilitated by desmosomes, focal adhesion points, zonular adherans and tight junctions (Proksch et al., 2008). These various adherence mechanisms collectively make the epidermis a very strong network, tightly regulating the barrier between the inside and outside of the body. The epidermis is typically 1-4mm thick in humans and is comprised primarily of differentiated keratinocytes, melanocytes and monocytes, as well as lipid layers and extracellular proteins. The keratinocytes differentiate as they move away from the basement membrane and form different strata (Kanitakis, 2002). In order of proximity to the basement membrane, they are: *stratum basale*, *stratum spinosum*, *stratum granulosum* and *stratum corneum* (Figure 1.1). *The stratum basale* contains the dividing germ line keratinocytes, as the cells differentiate they move from the basal layer progressively through the epidermis (Fuchs, 2008). The *stratum spinosum* is characterised by the formation of desmosomes, which hold adjacent cells together, giving this layer a strong structural role. The *stratum granulosum* contains granular cells, which have a more secretory role than the preceding layer, and are instrumental in the secretion of lipids, which are important in barrier function (Harding, 2004).

The *stratum corneum* (SC) is an interlinked network of terminally differentiated keratinocytes (corneocytes) that exhibit reduced metabolic activity and differs significantly from the other epidermal cell layers. Corneocytes have shed their nuclei and organelles and reside within a covalently-linked lipid cornified envelope. This envelope is a highly cross-linked sheet of proteins (e.g. involucrin, loricrin, filaggrin, trichohyalin) where the common cell membrane phospholipids are replaced by ceramides (Kalinin et al., 2002). These corneocytes are interspersed with secreted lipids made up of ceramides, cholesterol and free fatty acids (Lampe et al., 1983; Madison, 2003), which together with the cells create a hydrophobic, chemical and mechanical barrier for the skin.

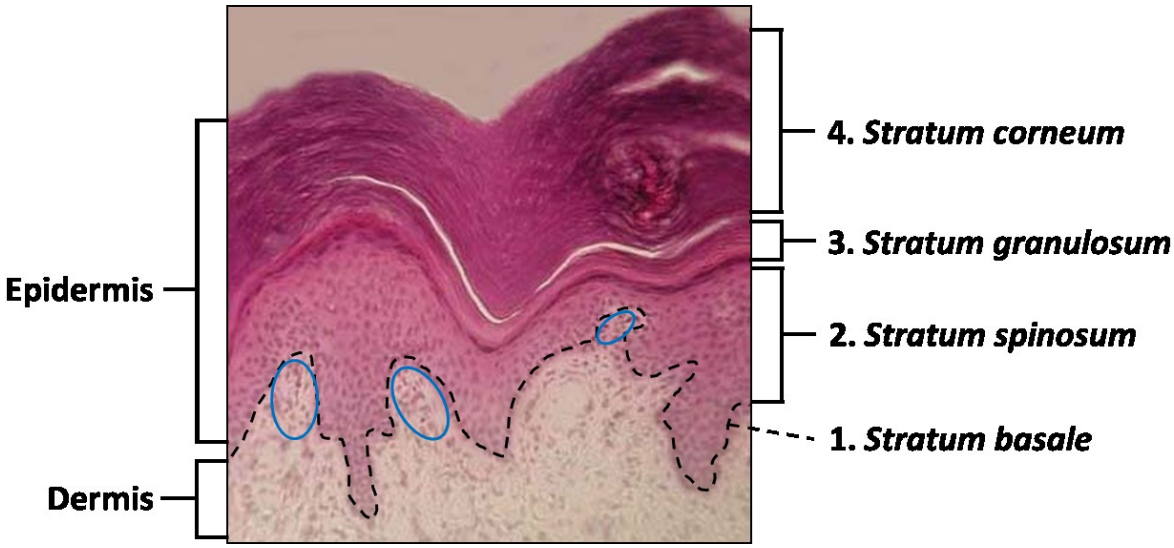

Figure 1.1. Cross section of human skin

Haematoxylin and eosin stained human skin section showing the squamous stratified epithelium. The epidermis is divided into 4 layers deriving from differentiated epidermal stem cells (blue circles in papules): 1) the basal layer or stratum basale, 2) the spinous layer, 3) the granular layer; and 4) the cornified layer or stratum corneum (http://histol.narod.ru/images/epithelia/epith-12.jpg reproduced with kind permission from owners).

The dermis accounts for 15-20% of the human body's total weight and sits between the epidermis and the subcutaneous fat. It provides nutrients and oxygen to the epidermis as the latter contains no vasculature and must rely on diffusion of nutrients between cells. It also contains lymphatic vessels that transport immune cells to and from the skin. The dermis ranges in thickness from 1 mm on the eyelid to 5 mm on the back and thighs and provides mechanical protection for the body as well as insulation and is

made up of extracellular matrix proteins, mainly collagen, secreted by fibroblasts. The cellular component of the dermis is primarily made up of fibroblasts, monocytes and macrophages. It projects into the epidermis in a papillary pattern and is separated from the latter by a basement membrane (Watt and Fujiwara, 2011). The basement membrane is comprised primarily from laminin secreted by keratinocytes (and possibly fibroblasts) complexed with nidogen, type IV collagen and fibrillar collagen secreted by fibroblasts (Fleischmajer et al., 1995).

1.2.2 Barrier function and basic skin immunology

Skin acts as a first line of defence in several ways:

1. The different layers of the skin act as barriers between the inside and the outside of the body.
2. The lipid envelope forms a barrier against polar fluids such as water.
3. Cross-linked proteins create a mechanical barrier against physical penetration into the skin

The different skin layers act as barriers between the inside and the outside of the body, and also contain immune cells to counter infection by external pathogens such as bacteria, fungi and parasites. However, commensal microflora present in the skin have also been shown to assist the immune system, by influencing the function of local T-cells (Naik et al., 2012). The lipid envelope forms a barrier against polar fluids such as water, and the epidermis and dermis both contain antigen presenting cells which sample the environment and under the right conditions present peptides to the immune system in order to modulate the appropriate response. The basement membrane, which separates the dermis and epidermis, acts as a secondary barrier. Melanocytes in the epidermis also help to shield the skin cells from UV damage (Friedmann and Gilchrest, 1987).

Two types of antigen presenting cells (APCs) reside in the epidermis and dermis respectively: Langerhans cells (LCs) and dermal dendritic cells (dDCs). Immune recognition in the skin is carried out by these cells, which present peptides from exogenous and endogenous proteins, in association with major histocompatibility complex (MHC) proteins, to T-cells in the lymph nodes. The antigens are obtained by endocytosis, pinocytosis or infection from pathogens (Kaplan et al., 2006). To present

these antigens, the cells must be induced to mature and migrate, which is thought to be the result of pathogen and stress markers received by the cells as a result of tissue insult to the skin or its barrier at the time of sensitization (Gallucci and Matzinger, 2001). These can include the presence of reactive oxygen species (ROS), cellular cytokine release and intracellular breakdown products of apoptosis. In the presence of these factors, the APCs are induced to migrate towards lymphatic vessels, which transport them to the draining lymph nodes where they come into contact with naïve T-cells.

Langerhans cells reside in the epidermis and are uniformly distributed in the tissue, with processes that protrude between epidermal keratinocytes, forming a network which spans most of the epidermis in three dimensions. Skin dendritic cells can be differentiated by the surface markers they express. Cluster of differentiation molecule 1a (CD1a) is an MHC-like molecule which presents non-protein antigens to T-cells (Sieling et al., 1995). Langerin is a C-type lectin which is thought to aid in the detection of fungal pathogens (de Jong et al., 2010) and causes the formation of the Birbeck granules (Valladeau et al., 2000). Factor XIIIa is a pro-transglutaminase which acts as a blood clotting factor in the blood plasma and platelets and can also be found on monocytes and macrophages (Muszbek et al., 1996) and can be used to differentiate LCs from dDCs (Cerio et al., 1989). Langerhans cells are $CD1a^{+}$, $FXIIIa^{-}$ and prior to maturation, express Langerin on the extracellular surface and in intracellular Birbeck granules, which are characteristic of LCs. It is also thought that LCs are necessary to induce contact hypersensitivity reactions (Bennett et al., 2007). However, other research suggests that contact hypersensitivity can be induced in the absence of LCs and that dermal dendritic cells are also able to elicit ACD (Fukunaga et al., 2008).

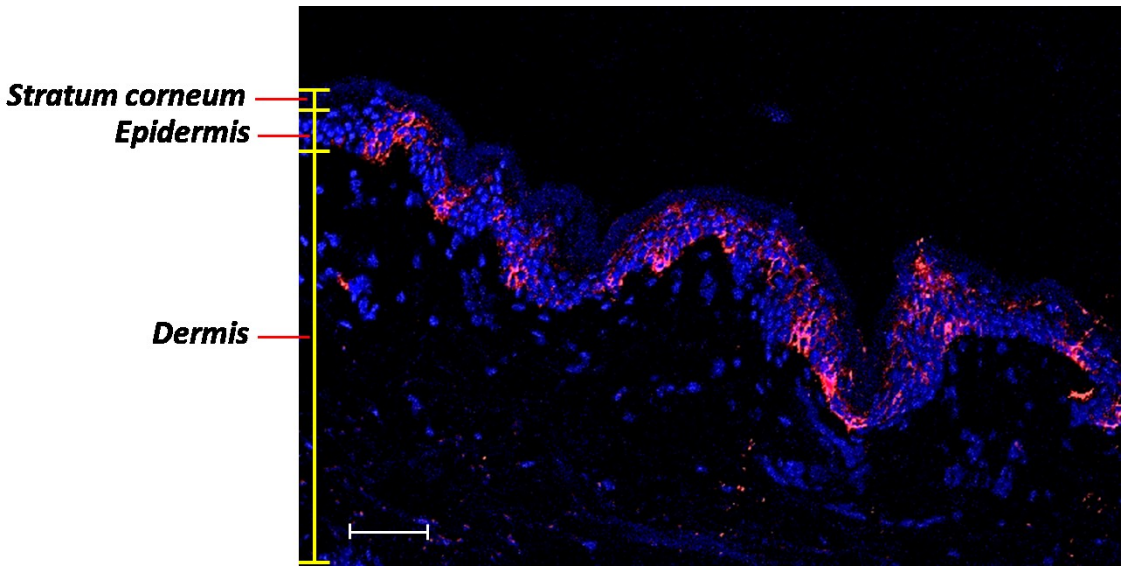

Figure 1.2. Cross section of human skin showing Langerhans cells

A confocal micrograph showing the Langerhans cells (red) along the entire length of the skin section, throughout the epidermis. LCs are labelled with anti-Langerin mouse primary antibody and anti-mouse alexafluor 546 secondary antibody. To-Pro 3 nuclear stain is shown in blue. (original data). Scale bar represents 60 µm.

The APCs in the dermis are dendrocytes which are factor XIIIa^{+} and generally CD1a^{-}, however some sub-populations are thought to express Birbeck granules and the CD1a antigen, suggesting perhaps that some dermal dendritic cells (dDCs) have a similar lineage to LCs. They express high levels of MHC class II molecules on their cell surface and thus are able to present antigens obtained through endocytosis and also makes them more efficient at presenting antigen to T-cells versus e.g. macrophages which express lower levels (Trombetta and Mellman, 2005). In contrast to LCs, dDCs are more likely to be involved in immune responses to specific viral (Allan et al., 2003) and parasitic (Ritter et al., 2004) infections. It is likely that LCs and dDCs each play slightly different roles with respect to acquisition of antigens from different pathogens, but it is not yet clear if there is a definitive distinction with regard to contact hypersensitivity and it is likely that either APC can process haptenated proteins and present them to T-cells in the lymph nodes.

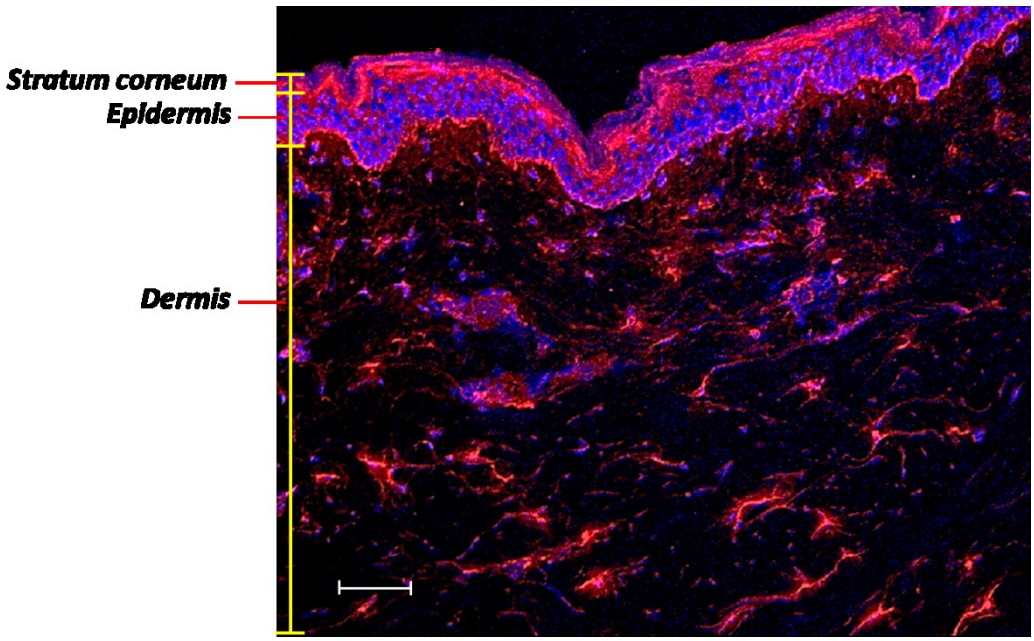

Figure 1.3. Cross section of human skin showing dermal dendritic cells

Confocal micrograph showing dermal dendritic cells (red) throughout the dermis. Dermal dendritic cells are stained with anti-FXIIIa rabbit primary antibody and anti-rabbit alexafluor 546 secondary antibody. To-Pro 3 nuclear stain is shown in blue. (original data). Scale bar represents 60 µm.

1.3 Pathologies of the skin

The skin is the body's primary protective interface to outside stressors and as a result it is prone to a number of pathological conditions brought about by chemical and environmental factors (Madison, 2003). Some skin conditions such as atopic dermatitis have genetic determinants (Brown and McLean, 2009; Morar et al., 2006) and are increasing in prevalence (Williams and Flohr, 2006).

1.3.1 Innate responses to chemicals and pathogens

Irritancy is caused by insult to the skin's barrier and damage to epidermal cells. This could be from a detergent, strong pH or solvent. Such substances may remove lipid molecules from the stratum corneum, allowing moisture to leave the skin, which in turn stresses the epidermal cell layers (Malten, 1981). Some chemicals affect cells directly, damaging them and thinning the epidermal layer. Innate responses also occur as a first line of defence against pathogens such as bacteria, fungi, parasites and viruses (Kupper and Fuhlbrigge, 2004) by detecting common molecular patterns in microbial proteins, known as pathogen-associated molecular patterns (PAMPs). The follow-on effects of innate immune activation damage can be inflammation where cytokine and chemokine

signalling recruits additional immune cells to an effected area. This is achieved by creating a molecular gradient for other immune cells and increases vascular porosity, leading to an influx of fluid, which causes swelling (oedema). Irritant damage and UV damage also cause a reddening of the skin, due to increased blood flow near the skin's surface, which is known as erythema.

All of these conditions involve primarily innate responses, which are non-specific and only require broad conditions to trigger.

1.3.2 Allergic contact dermatitis

Allergic contact dermatitis (ACD) is a type IV delayed hypersensitivity reaction, characterised by taking several days to develop and is mediated by T-cells (Coombs, 1975). This is an acquired immune response to proteins in the skin which have been modified by a specific xenobiotic agent to give an immunogenic epitope. Typically, symptoms occur approximately two to three days after the chemical has come into contact with the skin and present as itching (pruritis), swelling (oedema), redness (erythema), blisters and, in extreme cases; oozing, scabbing and scaling. Itching always occurs and rashes vary in severity and often contain blisters. These symptoms generally last as long as the allergen is in contact with the skin, plus as long as is required for the skin damage to heal.

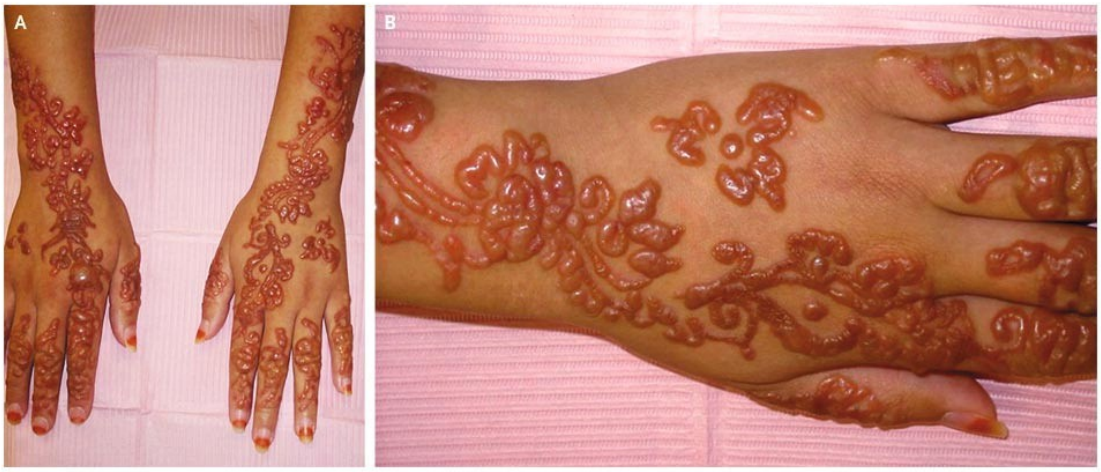

Figure 1.4. An example of how allergic contact dermatitis presents on skin.
In this instance, the dermatitis has occurred due to an allergic reaction to PPD, a common contact allergen. Reproduced with permission from (Evans and Fleming, 2008) , Copyright Massachusetts Medical Society.

1.4 The mechanisms of ACD

The process of ACD is thought to occur through several stages:

1.4.1 Penetration of a xenobiotic into the epidermis

An important property of any skin sensitizer is its ability to penetrate through the stratum corneum to generate haptens near to or within APCs. Movement through the SC requires that any sensitizer should be hydrophobic or amphipathic to traverse the lipid envelope. The hydrophobicity of a compound can be determined by its partition coefficient, or Log P value, which is the relative miscibility of a compound between polar and non-polar solvents (Abraham et al., 1995). The higher the Log P value, the more hydrophobic a compound is and thus the more readily the compound can move through the lipid-heavy stratum corneum and into the epidermis. However, chemical allergens and proteins can sensitize by penetrating into skin if the barrier is damaged (Berard et al., 2003; Smith Pease et al., 2002), meaning that the ability to move through the SC is not an exclusive requirement for chemical sensitizers.

1.4.2 Haptenation of proteins

For a chemical to haptenate proteins, it must have reactivity sufficient to alter the structure of exposed amino acids and to generate neo-antigens to be presented to naïve T-cells (Weltzien et al., 1996). There are several different types of reaction that can commonly occur between these chemical agents and amino acid residues and these are summarised below.

1) Nucleophile-electrophile reactions

Nucleophilic reactions occur when the compound of interest is highly polar and contains an electrophilic group able to attack an electron-rich nucleophilic region of an amino acid. This can happen in various ways including substitution reactions, where a nucleophile replaces a group on the chemical molecule at a saturated or unsaturated carbon, Michael addition, where the nucleophile is added to an unsaturated carbonyl group on a molecule, and carbonyl group condensation reactions where the nucleophile displaces water from the recipient molecule.

2) Nucleophilic aromatic substitution

Conjugation of some electrophilic chemicals to amino acid residues takes place as a nucleophilic aromatic substitution (SNAr) reaction. This occurs when the nucleophilic side-chain of an amino acid residue (e.g. Cys, His, Lys, Arg, Met, Tyr) or the terminal amine group of a protein attacks an unsaturated carbon centre on an electrophilic centre. The nucleophilic amino acid side-chain displaces a leaving group from the electrophile, in the case of the extreme sensitizer DNCB, a chlorine. The displaced chlorine from DNCB will leave as part of an HCl molecule (Figure 1.6).

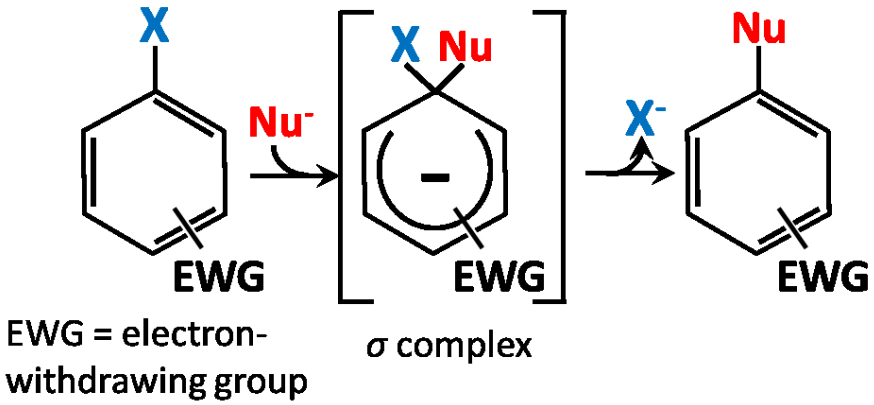

Figure 1.6. Nucleophilic aromatic substitution

A diagram showing a generic SNAr reaction, where a nucleophile (Nu-) forms a complex with the electrophilic donor molecule before displacing the leaving group. In the case of DNCB haptenation, X is Cl⁻, Nu⁻ is an amino acid side chain or N-terminal amine group and the final stage would be a dinitrophenyl protein adduct with HCl leaving the reaction.

3) Michael addition

This is a chemical modification that is often associated with sensitization to plant sesquiterpene lactones (Bleumink et al., 1976) and some fragrance chemicals (Divkovic et al., 2005). It involves the addition of a nucleophile, in this case again from an amino acid side chain; to a central carbon of a recipient molecule, essentially, extending the carbon backbone (Figure 1.7).

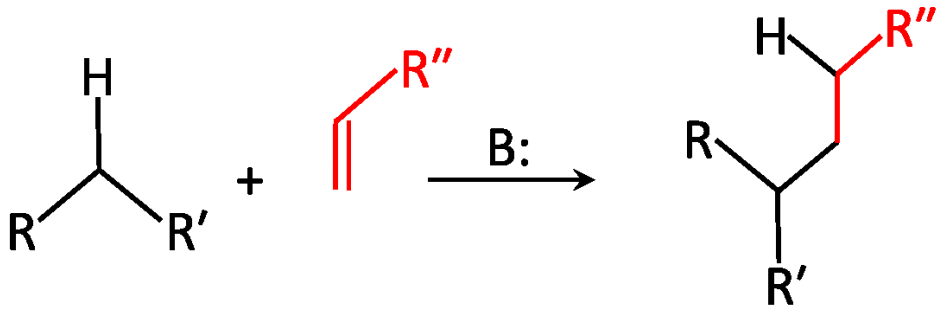

Figure 1.7. Michael addition reaction

Generalised diagram of a Michael reaction showing R and R' as two groups on a nucleophile electron donor (e.g. the side chain of a lysine residue) reacting with an electrophile R'' and a base B: to give an addition of the R'' without a leaving group.

1.4.3 Bioactivation: pro and pre-haptens

Many chemical sensitizers are not able to react with and modify proteins without first undergoing chemical activation, usually through an enzymatic modification. In the skin, multiple enzymatic pathways are used to detoxify compounds and make them more hydrophilic so that they may be disposed of in urine or bile (Gerberick et al., 2008). This takes place as a two stage response. Phase I is a modification step for rendering molecules more polar and thus water-soluble and is catalysed by enzymes such as cytochrome P450, alcohol and aldehyde dehydrogenases, monoamine oxidases, flavin-containing monooxygenases and hydrolytic enzymes. Phase II involves conjugation of reactive molecules to endogenous antioxidant molecules such as glutathione for the purpose of neutralizing reactive molecules and clearing potential toxins from the cell. Phase II enzymes include acetyltransferases, UDP-glucuronosyltransferases, sulphotransferases and glutathione S-transferases (Krishna and Klotz, 1994). The first phase, while intended to neutralise potentially harmful molecules, can render some substances more reactive, which is a crucial step in haptenation for some sensitizers

such as cinnamic compounds (Elahi et al., 2004; Niklasson et al., 2014; Smith et al., 2000) and diphenylthiourea (Samuelsson et al., 2011). Oxidation by contact with air has also been shown to allow some chemicals to become protein reactive, including geranial (Hagvall et al., 2011) and linalool (Skold et al., 2002), thus it remains possible that there are a variety of activating factors which broaden the number of potential sensitizers greatly and make it difficult to screen chemicals by structure alone.

1.4.4 Antigen processing and MHC loading

The acquired immune response is dependent on the presentation of antigens to the T-cells by professional antigen presenting cells (APCs) such as dendritic cells, B-cells and macrophages. In most cells, endogenous proteins are degraded within the proteasome and presented on the cell surface bound to major histocompatibility complex (MHC) class I molecules, thereby constitutively presenting a sample of the cell's protein content. These heterogeneous epitope libraries allow the immune system to identify cells that are potentially infected with pathogens and should be destroyed (Neefjes et al., 2011; Watts, 1997).

MHC class II molecules are used to present a sample of peptides at the cell surface derived from proteins that have been taken into the cell by endocytosis. Peptide loading to MHC class II molecules occurs within a different pathway to that of MHC class I molecules insofar as the former derives peptide antigens from proteins digested in the endocytic pathway and the latter from proteins within the cell (Trombetta and Mellman, 2005). Professional APCs such as Langerhans cells and dermal dendrocytes express high quantities of MHC class II molecules as they are directly responsible for priming the immune response to pathogens and other foreign material. When a haptenated protein is processed in a dendritic cell, some of the peptides that conjugate with the MHC molecules and are presented on the cell surface are thought to contain amino acid residues which have been modified by the hapten (Weltzien et al., 1996). Due to the conformational difference between the haptenated peptide and its unmodified equivalent, an MHC molecule loaded with a peptide-hapten adduct may be recognised as foreign by the immune system (Divkovic et al., 2005; Martin and Weltzien, 1994).

1.4.5 Irritancy, innate immunity and DC migration

Before recognition of the haptenated peptide can take place, an APC displaying the immunogenic peptides must migrate through the lymphatic system into a regional

lymph node (Saint-Mezard et al., 2004). This is not specifically triggered by the processing of foreign or modified proteins, but by noxious stimuli resulting from pathogen infiltration into the skin or epidermal damage and water loss (Gallucci and Matzinger, 2001). These events within the epidermis can result in further fluid loss, apoptosis, the generation of reactive oxygen species and signals of general tissue damage, e.g. platelet activating factor. As such, sensitization requires two factors: the modification of endogenous proteins by a chemical agent and pathogenic insult to the epidermal layer, resulting in APC migration (Vocanson et al., 2009).

Cells are also able to detect insult by protein-reactive electrophiles. Kelch-like ECH–associated protein 1 (Keap1) is a protein which contains reactive cysteine residues and associates with nuclear factor-erythroid 2-related factor 2 (Nrf2), a transcription factor which up-regulates the expression of antioxidant response elements (AREs). Certain chemicals can modify cysteines in Keap1, causing it to dissociate from Nrf2, which is then able to accumulate within the nucleus and up-regulates the expression of AREs, including many of the phase II enzymes mentioned earlier (Dinkova-Kostova et al., 2002). This increases the inflammatory response and has been shown to be relevant to a number of contact sensitizers which modify cysteine residues (Natsch and Emter, 2008).

During tissue insult, epidermal keratinocytes release cytokines such as interleukin-1 alpha (IL-1α) and tumour necrosis factor alpha (TNF-α). These molecules stimulate fibroblasts in the dermis, which secrete chemokines that create a molecular gradient along which APCs move towards the lymphatic vessels in the dermis where they can migrate to draining lymph nodes (Brand et al., 1992; Cumberbatch et al., 2000; Ouwehand et al., 2010b; Pickard et al., 2009; Toebak et al., 2006).

1.4.6 Antigen presentation and T-cell activation

After migration to the draining lymph node, APCs presenting an immunogenic peptide on an MHC molecule on the cell surface, can then activate T-cell recognition by a T-cell receptor (TCR), leading to clonal expansion of the T-cell. The naïve T-cell matures and differentiates to produce either memory T-cells which act as a response archive to a specific antigen; or effector T-cells, which mediate the acute immune response to the antigen. T-cell activation by APCs occurs when the antigen presented by an MHC molecule binds to the variable region of a T-cell receptor with a good affinity to form an immunological synapse and a co-stimulatory molecule on the T-cell interacts with the

MHC molecule (Grakoui et al., 1999). Antigen-specific T-cells are broadly categorised into the following sub-sets:

1) Cytotoxic T-cells (T_c)

These cells are characterised by the CD8 cell surface antigen and hence referred to as $CD8^+$ cytotoxic lymphocytes (CTLs) and are MHC class I restricted, meaning they only interact with MHC-I presented antigens. They respond to epitopes derived from within the cell and destroy cells which display immunogenic antigens in MHC class I molecules. This allows them to eliminate cells potentially infected with pathogens.

2) Helper T-cells (T_h)

These cells are $CD4^+$ and MHC-II restricted. They respond to antigens primarily obtained through endocytosis, which gives them the general role of responding to extracellular threats. Helper T-cells secrete cytokines to recruit macrophages and other lymphocytes, including B-cells to the site of detected antigen (von Andrian and Mackay, 2000). Helper T-cells are themselves divided into sub-sets, consisting of T_h 1,2 and 17 which are determined by the relative amount of different cytokines they are exposed to during differentiation. These sub-types are involved in different types of pathologies (Kidd, 2003; Steinman, 2007). Allergic contact dermatitis and contact hypersensitivity reactions tend to be associated with the T_h1 sub-set.

3) Regulatory T-cells ($_{Treg}$)

A sub-class of helper T-cells, they are $CD4^+$, $CD25^+$ and MHC-II restricted and act as inhibitory cells to mediate the strength of the immune response by secreting anti-inflammatory cytokines and limiting the response of cytotoxic T-cells. These cells are known as regulatory T-cells, or T_{reg} cells.

1.4.7 The elicitation of ACD

Allergic contact dermatitis is generally described as happening in 2 distinct stages: sensitization, where the T-cells are primed by the hapten epitopes; and elicitation, where subsequent contact with the sensitizer stimulates a more rapid and amplified response from the antigen-specific memory cells (Coombs, 1975).

Sensitization, which develops in approximately 10-15 days in humans, occurs when hapten-peptide epitopes are presented to naïve T-cells by APCs which have migrated to the lymph node. Since chemical sensitizers can remain in the skin for approximately 2 weeks after contact, elicitation can occur after a single application of the sensitizer; a process referred to as primary ACD (Saint-Mezard et al., 2003). This leads to the characteristic swelling and rash in a delayed hypersensitivity reaction. Once the tissue is free from the chemical hapten, the inflammation resolves, but the memory cells ensure that further challenge with the same hapten will trigger a more sensitive response. As well as T-cell activation, NKT cells from the liver may become active in response to haptenated proteins or inflammation markers caused by sensitization. These NKT cells can in turn activate antigen-specific IgM secreting B cells in the spleen (Vocanson et al., 2009), leading to a humoral response.

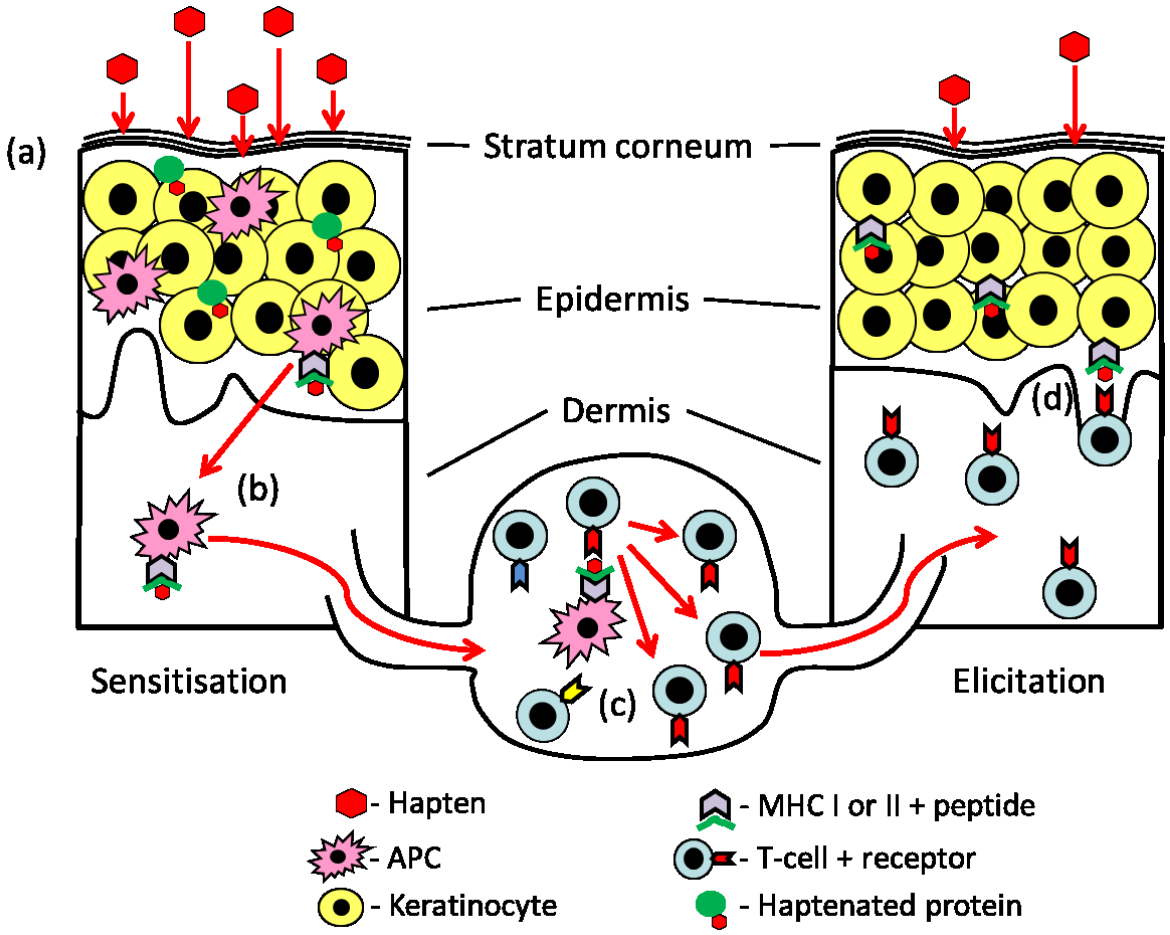

Figure 1.8. Overview of the mechanism of sensitization.

A diagram showing a basic model of contact sensitization: (a) Sensitizer enters skin through the SC and enters epidermal keratinocytes and APCs, haptenating proteins. (b) in response to tissue insult, the APCs migrate to the draining lymph node. (c) APCs present the haptenated peptides to naïve T-cells. If successfully stimulated, activated T-cells undergo clonal expansion and circulate via the blood and lymphatic system to the entire body, including the skin. (d) Subsequent challenge with the same sensitizer results in presentation of a hapten-peptide complex on the surface of epidermal cells. Antigen specific T-cells respond to affected cells by inducing apoptosis in epidermal cells presenting the relevant antigens and secrete cytokines promoting further immune cell infiltrate into the tissue.

1.5 2,4-dinitro-1-chlorobenzene (DNCB) as a model sensitizer

The model sensitizer 2,4-dinitro-1-chlorobenzene (DNCB) covalently modifies proteins by attaching a dinitrophenyl group to the side chains of susceptible amino acids (Figure 1.9).

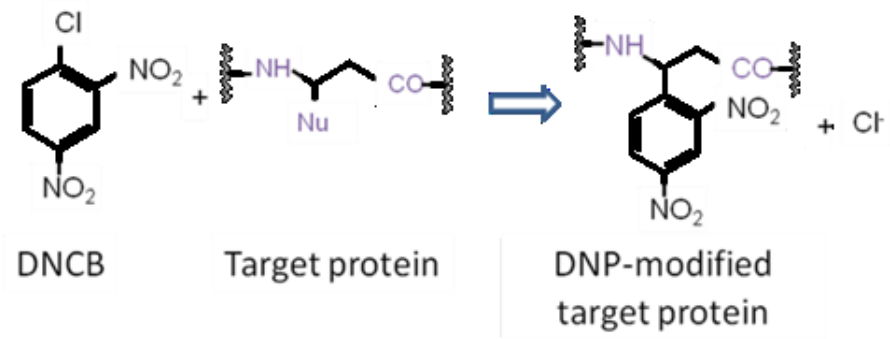

Figure 1.9. Dinitrophenylation of amino acid side chains

A reaction scheme for modification of a protein by dinitrochlorobenzene (DNCB). Modification results in the attachment of a dinitrophenyl group to the target protein.

Studies with DNCB have shown that sensitization occurs in a manner that is proportional to the dose of the sensitizer and also to the area of skin treated (Rees et al., 1990; White et al., 1986). A higher concentration of DNCB leads to more haptenation events and thus a higher number and variety of potentially immunogenic peptides to be presented by APCs. There is thus an increase in the number of APCs that have the opportunity to present the modified peptides (Figure 1.10).

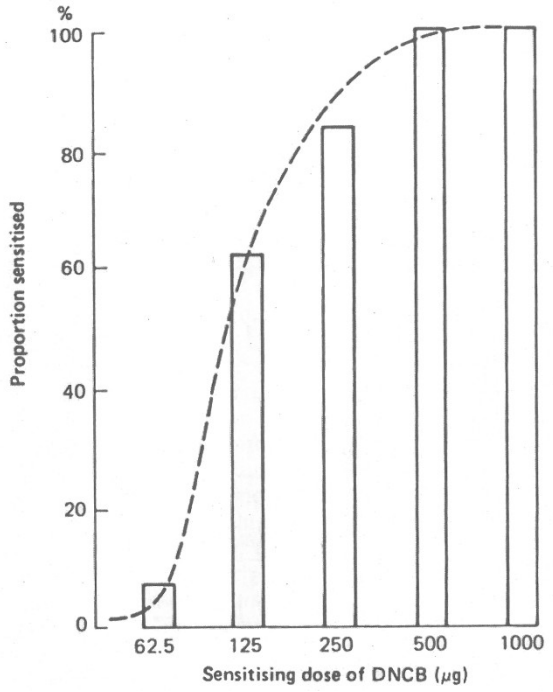

Figure 1.10. DNCB dose response

Graph showing dose response for DNCB patch tests on different test subjects. Taken from (Friedmann, 1990).

Further, if a larger surface area receives the dose, more dendritic cells are exposed to haptens. On a fixed surface area of, e.g., 3 cm diameter, the number of test subjects sensitized increases proportionally with the concentration of the sensitizer. Hence, if a dose concentration at which 100% are sensitized is applied to a far smaller area, say a circle with 1.5 mm diameter, fewer subjects are sensitized (table 1.1). This suggests that the number of dendritic cells in the affected area is a key factor in successful sensitization. The probability of naïve T-cells being activated by application of a sensitizing hapten is a factor of both dose and size of the affected area as these factors are representative of number of APCs and hapten-peptide adducts presented at their surface. Ultimately, dose and surface area are direct factors in probability of a sensitization event occurring.

Table 1.1. The effect of dose area on sensitization

The variability in subject sensitization percentage with difference in DNCB treated areas. An equivalent dose in μg/ cm^2 applied to a smaller area results in less people sensitized. Table from (Friedmann, 2006).

	Application site		Sensitizing dose			
Row	Diameter (cm)	Area (cm^2)	Total (μg)	Concentration (μg/cm^2)	Number of subjects	Percentage sensitized
1	3	7.1	1000	142	24	100
2	3	7.1	500	71	40	100
3	3	7.1	250	35.4	30	83
4	3	7.1	125	17.7	30	63
5	3	7.1	62.5	8.8	24	8
6	1.5	1.8	62.5	35.4	7	86
7	2.1	3.5	58	16.4	22	55
8	3	7.1	116	16.4	34	50
9	4.25	14.2	232	16.4	15	66
10	1 cm felt	0.8	30	38	28	93
11	3 mm felt	0.08	3	38	15	26

Dinitrophenyl modifications on proteins can be analysed in a number of ways. Antibodies can be raised against the DNP antigen by using proteins modified with DNCB to generate polyclonal antibodies. Commercially available antibodies raised against e.g. dinitrophenyl human serum albumin (Sigma, D9781) or dinitrophenyl keyhole limpet haemocyanin (Life Technologies, A-6430) can be obtained. Antibodies have been used for the detection of DNCB-modified proteins by immunofluorescence (Pickard et al., 2009), immunohistochemistry (Carr et al., 1983) and western blot (Dietz et al., 2010). As well as antibodies, autoradiography has also been used to detect adducts (Pickard et al., 2007). Another way to analyse hapten modifications is by mass spectrometry, which is detailed below.

1.6 The proteomics approach

The identities of proteins that are targets for skin sensitizers are poorly understood. One way to approach this issue is to analyse proteins or peptides from the skin that are modified following exposure to a specific sensitizer. It is also possible to examine responses in simpler systems, e.g. in cultured keratinocyte-like cells such as the HaCaT cell line (Boukamp et al., 1988) or to look at the modification of individual model proteins like human serum albumin (Aleksic et al., 2007; Bertucci and Domenici, 2002) or the skin proteins cytokeratin-14 and cofilin (Aleksic et al., 2008).

Protein modifications can be characterised by digesting proteins and analysing them at the peptide level to identify changes in mass, equivalent to the addition of a known chemical hapten. For example, DNCB confers a dinitrophenyl group which increases mass by 166.0015 Da. This characterisation can be accomplished by mass spectrometry, which separates ionized peptides according to the mass to charge (*m/z*) ratio, allowing for the differentiation of a modified peptide from its unmodified equivalent. Analysing a digest from proteins treated with DNCB versus a vehicle control should reveal peptides in the test sample with an *m/z* value which corresponds to a known peptide with an altered mass corresponding to the addition of the dinitrophenyl (DNP) hapten. DNCB modification of proteins has previously been carried out using human serum albumin (HSA) as a model protein where 10 amino acid residues were found modified by DNCB using a combination of MALDI mass spectrometry and ESI-MS/MS (see sections 1.6.3 and 1.6.5)(Aleksic et al., 2007).

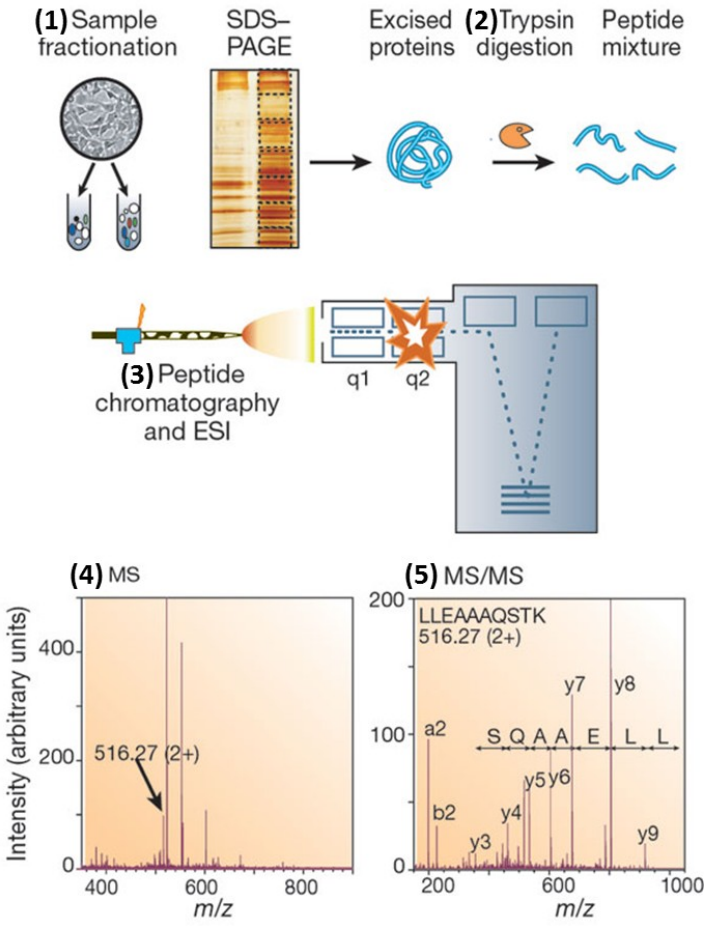

Figure 1.11. Mass spectrometry based proteomics

Illustration of a typical protemics workflow. Each of the steps shown will be described in more detail in this chapter. A protein lysate is obtained from cells or tissue, separated using SDS-PAGE, digested with trypsin, then further separated using liquid chromatography and analysed in a quadrupole time of flight (QToF) mass spectrometer. Reprinted by permission from Macmillan Publishers Ltd: Nature (Aebersold and Mann, 2003) , copyright 2003.

1.6.1 Sample fractionation

Whole cell lysates are extremely complex and as such, characterising the full proteome can be challenging, due to a wide dynamic range between the least and most abundant proteins. Further complexity given by the presence of splice variants, isoforms and post translational modification of proteins makes a full analysis of an entire proteome very difficult. To try and address these challenges, it is often necessary to reduce this complexity by employing one or more methods of fractionation. Some common methodologies are now discussed.

1) 1-D gel electrophoresis

Here protein mixtures are separated by molecular weight using SDS-PAGE prior to being excised, digested in gel using a site specific protease and the peptides extracted and analysed by LC-MS (GeLC-MS)(Nicholas et al., 2006; Wang et al., 2009). The approach is inexpensive, technically straightforward and has the added benefit of removing salts and other small molecular weight components of the lysate which might otherwise interfere with analysis of the sample.

2) Isoelectric focussing (IEF)

Isoelectric focussing can be used to separate analytes according to their isoelectric point. One method uses an immobilised pH gradient (IPG) along a gel. Analytes move along the gel driven by electrical current until they reach a point in the pH gradient where they are electrically neutral, their isoelectric point (O'Farrell, 1975). A relatively recent improvement in this technique results in the analytes eluting out of the gel into an adjacent solution, providing convenient recovery of the focussed analytes (Chang et al., 2001). One widely used system which utilises the elution of analytes into a liquid phase is the OFFGEL system (Agilent), which provides good, highly reproducible separation of both proteins and peptides (Hubner et al., 2008); (Hoerth et al., 2006).

3) 2-D gel electrophoresis

Two-dimensional SDS-PAGE allows for greater separation of complex protein mixtures than simple SDS-PAGE, by first separating proteins according to isoelectric point using IEF and then separating the proteins orthogonally by SDS-PAGE according to their molecular weight. Though useful for giving high-resolution separation and retaining the relative molecular weight and isoelectric point values of the proteins, this method is not easily automated and only allows limited resolution of proteins with very high or low molecular weight, pH or hydrophobicity (Hanash, 2000; Rabilloud et al., 2010).

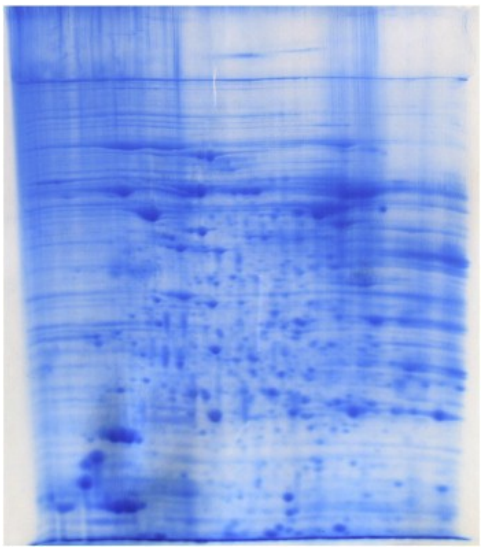

Figure 1.12. 2-Dimensional gel electrophoresis

A 2-dimensional gel stained with Coomassie blue showing proteins extracted from mouse liver mitochondria. The IEF is responsible for the horizontal separation and the SDS-PAGE the vertical. Reprinted from (Rabilloud et al., 2010).

4) Liquid chromatography

Liquid chromatography uses a stationary phase inside a column to separate biomolecules in solvent based on their polarity. Most proteomic work utilises high-performance liquid chromatography (HPLC) or ultra-performance liquid chromatography (UPLC) which use much smaller diameter mobile phase columns under high pressure for greater separation of proteins and peptides (Aebersold and Mann, 2003; Swartz, 2005). Reversed phase liquid chromatography (RPLC) is typically used in proteomics and uses a stationary phase which is less polar than the mobile phase containing the sample.

A typical stationary phase used for separating peptides is C18 silica (a C4 variant may also be used to separate larger molecules), which is a $(CH_2)_{17}CH$ chain anchored to silica, packed into a column. Hydrophobic interactions between the long carbon chains binds peptides from an aqueous stationary phase, allowing contaminants to be washed through before eluting the peptides by gradually increasing the percentage of an organic phase, typically acetonitrile (CH_3CN) flowing through the column. The relative hydrophilicity / hydrophobicity of each peptide will determine at which stage each will elute, providing separation of the peptide sample. Liquid chromatography can be used to create distinct fractions by collecting the eluate at timed intervals and directly analysing each fraction. More recently however, LC systems are configured to deliver the eluate directly into a mass spectrometer, which allows for greater automation and reproducibility, as well as eliminating boundary effects where molecules elute between fractions. Each ion analysed by the mass spectrometer will have an associated retention time value which corresponds to the time it was eluted from the LC capillary (Figure 1.13.).

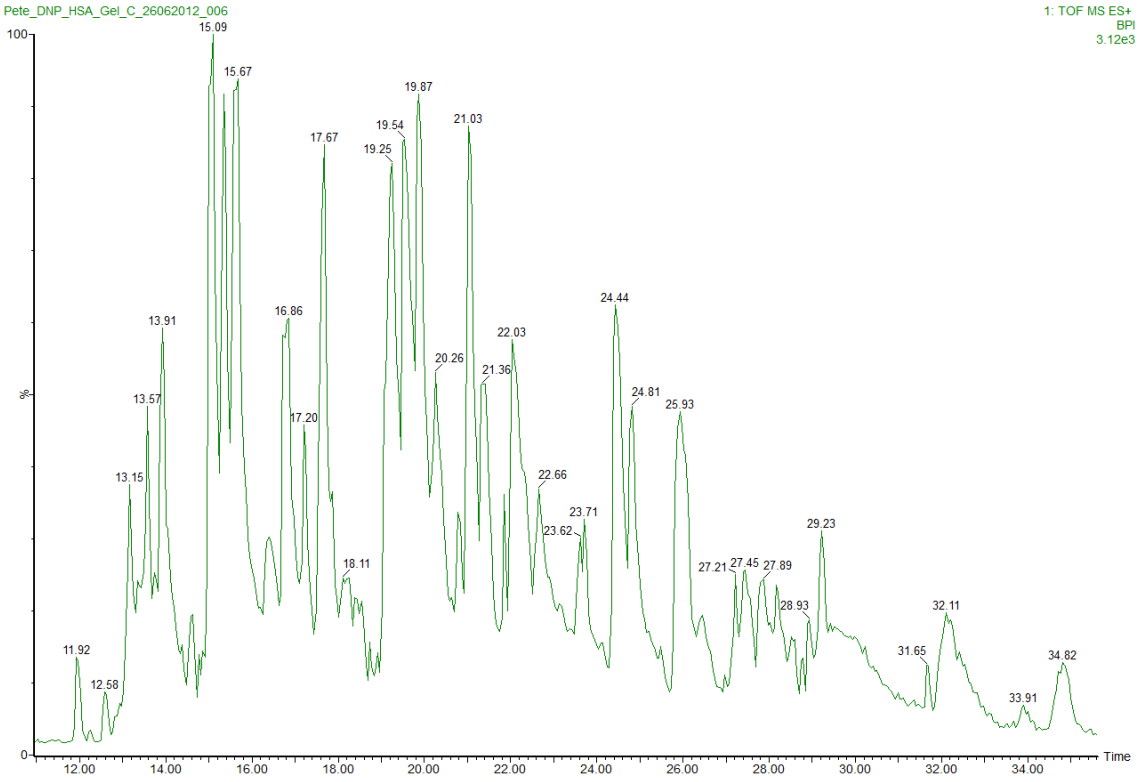

Figure 1.13. Liquid chromatography chromatogram

An example of a base peak intensity (BPI) chromatogram which shows the most intense peaks from each point of the chromatography elution as relative abundance as a response to time. Original data showing a chromatogram for a digest of human serum albumin.

Other types of LC columns such as strong cation exchange and strong anion exchange separate molecules by acidic / basic interactions to selectively bind and elute peptides based on their charge. These types of column are often used as an orthogonal dimension of separation (Chen et al., 2006).

1.6.2 Mass spectrometry ion sources

Mass spectrometry involves analysing molecules in the gas phase under the influence of an electrical gradient. Therefore, the first step of mass spectrometry is to get the sample into the gas phase by ionisation.

1) Matrix assisted laser desorption ionisation (MALDI)

One method used for ionising samples is matrix-assisted laser desorption / ionisation (MALDI). In this method, a low molecular weight UV absorbing compound (the 'matrix') is mixed with the sample, spotted onto a MALDI plate and allowed to dry to a crystalline matrix with embedded analyte. The matrix typically absorbs laser energy in a UV region not absorbed by the peptides. Thus, when a laser is fired at the samples, energy absorbed by the matrix is passed indirectly to the peptides, desorbing them from the surface of the sample plate and simultaneously ionising them in the gas phase (de Hoffmann, 2007). Two typically used matrices are α-cyano-4-hydroxycinnamic acid (CHCA) and 2, 5-dihydroxybenzoic acid (DHBA).

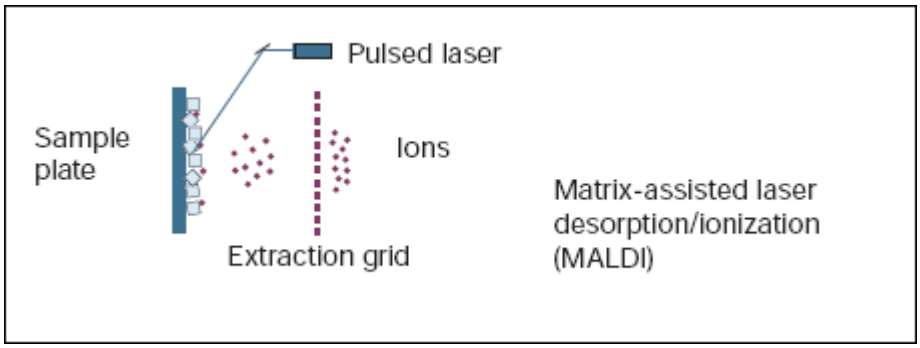

Figure 1.14. Matrix-assisted laser desorption ionisation

Diagram outlining MALDI sample ionisation. Dried sample and matrix are shot with a UV laser which excites the matrix, leading to vaporisation of the matrix along with the sample, but without directly exciting the sample. Ions are delayed at an extraction grid preventing any time of flight discrepancy before entering the analysis stage. Reprinted by permission from Macmillan Publishers Ltd: Nature (Aebersold and Mann, 2003) , copyright 2003.

MALDI mass spectrometers are usually used in combination with time-of-flight (Tof) mass analysers, though many mass spectrometers can in theory be integrated with a MALDI ionisation source.

2) Electrospray ionisation (ESI)

Electrospray ionisation (ESI) is an ionisation technique that introduces samples to MS by passing them in solvent through a capillary tube held at a high electrical potential. This results in a spray of charged particles, known as an electrospray. The sprayed particles undergo Rayleigh fission ('Coulomb explosions'), desolvating, generating ions that can be accelerated in the mass spectrometer. This ultimately results in the production of multiply charged ions that are devoid of solvent.

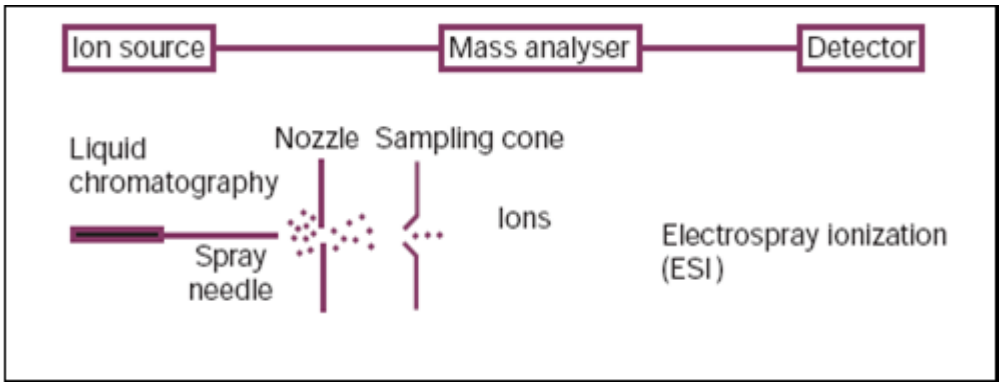

Figure 1.15. Electrospray ionisation

Diagram illustrating the process of ESI. The sample is injected into a fine needle which is heated between 40-100°C and kept at an electrical potential 3-5 kV relative to the sampling cone. Upon leaving the needle, the sample vaporises and the charged analytes travel along the potential difference, into the sample analyser. Reprinted by permission from Macmillan Publishers Ltd: Nature (Aebersold and Mann, 2003) , copyright 2003.

1.6.3 Quadrupoles

Some mass spectrometers employ a quadrupole mass filter. Quadrupoles consist of 4 metal rods, with each opposite pair being electrically connected. Radio frequency (RF) voltage is applied to the rods which creates an electrical field which can be modulated in a way which will only provide a stable trajectory through the quadrupoles for ions with a specific *m/z (de Hoffmann, 2007)*. It is possible to tune a quadrupole so that only ions with a specific *m/z* value can pass through at a given moment, allowing the isolation of specific peptides of interest (Figure 1.16). These peptides can be fragmented for tandem mass spectrometry (MS/MS), before being subjected to selection via an additional quadrupole positioned after a dissociation stage.

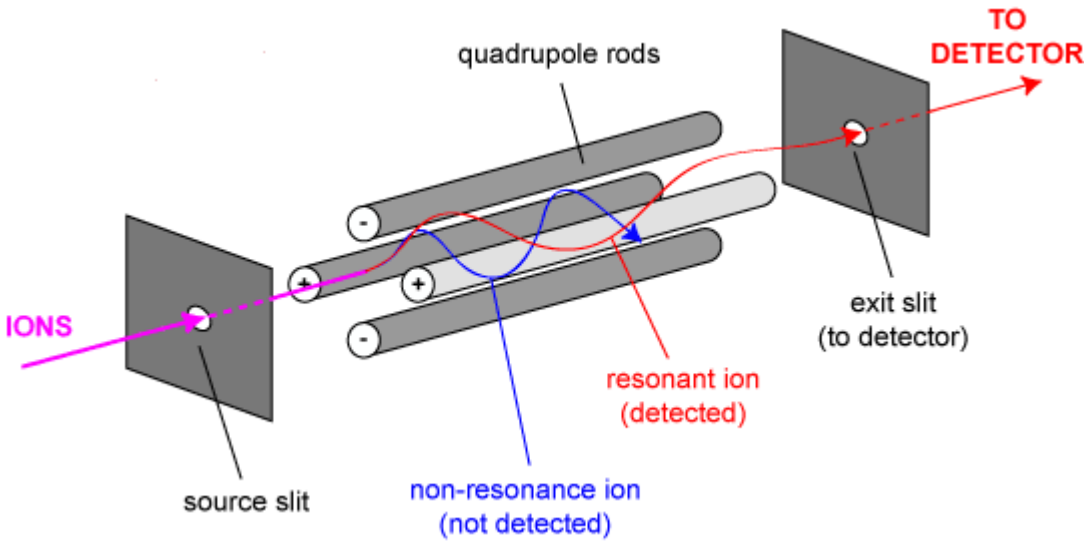

Figure 1.16. Quadrupoles

Diagram showing basic Q-Tof with quadrupole allowing an ion of a specific m/z to pass through (red) while rejecting all other molecules (blue). Image taken from http://www.bris.ac.uk/nerclsmsf/images/quadrupole.gif - permissions pending.

1.6.4 Mass analysers

Mass spectrometry (MS) applies an electrical current to ionised analytes under vacuum in order to determine their mass to charge (*m/z)* ratio (Figure 1.17).

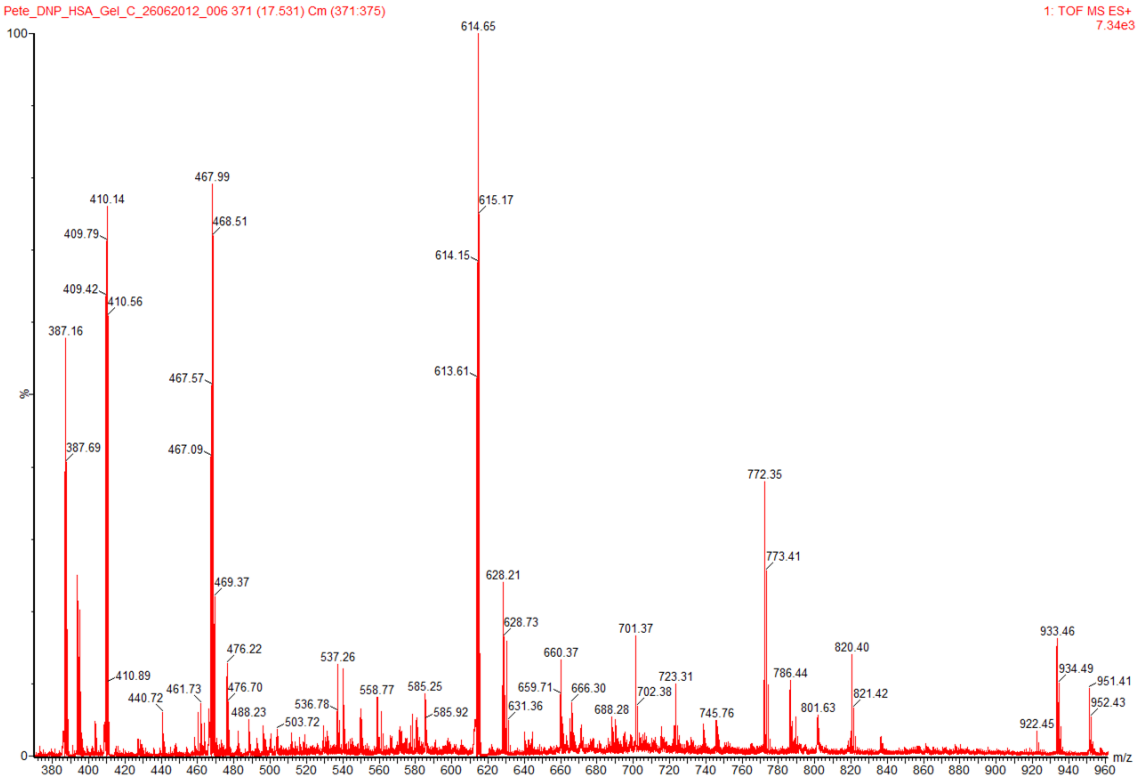

Figure 1.17. Mass spectra

An example of mass spectra, showing relative abundance versus m/z. Original spectra from a tryptic digest of human serum albumin.

This is achieved using a number of methods, some of which are outlined below.

1) Fourier transform ion cyclotron resonance (FT-ICR) and Orbitrap mass spectrometry

FT-ICR detectors trap ions in a magnetic field and then excite them using a separate, oscillating magnetic field, which moves the ions in a cylindrical pattern, at which point, different ions are grouped into packets determined by their mass and charge. The *m/z* is detected by measuring the charge differential when the ion packets move close to a detection plate. These data are then converted to mass spectra by de-convolution by Fourier transform (Figure 1.18) (Buchanan and Hettich, 1993).

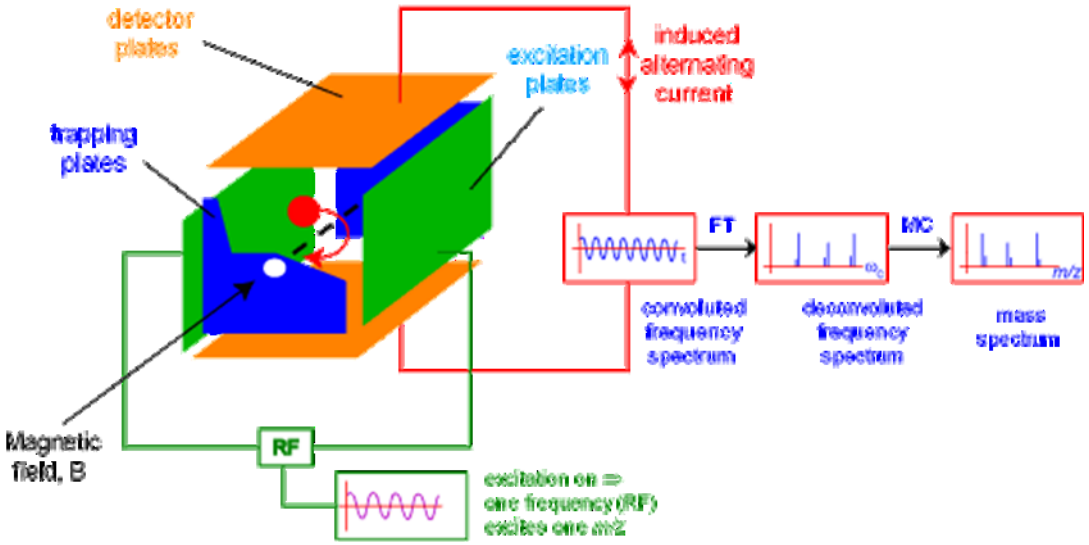

Figure 1.18. Fourier transform ion cyclotron resonance

Diagram showing the basic function of an ion cyclotron chamber. The trapping plates (blue) prevent the ions from leaving the chamber, the excitation plates (green) force the ions to move around the magnetic field and the detector plates (orange) record the information about the ion. The information is then deconvoluted by Fourier transform (FT) and mass calibrated (MC) to generate mass spectra. (Image taken from http://www.chm.bris.ac.uk/ms/images/fticr-schematic.gif).

Orbitrap mass spectrometers work in a similar way to FTICR in that the ions are trapped in a barrel shaped electrode with a spindle electrode in the centre around which the ions 'orbit'. This orbit is a balance between the ion's attraction to the central spindle electrode and the centrifugal force pushing it away. As well as moving around the central spindle, the ions also move back and forward along it in bands. The frequency of the bands' oscillation is used to determine the *m/z* (Figure 1.19.) (Makarov, 2000).

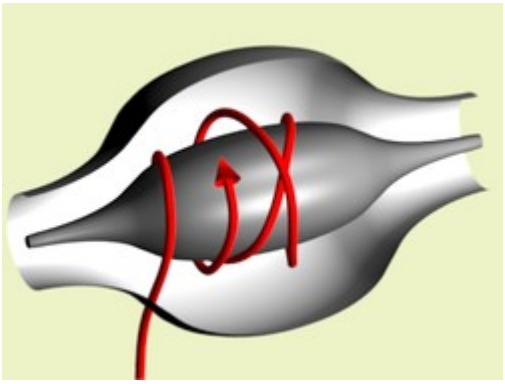

Figure 1.19. Orbitrap mass spectromter

Image depicting an orbitrap, with red arrow showing an example of the movement of ions around the spindle electrode. (Taken from http://en.wikipedia.org/wiki/File:Orbitrappe.png and used under creative commons).

Both FTICR and Orbitrap benefit from having higher resolution which provides significant improvements in mass accuracy.

2) Time of flight mass spectrometry

Time of flight (Tof) mass spectrometry measures the *m/z* of ions by passing them into a vacuum tube along which they travel at a speed which is determined by their mass and charge, until they reach the detector, which measures the electrical change caused by the ion. The time between the ion being passed into the Tof chamber and it reaching the detector is the time of flight of the ion. A Tof attached to a MALDI source (see section 1.6.2) is shown in Figure 1.20. The sample is ionised and enters the gas phase where it travels along a vacuum tube and is reflected by a series of electrostatic mirrors, known as a reflectron and then into the detector. The reflectron compensates for ions of the same mass travelling at different velocities, by slowing their velocity proportionate to their mass and charge, ergo smaller *m/z* particles will enter and leave the reflectron

more quickly than larger ones (Aebersold and Mann, 2003). Reflectrons also increase the Tof distance due to the ion travelling the distance to the reflectron and then back to the detector, thus increasing the resolution.

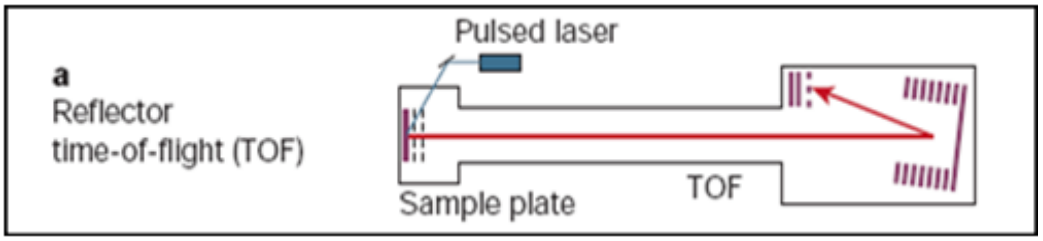

Figure 1.20. Time of flight mass spectrometry

Diagram illustrating a Tof analyser with reflectron mirror. Reprinted by permission from Macmillan Publishers Ltd: Nature (Aebersold and Mann, 2003) , copyright 2003.

1.6.5 Tandem mass spectrometry

Tandem mass spectrometry (MS/MS) uses fragmentation of peptides within the mass spectrometer to facilitate the elucidation of peptide sequence. During transit through the mass spectrometer, peptides can undergo collisionally induced dissociation (CID), via bombardment with high energy atoms of an inert gas, such as Ar or N_2, which partially degrades the peptide into smaller fragments, or product ions. These are subsequently measured in mass analyser. For CID to occur effectively, a peptide should carry a charge state of at least +2. Additional fragmentation methods used are electron transfer dissociation (ETD), which utilises free radical anions to fragment ions typically with charge states greater than +3. This softer fragmentation method is ideal for studying post translation modifications such as phosphate groups, which can be cleaved off in higher energy collision methods. One other fragmentation method used is higher energy collisional dissociation (HCD), which uses immonium ions to fragment peptides and is particularly good at analysing post-translationally modified peptides (Olsen et al., 2007).

Tandem mass spectra can be used to determine the sequence of peptides by interpolation of peptide product ion spectra generated from fragmentation of a peptide ion. Assuming that the peptides will be fragmented at each amide bond, all combinations of fragments from the full length peptide to single amino acid residues can be observed and used to deduce the peptide sequence. Dependent on which enzyme is used to digest the protein prior to analysis, the first and last residue can be predicted

and identified by their *m/z* value. The remaining sequence can be determined by measuring the difference in *m/z* between the K/R origin peak and the next peak detected which corresponds to the additional mass of a known residue *m/z* (Figure 1.21.).

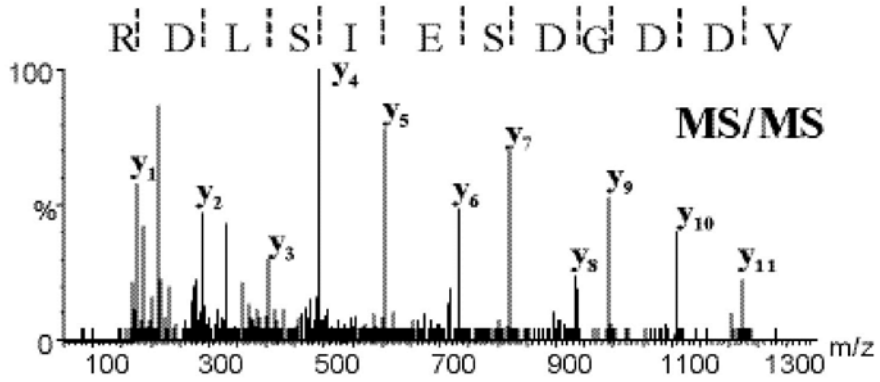

Figure 1.21. Tandem mass spectrometry fragment ions
A fragmentation spectra of a peptide, showing the labelled y-ions corresponding to their amino acid residues. Taken from (Elortza et al., 2003).

1.6.5.1 Data dependent acquisition (DDA)

DDA is a mode of acquisition that can be used to determine the partial or complete sequences of peptides by analysing peptides of high intensity in a sample (hence data dependent) by *m/z* in a sample during an initial MS pass. This is known as a precursor ion or survey scan. The quadrupole is then used to select only these top ions for fragmentation in the collision cell. This method can also be configured to analyse an inclusion list of anticipated precursor masses for selected precursor ions and/or specific retention times which fulfil certain criteria. For example, the DDA parameters can be set to only include ions with a charge state of +2 or above, which improves the signal to noise ratio by excluding singly charged which often represent noise in peptide analysis. Since DDA selects only the high intensity ions, many modified peptides would not be included; hence data independent analysis is preferred.

1.6.5.2 Data independent analysis and MS^E

Data independent analysis can be performed on mass spectrometers with quadrupoles and involves the continual fragmentation of all precursor ions by alternating between low and high energy in the collision cells. This results in a large array of multiplexed MS/MS which is reconciled by using the elution profile of the precursor ions to match them up to their associated fragments (Silva et al., 2005). The primary advantage of

MS^E analysis is that the majority of ions in the sample can be analysed at once, enabling low-level ions such as haptenated peptides to be detected.

1.6.6 Analysis of MS data

Before raw mass spectrometry data can be analysed, it must first be converted into peak lists of differently charged ions in isotope clusters matched to LC retention times which can subsequently be interrogated using a search algorithm. After the generation of spectral peak lists, the data can be searched for ions which correspond to peptides of known mass and sequence and subsequently used to identify the protein or proteins within the sample. Some software packages which exist for the searching of MS data include MASCOT (Perkins et al., 1999), PepIDENT (Gras et al., 1999), ProFound (Zhang and Chait, 2000), X!Tandem (Craig and Beavis, 2004), SEQUEST (Eng et al., 2004) and Andromeda (Cox et al., 2011). However, ProteinLynx Global Server (PLGS) must be used to process data and produce peak lists from MS^E analysis, so if this method is used, PLGS is the only option.

PLGS is a software package developed by Waters MS Technology (Manchester, UK) who also developed the MS^E mass spectrometry technique. The software allows the creation of peak lists from MS^E data as well as subsequent database searching from the peak list. Because MS^E generates fragmentation data continuously during analysis, the fragment ions need to be correlated with their parent ions before the sequences can be determined. This is accomplished using an algorithm which determines the accurate mass retention time (AMRT) of ions (Silva et al., 2005). This works by deriving a monoisotopic mass and charge from detected ions and compiling these detections into a peak list. Once these lists have been generated, the data can be searched against a protein database specified by the user. This process uses the *m/z* of precursor ion and their corresponding fragment ions to determine the sequence of each precursor peptide and then match this against predicted ions corresponding to peptides generated by the proteolysis method used within the specified protein database. Common modifications to peptides such as oxidation of methionine, carbamidomethylation of cysteine and deamidation of glutamine can be incorporated into the search algorithms. This compensates for peptide modifications caused by common side-reactions during sample preparation, but also takes into account intentional modification such as iodoacetamide derivatisation. This function is also essential when searching for protein adducts, such as that conferred by DNCB modification.

One problem with matching peptides to a large database of proteins is the possibility that a certain number will always match by chance alone. In order to provide a measure of this error, peptides can also be searched against a decoy database, which often uses scrambled, random or reversed sequences in order to show how many of the peptides are identified by random chance. This 'false discovery rate' (FDR) can be incorporated into database searches to exclude some peptides which appear to match too readily with decoy sequences, improving confidence in the positive identifications resulting from the analysis. Once has been completed, the database search will result in a list of proteins from the specified database which were detected in the sample, including details of any user-specified modifications to the peptide. For each protein, the peptides detected as part of that protein, as well as the relevant ion information (e.g. LC retention time, *m/z*, peptide score) will be listed.

1.7 Aims and objectives

We know that in order to sensitize an individual, any chemical must be able to penetrate into the skin to modify proteins and generate immunogenic hapten-protein complexes which stimulate T-cells of the immune system. To develop effective *in vitro* alternatives to animal testing, it is necessary to understand the responsible mechanisms in detail. The full process of sensitization is currently poorly understood, despite a great deal of research examining a variety of its aspects. The purpose of this project is to investigate the roles of protein modification in the process of ACD using the model sensitizer DNCB. To achieve this, the study needs to:

1 – Compare DNCB modification of proteins between a keratinocyte-derived cell line (HaCaT) and *ex vivo* human skin.

Protein modification will be visualised using anti-DNP antibodies to detect protein adducts in cultured cells and human skin explants.

2 – Determine the relative immunoreactivity of cell line proteins modified with the model sensitizer, DNCB.

This can be accomplished using protein lysates from cells which have been treated with DNCB to stimulate T-cell proliferation in the peripheral blood mononucleocytes of individuals sensitized to DNCB.

3 – Investigate the dynamics of covalent protein modification by DNCB using a model protein, human serum albumin.

This will be achieved through mass spectrometric analysis of dinitrophenyl modifications conferred to human serum albumin which has been incubated with DNCB at different doses and times.

4 – Explore a link between hapten lability and immunoreactivity

Using synthetic peptides, the difference between DNP-Cysteine and DNP-Lysine will be explored using DNP-specific lymphocyte proliferation, western blot analysis of monocytes after processing the peptides and mass spectrometric analysis of the removal of DNP groups by a process called thiolysis.

2 MATERIALS AND METHODS

2.1 Cell culture

All cell culture products were supplied by Life Technologies, unless otherwise specified.

The immortal human keratinocyte line, HaCaT cells, at passage 40 (CLS, Eppelheim, Germany) were cultured in Dulbecco's modified Eagle medium (DMEM) with 25 mM glucose, 1 mM sodium pyruvate, 40 μM phenol red and 4 mM l-glutamine with 1% added penicillin and streptomycin (Sigma) and 10% added foetal calf serum gold (PAA). HaCaT cultures were observed until 70-80% confluent and then passaged by discarding medium and washing adherent cells twice with phosphate buffered saline (PBS) and incubating for 10 minutes with 0.05% EDTA / trypsin (Sigma Aldrich). After 10 minutes, the reaction was stopped using an equal volume of culture medium and the detached cells were centrifuged at 340 x g for 5 minutes. The pellet was re-suspended in culture medium and split between new culture flasks.

Cells were banked by pelleting as per passaging steps and re-suspending the pellet in culture medium, foetal calf serum and dimethyl sulphoxide (DMSO, Sigma) in a 7:2:1 ratio respectively and freezing at -80 in a Nalgene freezing container (Sigma) with isopropyl alcohol, prior to storage in liquid nitrogen.

2.2 Treatment of HaCaT and primary keratinocyte cells with DNCB & [^{14}C]-DNCB

10 mM 1-chloro-2,4-dinitrobenzene (DNCB, Sigma) was prepared by dissolving 2.025 mg in 1 ml of DMSO (Sigma). 10 mM [^{14}C]-DNCB was made by diluting a 100 mM stock solution of [^{14}C]-DNCB in ethanol 1 in 10 into ethanol. HaCaT cells were cultured in 20 ml of DMEM to which the DNCB or [^{14}C]-DNCB in ethanol was added to the required concentrations. Primary keratinocytes were treated in 20 ml of serum-free medium and were treated with ordinary DNCB.

2.3 Culture of primary keratinocytes

Primary epidermal keratinocytes (HPEK, CellNTech) were cultured in serum-free medium with 1% added penicillin and streptomycin (Sigma). Primary cells were not passaged. DNCB-treated cells were removed by discarding medium, washing twice with sterile PBS and then incubating for 15-25 minutes with enzyme-free cell

dissociation buffer (Gibco), after which cells were centrifuged at 340 x g for 5 minutes and free DNCB was removed by washing the pellet 3 times using re-suspension with sterile PBS followed by centrifugation. The washed pellet was then lysed (see section 2.10).

2.4 Preparation and treatment of human skin

Skin samples from donors undergoing mastectomy at the Princess Anne hospital, Southampton were supplied in PBS. Samples were deemed suitable if they had an uninterrupted surface area large enough to accommodate one or more experiments plus control. Samples were cleaned using PBS and the subcutaneous fat removed before being cut into approximately 1 cm^2 pieces and placed one piece per well of a 6 well plate on 1ml RPMI + 10% FCS. Each 1 cm^2 section of skin was treated by using petroleum jelly to attach a 6 mm silicon rubber O-ring (RS components), into which 50 µl of DNCB in acetone or [^{14}C]-DNCB in ethanol could be placed. After treatment, a 6 mm biopsy punch (Medisave) was used to remove the skin from inside the O-rings and the excised sample was immediately frozen by placing into a 7 ml bijou tube then immersed in liquid nitrogen.

2.5 Sectioning and fixation of *ex vivo* human skin

Biopsy-punched skin samples were set into an optimal cutting temperature (OCT) compound (Tissue-Tek) and sectioned to a thickness of roughly 10 µm using a cryostat (Leica Cryostat CM1850, Milton Keynes, UK) kept at -25°C and transferred onto poly-L-lysine treated microscope slides provided by the University of Southampton School of Medicine Biological Imaging Unit. The slides were allowed to equilibrate at room temperature overnight in a sealed container with silica dessicant and then fixed by submersion in ice cold acetone for 10 minutes.

2.6 Separation of epidermis from *ex vivo* human skin and lysis of epidermal cells

Biopsy-punched skin samples were washed 3 times with PBS and incubated individually with 5 ml of warm 20 mM EDTA at 37° C for 3 hours, with the EDTA replaced once per hour. The EDTA was then discarded and the epidermis separated from the rest of the skin with forceps and placed into 0.1 M TEAB + 0.1% SDS.

Non-radioactive epidermis was lysed using a FastPrep savant, in tubes containing 1.4 mm ceramic spheres.

Epidermis treated with [^{14}C]-DNCB was lysed by cutting the epidermis into approximately 1 mm^2 pieces with a scalpel and then ground in a tissue homogeniser (Fisher) in 200 µl of 0.1 mM TEAB + 0.1% SDS.

2.7 Culture of HaCaTs on microscope slides and fixation of adherent cells

HaCaT cells were pipetted into each well of two 8-well slides (Camlab) at a concentration of 1 x 10^6 cells per ml of DMEM medium and left overnight to adhere and multiply to approximately 60% confluency (confirmed by phase microscopy). Each well was then treated serially 1 µM increments from 0 to 11 µM DNCB in DMSO with a final concentration of 0 to 0.11% DMSO respectively and incubated at 37°C. After 3 hours, the medium was discarded and the well frame removed. The cells were washed with PBS and then incubated in 4% paraformaldehyde for 10 minutes at room temperature before being quenched with 10 mM ammonium chloride and washed with PBS.

2.8 Immunofluorescence detection of dinitrophenyl epitopes, dendritic cells and nuclei in sections of human skin and HaCaT cells

Fixed skin and HaCaT cells were pre-treated with blocking buffer (PBS containing 10% foetal calf serum and 1% bovine serum albumin) for 1 hour, washed 3 times with PBS and then dried at 37 °C for 10 minutes. Goat polyclonal anti-dinitrophenyl antibodies (Sigma) were diluted 1 in 600 into blocking buffer and applied to skin and HaCaT cells for 1 hour, washed 3 times with PBS and oven dried at 37 °C for 10 minutes. Mouse anti-goat antibodies conjugated to fluorescein isothiocyanate (FITC, Sigma) were diluted 1 in 350 into blocking buffer and applied to skin & HaCaTs for 1 hour, washed 3 times with PBS and oven dried at 37 °C for 10 minutes.

Langerhans cells were visualised using monoclonal mouse anti-Langerin (Beckman Coulter) antibodies at a 1 in 100 dilution, secondary detection was with donkey anti-mouse alexafluor546 (Life Technologies) used at a 1 in 500 dilution. Dermal dendritic cells were stained using polyclonal rabbit anti-FXIIIa (Abcam) at a 1 in 25 dilution, secondary detection was with donkey anti-rabbit alexafluor546 (Life Technologies) at 1 in 500. All staining and wash steps were carried out as detailed above.

The nuclear stain, To-Pro-3 (Life Technologies), was diluted to 1 in 1000 in PBS and applied to skin and HaCaTs for 10 minutes, washed 3 times with PBS and oven dried at 37 °C for 10 minutes. Vectashield (Vector Labs) was then added to cover each sample and covered with a glass coverslip which was then sealed with clear nail varnish and left at 4 °C with desiccant until needed.

2.9 Fluorescent and laser confocal microscope analysis of immune-stained human skin and HaCaT cells

Fluorescent microscope images were acquired using a Zeiss Axioskop 2-MOT with Zeiss Axiocam camera. Sections were imaged at 200 x magnification with each channel (488 nm filter for FITC, 548 nm for To-Pro-3) and images were captured using the software optimised to show minimal signal intensity for vehicle treated skin (cells were only analysed using confocal microscopy) then overlaid using GNU Image Manipulation Program (GIMP). The gain and contrast in GIMP was normalised for vehicle treated skin and the settings were applied equally to all images.

Laser confocal microscope images were taken using a Leica TCS-SP5. Sections were imaged at 200 x magnification from two channels optimised for FITC and To-Pro-3 with the outputs set to green and blue respectively. Z-plane images were taken at 1 µm intervals at 1024 x 1024 resolution. The gain and offset values for the laser in each channel were optimised to show minimal signal in vehicle-treated samples in HaCaTs. These settings were then used for all skin and HaCaT samples. Images taken were converted to maximum projections of the z-planes before analysis. Each sample was imaged at 3 locations where skin or cell morphology was considered typical of the sample.

2.10 Cell lysis and protein extraction for SDS-PAGE

Vehicle and DNCB-treated HaCaT cells and primary keratinocytes were lysed by adding 300-500 µl of 100 mM triethyl ammonium bicarbonate (TEAB) + 0.1% sodium dodecyl sulphate (SDS) + protease inhibitor cocktail (Roche) to a centrifuged cell pellet and mixed by pipetting up and down 5-10 times. DNA was sheared by probe sonication followed by passing the lysate through an insulin syringe repeatedly until viscosity was no longer apparent. The lysate was then centrifuged at 15,000 x g for 15 minutes and the supernatant was removed and stored at -20°C until needed.

2.11 Determination of protein concentration by bicinchoninic acid (BCA) assay

A BCA protein assay kit (Sigma) was used as per the manufacturer's instructions. Protein standards were prepared by dissolving 1 mg of human serum albumin in 1 ml of the cell lysis buffer used and then a serial dilution from 0.1 – 1.0 mg/ml was prepared. Cell lysates were used undiluted and as a 1:5 dilution. Standards and cell lysates were mixed 1:10 with BCA + copper II sulphate and incubated for 30 minutes at 37°C then the absorbance was read at 562 nm and the concentration of protein in the lysates was determined by plotting against the standards.

2.12 SDS-PAGE separation of proteins from lysates of cell lines and epidermis from *ex vivo* skin

Protein lysates were mixed 3:1 with 4 x Laemmli buffer (glycerol, SDS, bromophenol blue – dithiothreitol was added unless otherwise indicated in chapter experimental setup section) in a 3:1 ratio and roughly 20 μg run using 4-12% Bis-Tris pre-cast gels (Life Technologies) in an XCell electrophoresis tank (Life Technologies) at 200 volts for approximately 50 minutes or until the dye front had reached the end of the gel. Gels were then fixed and stained using Coomassie blue solution (40% methanol, 10% glacial acetic acid and Coomassie blue added until solution is deep blue without being opaque), then de-stained using 40% methanol, 10% glacial acetic acid.

2.13 Detection of dinitrophenyl adducts using western blot

All western blot equipment and reagents were supplied by Life Technologies unless otherwise indicated. Proteins were transferred from SDS-PAGE gels to PVDF membranes using the iBlot system by running gels against PVDF membrane cartridges using a standard western transfer program for 7 minutes. Each membrane was first washed in 8ml methanol followed by three to five washes of de-ionised water and then incubated at room temperature in a WesternDot staining dish with 8 ml of WesternDot blocking buffer for 1 hour. Polyclonal rabbit anti-dinitrophenyl antibodies were diluted to 1 in 5,000 in wash buffer (tris-buffered saline, 0.5% tween). The blocking buffer was discarded and 8 ml of the primary antibody solution was added to each membrane and incubated at room temperature overnight and then discarded. Each membrane was then washed 3 times for 5 minutes with 15 ml of wash buffer. Biotin-XX-goat anti-rabbit antibodies were then diluted 1 in 2,000 with wash buffer and 8 ml was added to each

membrane and incubated at room temperature for 1 hour and then the antibody solution was discarded and the membrane washed 3 times for 15 minutes with wash buffer at room temperature. IRDye800 streptavidin conjugate (LiCor) was diluted to 1 in 4,000 with blocking buffer and 8 ml was incubated with each membrane at room temperature for 1 hour before being discarded. Each membrane was then washed 3 times with 15 ml of wash buffer and once with 20 ml of de-ionised water before being dried. Each membrane was imaged using an Odyssey imaging system (LiCor) using ultraviolet light. Membrane images were acquired at exposures of 0.5, 1.0, 1.5 and 2.0 transformed using Odyssey software (LiCor) to give distinct bands.

2.14 Densitometry analysis of anti-dinitrophenyl western blots: qualitative comparison of human skin with HaCaTs

Western blot images were analysed in ImageJ (National Institutes of Health) in the gel mode. Images were converted to greyscale and inverted to give a black background with white bands. A line was drawn from the top-most visible protein ladder band to the bottom-most visible protein ladder band and moved across the image until it rested on each lane, where histogram values were taken as a measure of pixel intensity along the line. The values were tabulated and plotted as intensity values on the Y axis against percentage distance down the lane on the X axis. The values for dinitrophenyl HaCaT lysates were then overlaid with the values for dinitrophenyl epidermal lysates and the protein ladder for qualitative comparison.

2.15 Detection of dinitrophenyl adducts using autoradiography

After protein staining and de-staining, gels containing radio-labelled dinitrophenyl HaCaT proteins were incubated at room temperature with 20 ml of Amersham Amplify fluorographic reagent (GE Healthcare) for 30 minutes on a rotary shaker and then washed 3 times with de-ionised water. Gels were then dried overnight in cellulose using a DryEase mini-gel drying frame and gel drying solution (Life Technologies) before being sealed in an autorad cassette with radiographic film (Kodak) and then incubated at -80°C for 8 weeks. Film was developed in a dark room by submerging film in developing fluid until the film became translucent, with gel band images visible as black bands, then washed in water and submerged in fixing solution for 5 minutes, washed in water and then air dried at room temperature for approximately 30 minutes.

2.16 Preparation of cell lysates for addition to lymphocyte assays

Method 1: HaCaT cells and primary keratinocytes were treated with DNCB in culture, extracted and pelleted as detailed in sections 2.1, 2.2 & 2.3. A proteaprep anionic cell lysis kit (Protea) was used with or without protease inhibitor cocktail (Roche) as denoted in results chapters. Lysis buffer was added to the washed cell pellet and sonicated on ice for 3 x 20 seconds before being centrifuged at 15,000 x g for 15 minutes and the supernatant retained. Acid-labile surfactant in the lysis buffer was degraded by the drop-wise addition of 10% trifluoroacetic acid until the pH was between 2-3 and then incubated at room temperature for 20 minutes.

Method 2: The washed cell pellet was re-suspended in 200 µl of 100 mM TEAB and transferred to a lysing matrix D centrifuge tube containing 1.2 mm ceramic beads (MP Biomedicals). 200 µl of 100 mM TEAB + 0.1% SDS was added, giving 0.05% SDS. The cells were disrupted using a Savant FastPrep (MP Biomedicals) 3 times at full speed for 20 seconds, with the sample cooled for 2 minutes on ice between cycles. Lysates were collected from the ceramic beads by vortexing briefly and centrifuging at 15,000 x g for 2 minutes, then removed with a pipette. Cell debris was removed by centrifugation at 15,000 x g for 10 minutes, after which the supernatant was assayed for protein content. SDS was removed from the sample by incubating for 5 minutes at room temperature in a detergent removal spin column (Pierce) after which the sample was collected by centrifugation at 1,500 x g for 2 minutes.

2.17 Isoelectric focussing fractionation of HaCaT proteins

All reagents used were supplied by Sigma unless otherwise stated. A stock solution of non-reducing fractionation buffer was prepared to 1.25x concentration by mixing 25.2 g urea, 9.1 g thiourea, 3 ml glycerol, 600 µl ph 3-10 non-linear immobilised pH gradient (IPG) buffer (GE Healthcare) with dH_2O up to 50 ml. For IPG gel rehydration, 2.24 ml of 1.25x stock solution was added to 0.56 ml of dH_2O. The protein sample was prepared by adding 1.44 ml of 2 mg/ml DNCB-treated HaCaT lysate was added to 5.76 ml of 1.25x stock fractionation buffer. A 3100 OFFGEL fractionation system (Agilent) was used with 4 pH 3-10 13cm gel strips (GE Healthcare) separated into 12 wells using a frame. Re-hydration solution was added to each well and left for 15 minutes to allow the gel to swell. 140 µl of protein sample was pipetted into each of the 12 wells and the wells were sealed. Electrode pads wetted with rehydration solution were placed at

either end of the gel next to the 12-well chamber. Mineral oil was then pipetted into each lane of the OFFGEL system containing a gel to a depth of half of the lane. Fractions were run using the setting OG12PRO0 (20 kVh, 8000 V, 20 µA, 50 mW). At the end of the run, fractions were removed from each well, pooled and dialysed against 4 changes of 2L of 50 mM ammonium bicarbonate at 4 °C for 12 hours per buffer change. Dialysed fractions were stored at -20 °C until use.

2.18 Isolation of PBMCs from human blood

Ten ml of venous blood was acquired by venupuncture from healthy volunteers into vacutainers containing heparin and layered on top of an equal volume of lymphoprep density gradient (Lymphoprep, Axis Shield) and centrifuged at 1,200 x g for 20 minutes with minimum acceleration and deceleration settings. The 'buffy-coat' layer of PBMCs was transferred into a 50 ml Falcon tube and made up to full volume with ice cold PBS and centrifuged at 300 x g for 5 minutes. The supernatant was discarded and the pellet re-suspended in ice cold PBS and made up to 50ml and centrifuged at 1,000 rpm for 5 minutes. After the supernatant was discarded, the pellet was re-suspended in RPMI + 5% human serum.

2.19 Lymphocyte proliferation assays (LPA)

Isolated PBMCs (see section 2.18) in medium were diluted to a concentration of $2x10^6$ per ml and transferred to 48-well plates (Nunclon) at 500 µl per well. Experiments were performed in triplicate. Baseline proliferation was measured from wells with no treatments added. Generic cell activity was monitored by adding phytohaemagglutinin (PHA). DNCB-specific response was measured by adding 3 µM DNCB. Response to HaCaT lysates was measured by adding 10 µg of lysate from 30 µM DNCB-treated HaCaTs, with vehicle treated HaCaT lysate used as a control. PBMCs were cultured with treatments at 37° C for 6 days before being incubated with tritiated thymidine for 6 hours and frozen at -20° C. Frozen cells were defrosted and transferred to a 96-well filter plate (Millipore) using a cell harvester (Perkin Elmer) and dried. 40 µl of scintillation fluid (Perkin Elmer) was then added to the wells containing cells and sealed before being read on a TopCount scintillation counter (Perkin Elmer).

2.20 Precipitation, non-reducing enzymatic digestion and peptide de-salting of protein lysates and fractions

Proteins and fractions were digested by making 50 µg of protein up to 100 µl with dH_2O. With vortex mixing after the addition of each, the following was added in steps: 400 µl of methanol, 100 µl of formaldehyde. Then 400 µl of dH_2O was added to precipitate protein. The solution was vortexed and then centrifuged at 13,000 x g for 1 minute. The aqueous layer was removed without disturbing the protein disc, then 400 µl of methanol was added and the sample briefly vortexed and centrifuged at 15,000 x g for 2 minutes. The methanol was removed and the tubes allow to air dry. Dried samples were re-constituted in 100 µl of pH 7.5 6M urea, 2M thiourea and 10 mM HEPES and incubated for 60 minutes at 60 °C, after which, 5 µM iodoacetamide (IAA) was added and the sample was incubated in the dark for 45 minutes. Endoproteinase Lys-C (Promega) was added at a ratio of 50:1 protein:enzyme and incubated at 37 °C for 4 hours, after which, 400 µl of 20 mM ammonium bicarbonate (pH 8.0) was added to dilute the urea to reduce interference with trypsin digestion. Modified trypsin (Promega) was added to the same 50:1 ratio as Lys-C and incubated overnight at 37 °C. Digested peptides were separated from undigested proteins and large peptides by centrifugation 3 times through 10 kDa molecular weight cut-off filter columns with 10% acetonitrile at 15,000 x g. The filtrate was then lyophilised to dryness using a concentrator plus (Eppendorf).

2.21 De-salting of peptides

All reagents were supplied by Protea unless otherwise specified. All centrifugation steps were performed at 2,000 x g. Lyophilised samples were re-suspended in 100 µl of spin tip reconstitution and wash buffer and mixed by vortex for 20 minutes. Functionalised C18 silica spin tips were centrifuged twice for 3 minutes with 50 µl of spin tip equilibration solution, then twice for 4 minutes with 100 µl of spin tip reconstitution and wash solution. The samples were then loaded into tips and centrifuged for 3 minutes. Salts and other contaminants were then removed by centrifugation 4 times for 4 minutes and once for 5 minutes with 150 µl of spin tip reconstitution and wash buffer. Peptides were eluted from the tips into fresh tubes using 2 washes with 50 µl of spin tip elution buffer, for 4 minutes and once for 5 minutes. Peptides were then lyophilised *in vacuo* at 30° C and stored at -20° C until needed.

2.22 MS^E analysis of peptides from HaCaT lysates and fractions

Lyophilised, de-salted peptides were re-constituted in 2% acetonitrile + 0.1% formic acid and 500-1000 ng was loaded onto a reverse phase trap column (Symmetry C18, 5 µm, 180 µm x 20mm, Waters) , at a trapping rate of 5 µL/min and washed for 10 minutes with buffer A prior to the analytical nano-LC separation using a C18 Reverse phase column (HSS T3, 1.8 µm, 200mm x 75µm, Waters). The eluted peptides were fractionated over a 90 minute continuous gradient from 1% acetonitrile + 0.1% formic acid up to 60 % acetonitrile + 0.1% formic acid, at a flow rate of 300 nL/min. Eluted samples were sprayed directly into a Synapt G2-S mass spectrometer (Waters) operating in MSe mode. Data was acquired from 50 to 2000 m/z using alternate low and high collision energy (CE) scans. Low CE was 5V and elevated collision energy ramp from 15 to 40V. Ion mobility was implemented prior to fragmentation using a wave height of 650 m/s and wave velocity of 40V. The lock mass Glu-fibrinopeptide, (M+2H)+2, m/z = 785.8426) was infused at a concentration of 100 fmol/µl with a flow rate of 250 nl/min and acquired every 60 seconds.

2.23 Incubation of human serum albumin with DNCB

Human serum albumin (Sigma) was made to 1 mg/ml in PBS and incubated at 37 °C with either 1500, 750, 150, 15 or 7.5 µM DNCB or deuterated DNCB in DMSO with non-treated controls, with the final concentration of DMSO not being more than 1%. At 1, 6, 24 and 192 hours (8 days), the reaction was stopped by mixing equal volumes of deuterated and non-deuterated samples 3 to 1 with SDS-PAGE sample buffer (Life Technologies) and heated for 10 minutes at 70 °C. Free DNCB and buffer salts were removed by running the samples on SDS-PAGE for 50 minutes.

2.24 In-gel protein digestion

Gels from the previous method were stained using Coomassie blue and then de-stained and the large band containing the modified or control HSA was excised as three equal-sized parts which were each placed into separate wells in 150 µl de-ionized water in a 96-well plate. Each part was then cut into approximately 1 mm^2 pieces using forceps. Digestion was carried out using an automated MassPREP™ robotic handling system (Waters, UK). Each of the following steps was performed at 40 °C and the supernatant removed and discarded unless otherwise indicated. Coomassie blue stain was removed using 50 µl of 100 mM NH_4CO_3 (Sigma) and 50 µl of acetonitrile (Fluka) per well and

incubated for 10 minutes. Gel pieces were then dehydrated by addition of 50 µl of acetonitrile and incubated for 5 minutes. Reduction of protein was performed by the addition of 50 µl per well of 10 mM dithiothreitol (DTT, Sigma) in 100 mM NH_4CO_3 and the gel pieces were incubated for 30 minutes. Free cysteines were alkylated by the addition of 50 µl of 55 mM iodoacetamide (Sigma) in 100 mM NH_4CO_3 incubated for 20 minutes. A wash of 50 µl of 100 mM NH_4CO_3 was added and incubated for 10 minutes. 50 µl of acetonitrile was then added and incubated for 5 minutes. 50 µl of acetonitrile was added to each well and incubated for 5 minutes before being removed. A further 50 µl of acetonitrile was added and left to evaporate for 15 minutes. 25 µl of 6 ng/µl sequencing grade porcine tryspin (Promega) in 100 mM NH_4CO_3 was added to each well and incubated for 15 minutes at 37°C. 10 µl of 100 mM NH_4CO_3 was added and gel pieces were incubated for 5 hours at 37°C. Peptides were extracted by adding 30 µl of extraction buffer (2% acetonitrile (v/v) + 1% formic acid (v/v)) to each well, incubating for 30 minutes at 37°C and 15 µl into a clean 200 µl 96 well microtitre plate. This extraction step was performed three times.

2.25 Nano-LC-MS^E data analysis of DNP-HSA

After digestion 10 µl of each sample in extraction buffer was run on a 30 minute linear gradient from 1% acetonitrile + 0.1% formic acid increasing to 50% acetonitrile + 0.1% formic acid and then to 85% to wash the LC column using a nanoAcquity UPLC system (Waters) online to the ESI ionization source of a Q-TOF Global Ultima (Waters). The mass spectrometer was configured to switch between low and high collision cell energy every second, with the quadrupole held in RF mode, allowing all ions to pass through. Glu-1-fibrinopeptide B was used as a lock mass standard. MS^E data was processed using Protein Lynx Global Server 2.4 (PLGS, Waters). The processing parameters used to create peak lists were set to detect automatically, with the exception of the intensity thresholds, which were set to 100 counts for low energy ions, 25 counts to high energy ions and 1000 counts for precursor ions. The workflow parameters used for identification of peptides were run on a human serum albumin SWISSPROT database with peptide and fragment tolerances set at 250 and 150 counts respectively. The minimum fragment ion matchers per peptide and protein were set at 3 and 7 respectively and the minimum peptide matches per protein was set at 1. The primary digest reagent was trypsin, with 2 missed cleavages allowed for. Variable modifications searched for were: carbamidomethyl cysteine, oxidated methionine, dinitrophenyl side-chain

modification of cysteine, histidine, lysine or tyrosine and dinitrophenyl modification of the N-terminus. The false discovery rate was set to 2%.

The full ion accounting file for each sample was filtered by records reporting a DNP modification, with in source fragments filtered out. All modified peptides identified as being present in the non-treated control were omitted. Each identified modification was verified by comparing each sample's base peak intensity chromatogram for each precursor mass against control and also comparing the MS at the relevant retention time to confirm absence in the control, as well as an isotope doublet to account for the deuterated modification.

2.26 Isolation and culture of human monocytes from peripheral blood mononuclear cells

After the isolation of PBMCs described in section 2.18, cells were incubated for 2 hours at 37 °C to allow monocytes to adhere to the surface of the culture wells. Other cells and the culture medium were then removed by gentle pipetting and fresh RPMI medium + 1% penicillin / streptomycin and 5% human AB serum (Life Technologies) was added for overnight culture.

2.27 Incubation of human monocytes with DNP-modified synthetic peptides in culture

Peptides with the sequences YLQQ**C**PFE and YLQQ**K**PFE, where the bold and underlined residues denote a DNP modification to the side-chain, were provided by Peptide Protein Research (Southampton, UK). Each peptide was incubated overnight at 8 µg/ml

2.28 Thiolysis of DNP groups from synthetic peptides using dithiothreitol

Reactions were performed in 100 µl using either Dulbecco's phosphate buffered saline at pH 7.4 or 50 mM sodium acetate plus 100 mM sodium chloride at pH 4.5. In each buffer, each of the two peptides detailed in chapter 2 section 2.27 were incubated at 5 µM concentrations with either no dithiothreitol (DTT) as a control or with DTT concentrations of 25 µM, 62.5 µM, 125 µM, 250 µM or 500 µM. Aliquots of 30 µl were removed at 1.5, 2.5 and 4.5 hours and the reaction was stopped by adding iodoacetamide (IAA) at a 5x molar excess of DTT and then increasing the pH to 8.0 by

addition of 0.1M sodium hydroxide. Microcon spin filters with 10 kDA molecular weight cut-off (Millipore) were washed three times with 400 µl of 10% acetonitrile (Fluka) for 25 minutes at 15,000 x g. Each sample was then washed through pre-washed filter column three times with 100 µl of 10% acetonitrile for 10 minutes at 15,000 x g. The filtrate was lyophilised *in vacuo* at 30° C and stored at -20° C until needed.

2.29 Mass spectrometric analysis of synthetic peptides

Peptides were de-salted and dried (see section 2.21) and then re-suspended in 30 µl of 1% acetonitrile + 0.1% formic acid and vortex mixed for 20 minutes. Peptides in solution were then run on a 20 minute linear gradient from 1% acetonitrile + 0.1% formic acid increasing to 50% acetonitrile + 0.1% formic acid and then to 85% to wash the LC column using a nanoAcquity UPLC system (Waters) online to the ESI ionization source of a Q-TOF Global Ultima (Waters). Glu-1-fibrinopeptide B was used as a lock mass standard. Thiolysed peptides were identified by a delta mass corresponding to the removal of a DNP group and replacement with a carbamidomethyl group, a net change of -108.9795 Da.

3 DETECTION OF COVALENT PROTEIN MODIFICATION IN HUMAN SKIN AND HACAT CELLS USING IMMUNOFLUORESCENCE AND IMMUNOBLOTTING

3.1 Introduction

To study the effects of a model sensitizer on human skin proteins, an assessment of the extent of covalent protein modification is required. Since the culturing of *ex vivo* skin, although possible, is less accessible, often representative systems are used (Boelsma et al., 1999; Deshmukh et al., 2012; Lehmann, 1997; van der Veen et al., 2013), this includes the use of cells lines (Lehmann, 1997) and organotypic models, such as reconstructed human epidermis (Elbayed et al., 2013). The use of immortalised keratinocytes requires analysis to determine if the proteins modified by chemical haptens are similar to those modified by the same chemical in human skin.

DNCB is classified as an extreme sensitizer and has an EC3 value of <0.1% (approx. 500 μM). The EC3 value refers to the w/v percentage of a chemical required to give a three-fold increase in T-cell proliferation after application to skin versus control in the murine local lymph node assay (LLNA) (Kimber and Weisenberger, 1989). DNCB is routinely used as a model chemical in contact allergy studies (Basketter et al., 2000; Dearman and Kimber, 1991) and reacts with specific nucleophilic amino acid side chains (Aleksic et al., 2009).

To restrict the extent of protein modifications to those which are clinically relevant, the dose used to treat *ex vivo* skin explants was determined from studies which sensitized humans to DNCB (White et al., 1986). Extrapolation from the data suggests that a dose of 50 $\mu g/cm^2$ DNCB is approximately the lowest which would be expected to sensitize 100% of healthy subjects and would hypothetically modify proteins in a way which is clinically relevant to the process of DNCB sensitization. However, it is not known exactly how much of the applied chemical reaches cells within the epidermis and thus it is necessary to examine cell viability data to determine the range of concentrations that can be applied to cell lines without inducing major toxicity. Research conducted with human monocytic cell lines indicate that DNCB effects are observed at concentrations equivalent to 9 μM in a 24 hour culture (Sakaguchi, Ashikaga et al, 2009). Furthermore, it may be possible to determine a range of doses in cells that show equivalent levels of

modification to that obtained in skin, by comparing the associated fluorophore intensity values corresponding to incorporation of DNP groups.

Detection of hapten-protein complexes (HPCs) has previously been performed in skin and cell lines by using polyclonal antibodies or antisera raised against a specific HPC using immunofluorescence, immunohistochemistry and western blots (Carr et al., 1984; Elahi et al., 2004; Pickard et al., 2009; Pickard et al., 2007). Immunofluorescence has also been used to determine the location of haptenation events in skin (Pickard et al., 2007; Simonsson et al., 2011). Radiolabelled sensitizers have been used to show the range of protein modification in cell lysates (Pickard et al., 2007).

This chapter investigates the effects of DNCB haptenation on epidermal keratinocytes by characterising the covalent modification of keratinocytes in *ex vivo* skin and the HaCaT cell line. This will be achieved using polyclonal antibody detection of dinitrophenyl groups on proteins in immunofluorescence and western blot experiments. The effectiveness of antibody detection of haptens will also be assessed using radiolabelled DNCB to verify western blot results.

3.2 Experimental design

Incubation of human skin and HaCaT cells with DNCB

To show the effects of both clinically relevant and excess doses of DNCB on *ex vivo* human skin, dosages were extrapolated from the literature (White et al., 1986). A dose of 50 μg/cm^2 was used at which 100% of people sensitize and 300 μg/cm^2 (a 6 fold increase) was used to demonstrate any effects caused by a dose of DNCB expected to cause significant epidermal cell death (Coquette et al., 1999). The DNCB was delivered to a defined area by attaching a 6mm silicone rubber ring to the skin's surface using petroleum jelly and applying DNCB dissolved in acetone inside the ring. Acetone was used to increase the penetration of DNCB into the epidermis (Heylings et al., 1996). Various incubation times were used to determine the rate of penetration, after which the skin within the silicone ring was removed from the surrounding skin using a biopsy punch (see chapter 2 section 2.4).

HaCaT cells were incubated either in chamber slides for immunofluorescence experiments or cell culture flasks for western blotting and autoradiography experiments (see chapter 2) and treated with DNCB dissolved in DMSO in culture medium to give the appropriate DNCB concentration while keeping the DMSO concentration below 0.2%. While acetone would have allowed for more direct comparison to the skin experiments, its toxicity precluded its use directly in media on cells. The concentrations of DNCB used were 1 μM increments from 1 to 11 μM for the immunofluorescence experiments and 4, 12 & 36 μM for the Western blot experiments.

Immunofluorescent analysis of DNP modifications in *ex vivo* human skin and HaCaT cells

Skin and adherent cells on slides were fixed and stained as described in chapter 2. Antibody concentrations were determined by titration of primary and secondary antibodies with sections of human skin treated with DNCB or vehicle in order to find a concentration which gave a specific positive signal for DNP adducts. The resulting antibody concentrations were also used to stain the HaCaT cells in chamber slides.

Fluorescent and confocal microscope analysis was optimized to minimise signal (auto-fluorescence) from the vehicle treated samples and maximise signal intensity from the

DNCB-treated samples. To determine the degree of variation in the experiments, 5 biological replicates were used for skin and 3 technical replicates were performed for each experiment. For both skin and cells, a technical replicate consisted of capturing microscope images from 3 areas of the slide or section. For each of these images, average FITC signal intensity was measured along 12 regions of interest. In total, each technical replicate consisted of 36 measurements.

Western blot analysis of DNP-modified epidermal and HaCaT cell proteins

Epidermis was isolated from DNCB and vehicle-treated *ex vivo* skin. HaCaT cells were treated with different DNCB doses or vehicle in culture flasks. Protein lysates were extracted, separated by SDS-PAGE and then transferred to PVDF membranes (see chapter 2 section 2.13). Rabbit polyclonal antibodies (Life Technologies, A-6430) were used to detect DNP modified proteins since the Sigma antibody used for the immunofluorescence (Sigma, D9781-2ML) did not give reproducible results in Western blot experiments (data not shown). Western blots were analysed by densitometry to determine how much overlap there was between the modification profiles of epidermal and HaCaT cell lysates. The extent of primary antibody recognition of DNP haptens was determined by general comparison to autoradiographs from control experiments using ^{14}C labelled DNCB.

3.3 Results

3.3.1 High dose DNCB effects in *ex vivo* skin

To determine the effects of excessive dosage, skin was treated with doses up to ~300 µg/cm^2 DNCB. The treated skin was sectioned and stained for DNP adducts and images captured by confocal microscopy (Figure 3.1.).

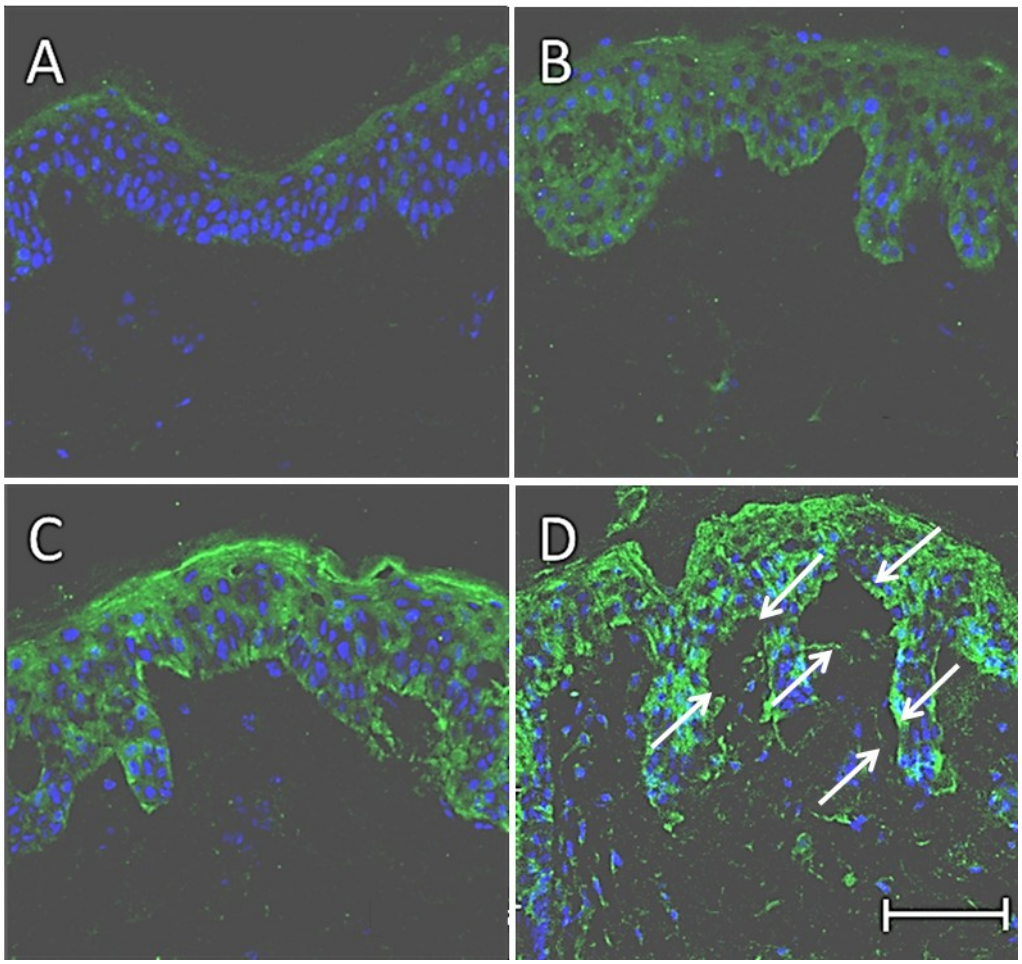

Figure 3.1. High dose DNCB may rupture the basement membrane
Confocal micrograph taken using a Leica TCS-SP2 laser confocal microscope, showing anti-dinitrophenyl detection in human skin sections treated with: (a) 100 µl acetone vehicle, (b) 35 µg/cm^2 DNCB, (c) 106 µg/cm^2 DNCB, (d) 318 µg/cm^2 DNCB for 16 hours. White arrows in panel D indicate blister formation in the skin and separation appearing at the dermal-epidermal junction. Detection of dinitrophenyl adducts was achieved using a goat polyclonal antibody raised against dinitrophenyl human serum albumin (Sigma), with secondary detection using anti-goat-FITC antibody (Sigma) at optimised concentrations. Nuclei were stained using To-Pro 3 (Life Technologies). Scale bar represents 60 µm.

Skin treated with a high dose of DNCB showed altered morphology of the epidermal-dermal junction and positive DNP staining within the dermis. This suggests that at high

doses, DNCB disrupts the basement membrane, allowing DNCB to penetrate the dermis. Also observed was an increase in the number of nuclei visible in the dermis possibly indicating either migrating Langerhans cells or dermal dendritic cells.

3.3.2 Penetration of DNCB into *ex vivo* skin during a 16 hour incubation

To maximise protein modification, incubation times were optimised. The clinically relevant dose of 50 µg/cm^2 DNCB was applied to 4 separate pieces of *ex vivo* skin taken from two patients, plus a vehicle control using 50 µl acetone (see chapter 2 section 2.4). These DNCB-treated skin samples were removed and snap frozen in liquid nitrogen at 0.25, 1, 4 and 16 hours after the vehicle solvent was no longer observed inside the O-rings. These samples were then sectioned and stained and images captured by fluorescent microscopy (Figure 3.2).

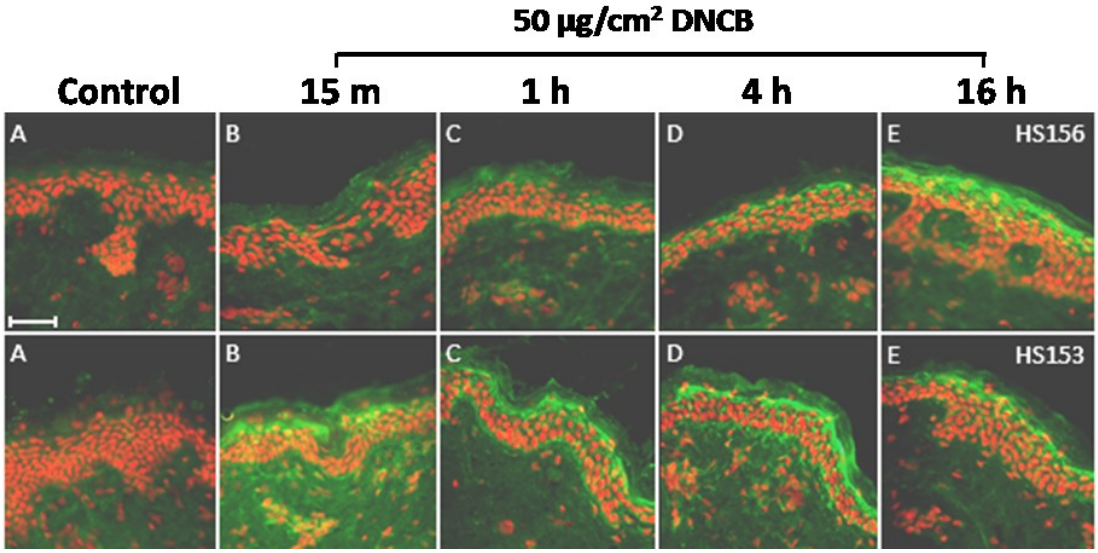

Figure 3.2. DNCB penetration into human epidermis over time

Immunofluorescent micrographs of skin from two patients designated HS156 (top row) and HS153 (bottom row). For each patient, the images are representative of the following treatments of DNCB: a) 0 h / acetone vehicle control, (b to e) 50 µg / cm^2 DNCB in acetone for: b) 15 minutes, c) 1h, d) 4h and 5) 16h. Anti-DNP stain is green, nuclear stain is orange. Scale bar represents 60 µm.

The two skin samples show varying levels of DNCB penetration through the epidermis. HS156 can be seen to be fully dinitrophenylated between 4 and 16 hours, while HS153 as early as 15 minutes. This may reflect skin barrier variability between patients. Using these qualitative experiments to assess the optimal incubation time of skin from a range

of donors would suggest that incubation for 16 hours would be sufficient to allow complete penetration in other skin samples.

3.3.3 Clinical dose analysis of dinitrophenyl proteins in skin

Duplicate skin samples (n=5) were treated with vehicle and 50 μg/cm^2 of DNCB for 16 hours and stained as in section 3.2. A significant amount of variation is observed in both positive dinitrophenyl detection and auto-fluorescent background can be observed in all five samples. However, penetration of DNCB and subsequent modifications was achieved throughout the epidermis with no distortion of the basement membrane or detection of DNP groups in the dermis (Figure 3.3).

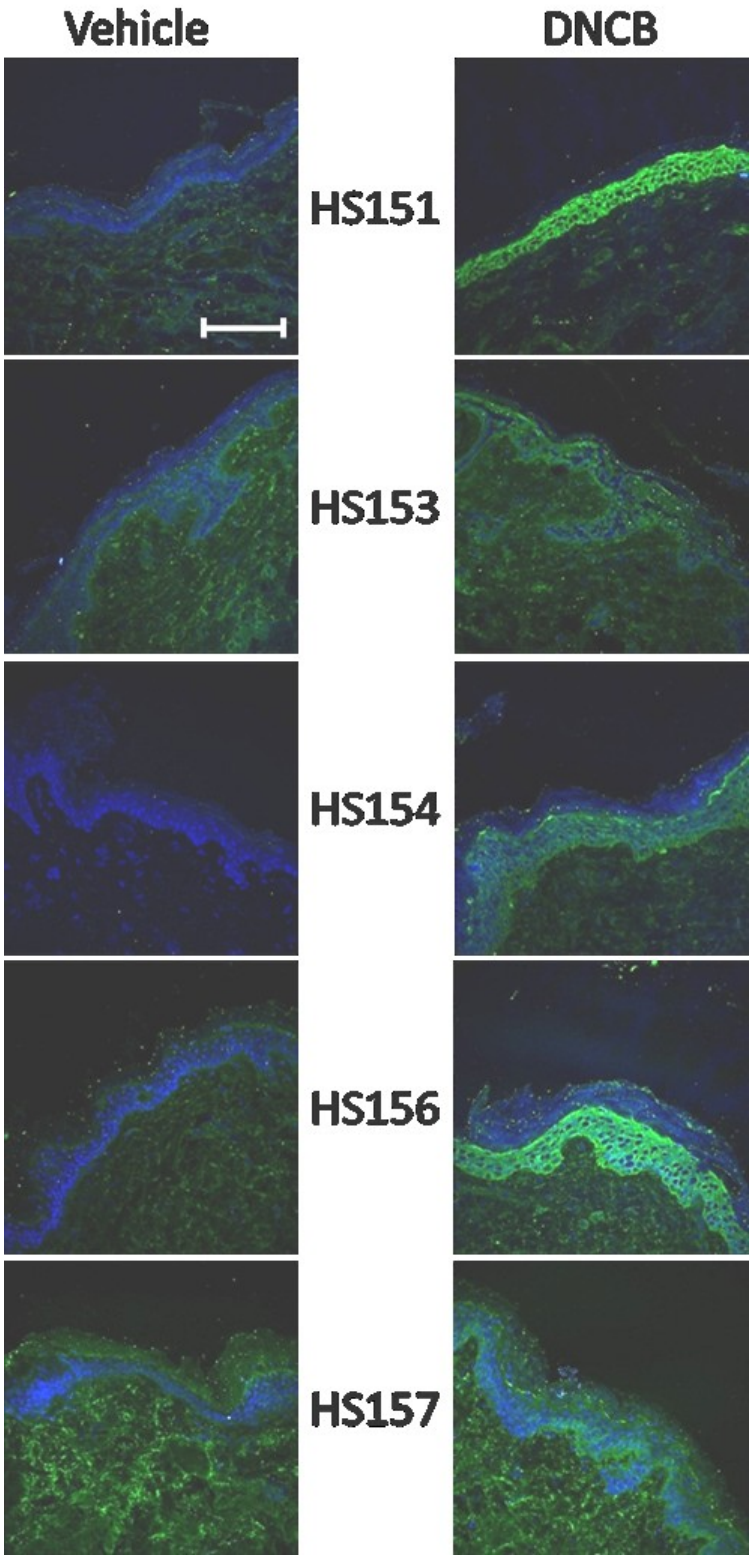

Figure 3.3. Variable penetration of DNCB into epidermis between donors

Laser confocal micrographs of ex vivo human skin from 5 patients (indicated by HSxxx patient ID) treated either with the vehicle acetone (left column) or 50 µg / cm^2 DNCB in acetone for 16 hours at 37°C. Detection of dinitrophenyl adducts was achieved using a goat polyclonal antibody raised against dinitrophenyl human serum albumin (Sigma), with secondary detection using anti-goat-FITC antibody (Sigma) at optimized concentrations. Nuclei were stained using To-Pro 3 (Life Technologies). Scale bar represents 60 µm.

To quantify the amount of haptenation in the skin samples, a region of interest was selected and quantification performed using the LAF software (Leica). Maximum projections of the z-planes for each of 3 recorded images per sample were used. For 12 regions of interest, lines were drawn across the epidermis from just beneath the stratum

corneum to just above the epidermal-dermal junction at approximately equal intervals and the average pixel intensity across each region of interest calculated (Figure 3.4).

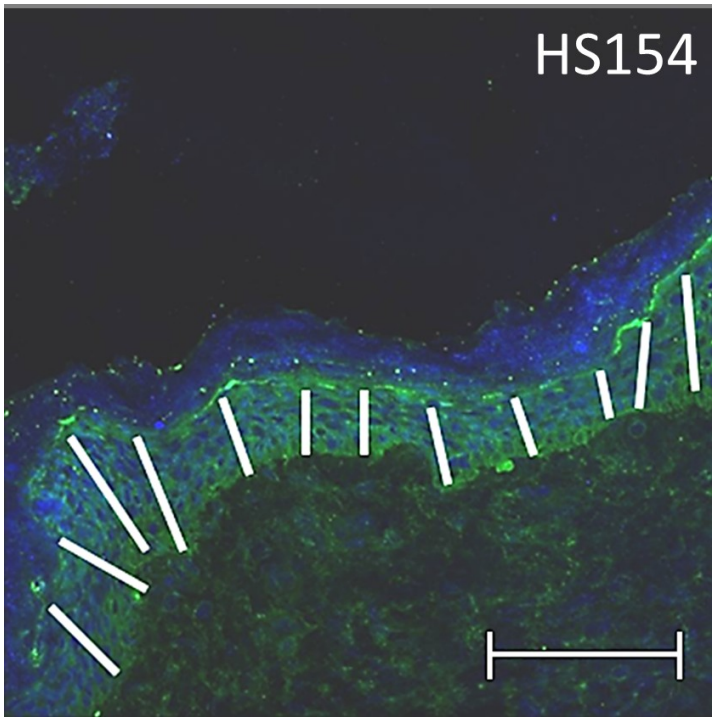

Figure 3.4. Analysis of immunofluorescence output

Ex vivo skin overlaid with white lines indicating how FITC intensity values were measured across the epidermis. Each line measures a value from 0 to 127 indicating the average pixel intensity along the line. Detection of dinitrophenyl adducts and nuclei was achieved as described in the text. Scale bar represents 60 µm. n = 3

The experiment was performed in triplicate and the average FITC values for all regions of interest were plotted as a bar graph (Figure 3.5).

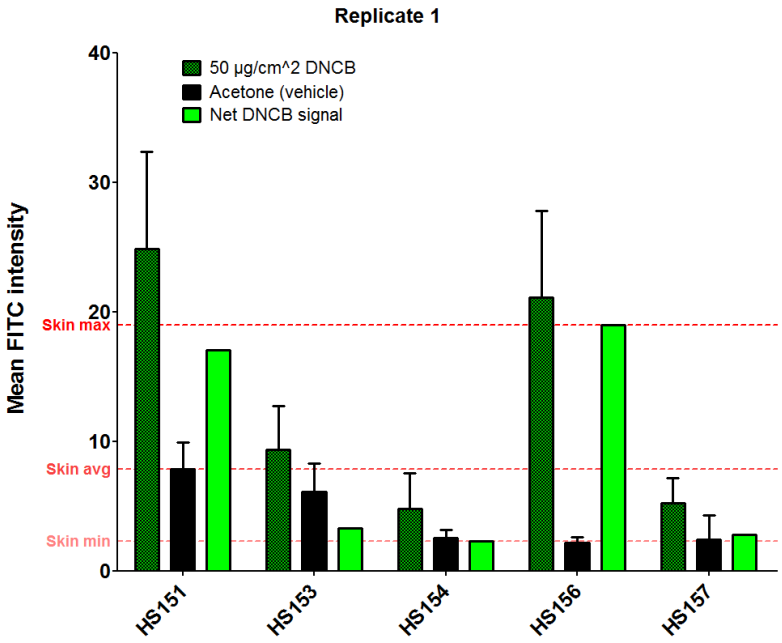

Figure 3.5. Protein modifications quantified as a function of fluorescence intensity

A bar chart showing the mean FITC intensity per patient. For each patient the mean FITC intensity for the acetone vehicle treated skin was subtracted from that of the DNCB-treated skin, giving the net DNCB signal. Lines were added to indicate the minimum, maximum and mean values of net DNCB signal. Representative of three technical replicates.

The amount of protein modified within the epidermis shows significant variation between donors, with 2 groupings of average FITC fluorescence intensity. Donors HS151 & HS156 had an average intensity value of ~17-19 while the other 3 donors had considerably lower intensity values from ~2.5 – 3.5.

3.3.4 Immunofluorescence of dinitrophenylated proteins in HaCaT cells

To examine the modification of proteins in HaCaT cells, cells were cultured in 8-well chamber slides and treated for 2 hours with concentrations of 0 to 11 µM DNCB in DMSO (see chapter 2 section 2.7). Cells were stained with the same antibodies and concentrations as used in the *ex vivo* skin experiments. The laser confocal microscope was calibrated to show DNCB-specific staining of the HaCaT cells (Figure 3.6.) (see chapter 2 section 2.9).

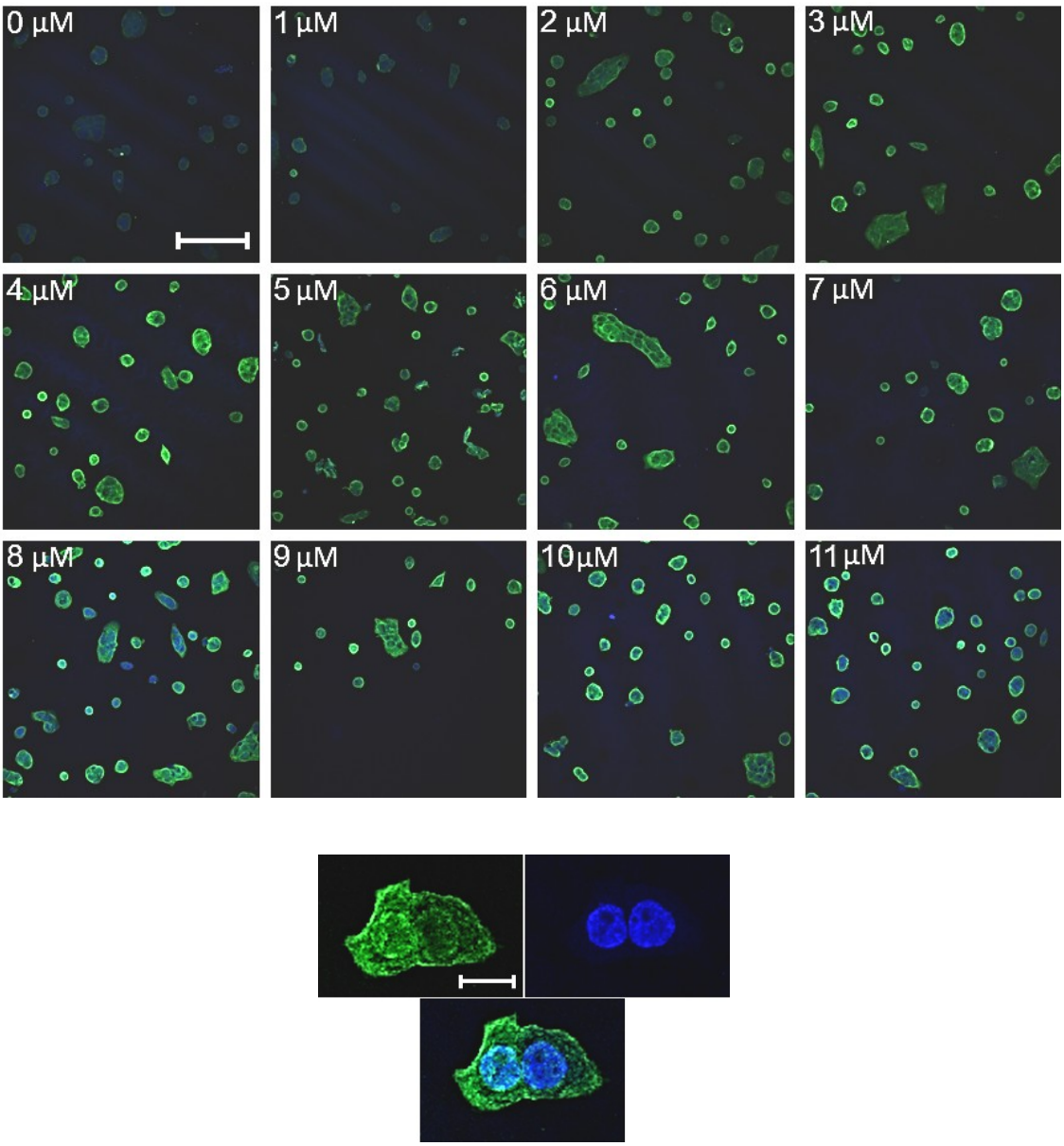

Figure 3.6. Immunofluorescence labelling of DNP adducts in HaCaT cells

(Top) Laser confocal micrographs captured using a Leica TCS-SP5 of HaCaT cells treated with DMSO vehicle (0.11% DMSO, 0 µM DNCB) and DNCB at micromolar concentrations indicated by the number in the top left of each image. Vehicle concentration ranged from 0 to 0.11% concentration. Scale bar represents 60 µm.

(Bottom) Higher magnification of HaCaT cells treated with 8µM DNCB showing the FITC (DNCB) and To-Pro3 (nuclei) channel outputs and the merged image. Scale bar represents 5 µm.

Average fluorescence intensity was measured for the FITC output of the HaCaT cells by measuring regions of interest across 12 distinct cells chosen in spiral sequence beginning from the top of each image so as to reduce sampling bias. The experiment was repeated in triplicate and the average FITC values for all regions of interest

calculated (36 values per replicate in total) and plotted as an X/Y scatter graph (Figure 3.7.).

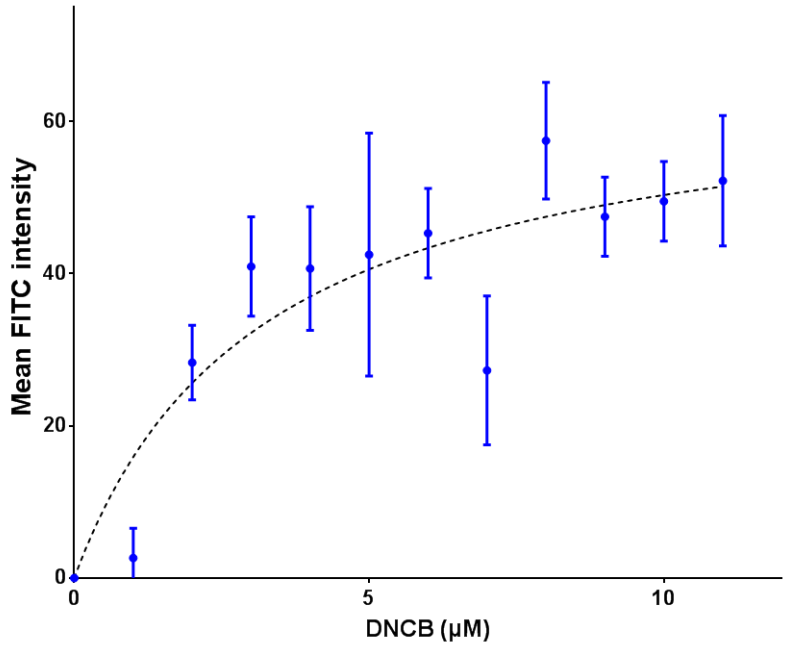

Figure 3.7. Haptenation response to DNCB concentration in HaCaT cells

Graph showing mean FITC intensity as a response to DNCB concentration in cell culture. A line of best fit was plotted using non-linear regression with a fit of 0.717 (R squared). Representative of 3 technical replicates.

The relationship to DNCB concentration appears to be a broadly hyperbolic standard dose response. Although the data shows a high level of variability, the large number of data points per dose (36 per dose for each replicate) allows for a relatively confident assignment of the standard dose-response curve. Little additional increase in DNP adducts is observed above 4 µM DNCB.

3.3.5 Comparison of modification dose-response in HaCaT cells using western blot

Protein extracts from HaCaT cells which had been treated with 0, 4, 12 and 36 µM DNCB in vitro, were separated using SDS-PAGE. Protein lysates were separated using duplicate gels, with one being fixed and stained using Coomassie blue and the other being transferred to a PVDF membrane for western blotting. The data show positive bands only on the proteins extracted from cells treated with DNCB (Figure 3.8).

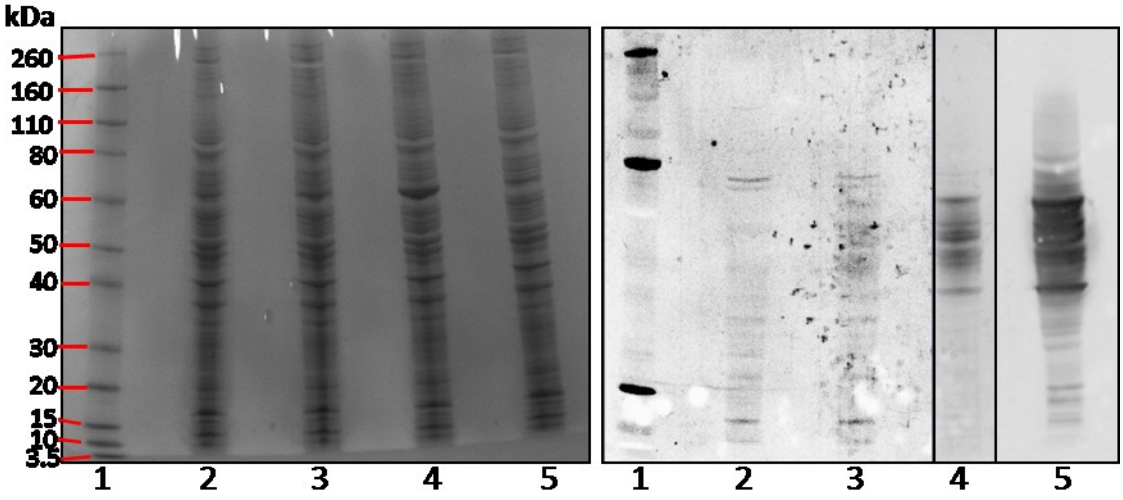

Figure 3.8. Western blot comparison of the distribution of DNP-proteins in HaCaT cell lysate treated with different DNCB doses

A photograph of a Coomassie stained gel (left) and UV emission from a western blot (right) showing the difference between lysates treated with DNCB and those without. The lanes contain: 1) 5 µl pre-stained protein standards, 2) 20 µg lysate of vehicle (DMSO) treated HaCaT cells, 4 (3), 12 (4) & 36 (5) µM DNCB treated HaCaT cells. All DNCB incubations were for 2 hours at 37 °C. A montage of images captured from the same membrane was created using three gain and contrast settings. Lanes 1-3 (right) are configured to maximise exposure of lane 3 versus lane 2, while lanes 4 & 5 are configured for maximum exposure of themselves. Banding in lane 2 (vehicle control) is probably due to non-specific binding of either the anti-dinitrophenyl or anti rabbit antibodies.

While the majority of modification seems to occur within a range between 40-70 kDa, a broader spectrum is observed with an increasing dose of DNCB including some high molecular weight proteins in the 36 µM sample. It should be noted that most human skin keratins have molecular weights within the 40-70 kDa range (Fuchs, 1995).

To continue assessment of the suitability of HaCaT cells, haptenation of proteins was qualitatively compared by running western blots on epidermis of *ex vivo* skin treated with 50 µg/cm^2 DNCB (and 300 µg/cm^2 when sufficient skin was available) and generating histograms of the banding intensity. Skin was DNCB-treated and the epidermis separated and prepared as described in chapter 2 sections 2.3 and 2.6 respectively. HaCaT cells were cultured, treated and lysed as described in chapters 2.1, 2.3 and 2.10 respectively. Western blot profiles showed more clearly defined bands for skin than for HaCaT cells, but the distribution of banding intensity was broadly similar between the two (Figure 3.9).

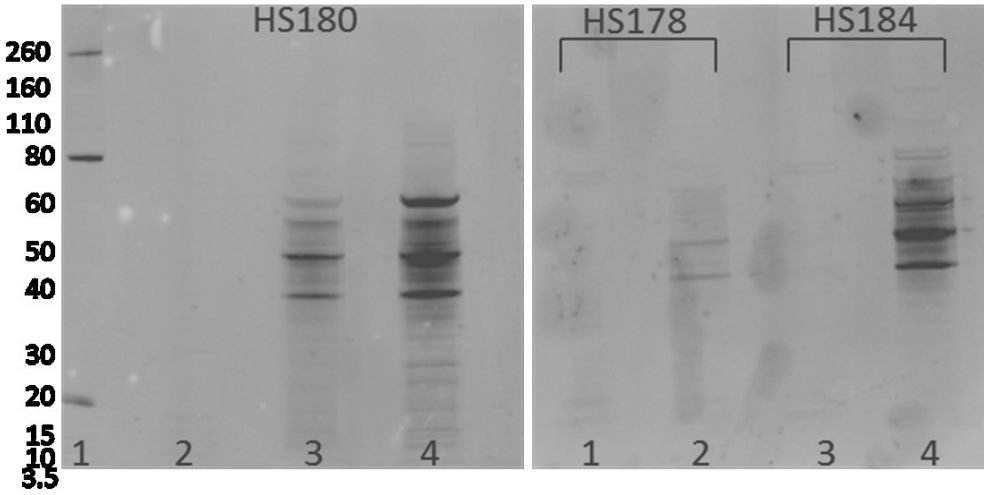

Figure 3.9. Western blot comparison of DNP-proteins in different skin donors
Photographs of UV emission from 2 western blots showing proteins extracted from human epidermis from 3 donors. The lanes contain: LEFT: 5 µl pre-stained protein standards (1), 20 µg lysate of epidermis isolated from vehicle (acetone) treated human skin (patient HS180) (2), 50 (3) and 300 µg/cm^2 (4) DNCB treated human skin. RIGHT: 1) 20 µg lysate of epidermis isolated from vehicle (acetone) treated human skin (patient HS178)(1) and 50 µg/cm^2 DNCB treated human skin (2), 20 µg lysate epidermis isolated from vehicle (acetone) treated human skin (patient HS184) (3) and 50 µg/cm^2 DNCB treated human skin (4).

The bands in the epidermal lysates are more clearly resolved than in the HaCaT lysates. The overall pattern, including the pronounced region between 40-70 kDa appears broadly similar between the two lysates and again could possibly indicate modified keratins (Fuchs, 1995). The difference in band intensity between the three skin donors suggests some variability in the amount of modification, which supports the immunofluorescence results.

For qualitative comparison between the western blots, histograms of the lanes were generated using ImageJ software and overlaid, showing that the modification profiles of the HaCaT cells and the skin were broadly similar, with the majority of signal indicating proteins between 40 to 70 kDa in size (Figure 3.10).

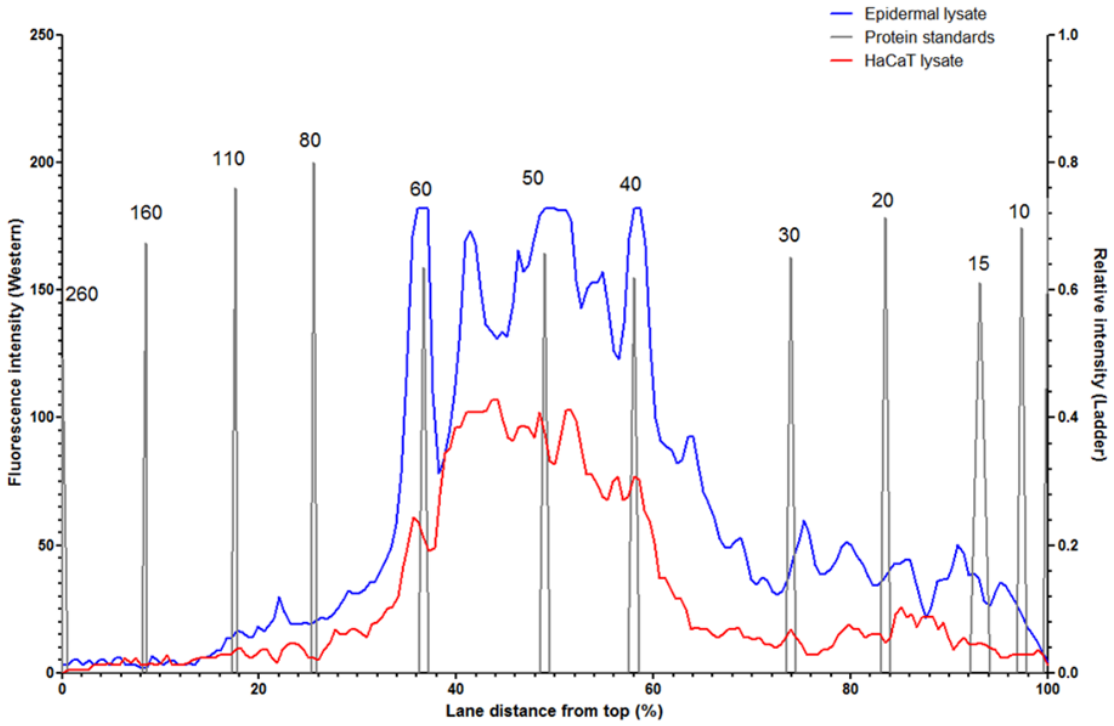

Figure 3.10. Densitometric comparison of DNP-protein lysate isolated from human epidermis and HaCaT cells

Densitometric analysis of band intensity of HS180 epidermal (blue) and HaCaT (red) lysate western blots. The majority of the area under the curve (AUC) lies between 40 to 70 kDa for each.

3.3.6 Validation of western blots using [^{14}C]-DNCB radiolabelling

Due to noticeable differences between the Sigma primary detection antibody used in initial investigations (data not shown) and the Life Technologies one here (shown in Figures 3.8 & 3.9), confirmation was required that the banding pattern observed using antibody detection represents the full spectrum of protein modification. Skin and cells were incubated with [^{14}C]-DNCB to provide a direct detection of dinitrophenyl proteins. Experiments were carried out using HaCaT cells and *ex vivo* human skin treated using the same methods as with non-radiolabelled DNCB (see chapter 2 sections 2.3 & 2.4). Protein lysates were separated using SDS-PAGE and visualised using Coomassie blue, de-stained and subsequently treated with a fluorographic amplification agent and incubated for 8 weeks on radiographic film (Figure 3.11).

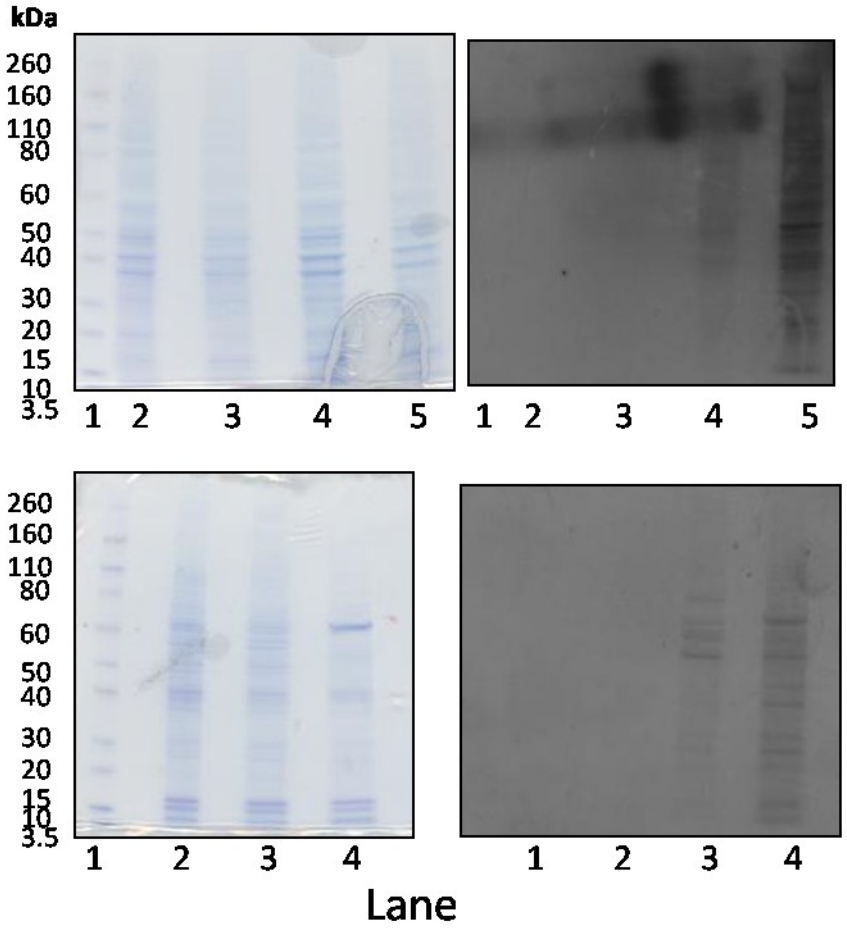

Figure 3.11. Autoradiographic detection of DNP-proteins in HaCaT cells and skin
Coomassie stained gels and their corresponding autoradiographs. The top 2 images show lysates of 2 hour DNCB-treated HaCaT cells, the bottom 2 show lysates of DNCB-treated human epidermis. The lanes contain: TOP: 5 µl pre-stained protein standards (1), 20 µg lysate of vehicle (ethanol) treated HaCaTs (2), 4 (3), 12 (4) and 36 µM (5) [^{14}C]-DNCB treated HaCaT cells. BOTTOM: 5 µl pre-stained protein standards (1),) 20 µg lysate of vehicle (ethanol) treated human epidermis (2), 50 (3) and 300 µg/cm^2 (4) [^{14}C]-DNCB treated human epidermis.

Densitometric analysis of the autoradiographs was not possible due to the faintness of the bands not allowing for clear separation of graph peaks (data not shown), however there were signals in a wider range of molecular weights than seen for the western blot studies.

3.4 Discussion

The effects of dose and time in the modification of proteins within *ex vivo* skin and HaCaT cells by DNCB were assessed by labelling with antibodies and radio-isotopes. The purpose of this work was to broadly compare protein modification between *ex vivo* and *in vitro* systems and to determine the suitability of HaCaT cells as a model for human skin.

Skin incubated with DNCB for 16 hours exhibited increased levels of positive staining in the dermis at the highest concentration of DNCB (Figure 3.1). There are also some indications that the integrity of the dermal-epidermal basement membrane has been affected, resulting in blister formation where the epidermis has separated from the dermis. It is possible that DNCB binding to amino acid residues in basement membrane proteins could alter its structural integrity enough to disrupt the barrier. It is not known what proportion of basement membrane proteins are nucleophilic and available for modification. It may be that generic degradation occurring in *ex vivo* skin upon culture may contribute to this effect. Modification throughout the epidermis occurs at the clinical dose of 50 $\mu g/cm^2$ without altering morphology compared to the vehicle-treated skin (Figs. 3.2 & 3.3), which suggests that only doses of DNCB above a certain threshold alter the skin morphology. An early study into the effects of DNCB in the epidermis suggests that full penetration into the epidermis occurs within 6 hours, with positive signals in the dermis concomitant with migrating Langerhans cells (Carr et al., 1984). This could explain the presence of the signal in the dermis, but not alterations in basement membrane integrity. A study using reconstructed human epidermis (RHE) has also shown that treatment with DNCB exhibits significant cytotoxicity with altered morphology and detachment of the basal cells from a polycarbonate substrate. The results from this study are comparable here since the 300 $\mu g/cm^2$ treatment equates to 1,680 μg/ml and the RHE experiments show a dramatic decrease in cell viability between 1,000 and 2,000 μg/ml (80% and 30% respectively) (Coquette et al., 1999). Other research highlights the importance of haptenation in the basal keratinocytes in relation to allergic contact dermatitis (Simonsson et al., 2011), which could suggest that greater protein modification occurs nearer the basement membrane. This could be due to increases in haptenation by DNCB at the higher pH present at the *stratum basale* (pH 6.8) relative to the *stratum corneum* (pH 5.5) (Dietz et al., 2010). Higher doses of DNCB could perhaps be capable of modifying extracellular matrix proteins at the dermal-epidermal junction to a degree which may interfere with the structure of the

basement membrane and its contact to basal keratinocytes (Bauer et al., 2011). Indeed, there is also some indication in chapter 5 of this thesis that DNCB modification may cause changes in the structure of proteins.

Immunofluorescence shows that DNCB penetration after 0.25, 1, 4 and 16 hours was variable between donors. One skin sample showed full penetration as early as 1 hour, while another didn't show full penetration until between 4 and 16 hours. Hence 16 hour incubations are needed to ensure maximum DNCB penetration. One published study showed that after 16 hours, the rate of modification, as determined by assaying the increase in formation of dinitrophenyl glutathione, approaches an asymptote. It should also be noted that the uncut *ex vivo* skin used in that study, retained most of its viability for up to 25 hours (Jewell et al., 2000).

The distribution of dinitrophenyl modified protein throughout the epidermis appears homogeneous between donors, suggesting that the difference may be caused by natural variation in the barrier qualities of donor skin. Studies examining the lipid varieties in the *stratum corneum* indicate that the composition is highly variable between individuals and of significant importance to barrier function, as determined by water loss (Norlen et al., 1999). However, factors such as the way the skin is stored, the time between excision and the set-up of each experiment could also be important (Jewell et al., 2000).

As with *ex vivo* skin, the distribution of dinitrophenylation throughout HaCaT cells in all doses appears widespread, suggesting promiscuous modification of a wide range of proteins in the cytosol and at membranes, or preferential modification of widely distributed proteins such as actin. The heterogeneous staining suggests that protein modification within the cell corresponds to distinct structures, the identity of which would need to be determined by further work.

To determine if DNP modifications in skin could be used to indicate a suitable dose of DNCB to treat HaCaT cells with, the mean FITC intensity of the HaCaT experiments was plotted against the mean, maximum and minimum net FITC signal from stained epidermis from all 5 donors (data not shown). The large variations between skin samples as well as the considerable variation within technical replicates of the HaCaT samples were such that a meaningful relationship could not be determined between the two.

Western blots from protein lysates from differentially DNCB-treated HaCaT cells show a variation in modification dependent upon the amount of DNCB the cells were treated with. This demonstrates that the antibodies are highly specific to DNP-protein at the concentrations used. The composite image (Figure 3.8) showing lysates of HaCaT cells treated with 4, 12 and 36 μM DNCB provides evidence that the amount and diversity of modified proteins increases with dose. This suggests either that saturation of more reactive proteins allows subsequent modification of those with lower reactivity, or that higher doses of DNCB alter protein expression within the cell, providing a different range of targets for modification.

Western blots of protein lysates of DNCB-treated epidermis and HaCaT cells have similar banding patterns to one another, although the epidermal lysates show more distinct bands. This could indicate that the barrier in skin has decreased the availability of some proteins, leading to a greater resolution between proteins linked to spatial availability in the tissue. The similarity is supported by the densitometry graph (Figure 3.10) which shows that the largest areas of signal generally overlap.

In contrast to the western blots which seem to show a narrow molecular weight range of modified proteins between 40 – 70 kDa, the modification profiles of the radiolabelled lysates show a far wider molecular weight distribution of DNCB labelled proteins (Figure 3.11). It is likely that the western blot detection is limited either by a selectivity bias of the antibodies to certain proteins, or could be due to eccentric transfer of proteins to the PVDF membrane. Other studies using western blot detection of DNP adducts do not show the same biased range of detection (Hirota et al., 2009; Megherbi et al., 2009) which supports the possibility of the differences being methodological in origin. There are keratins within this molecular weight range which are highly expressed by HaCaT cells (Boukamp et al., 1988) and in human skin (Fuchs, 1995), so it could be that these proteins are modified by DNCB and due to their abundance, suppress weaker signals from other modified proteins. Bovine serum albumin, present within the culture medium could explain the result similarly, however this does not explain the difference between the western blots and the autoradiographs. An important consideration when interpreting these data is a process called thiolysis, where DNP groups can be removed from cysteine, histidine and tyrosine residues by a reducing agent (Shaltiel, 1967). Thiolysis, which is dealt with in more detail in chapter 6 of this thesis, was only learned

of after this work had been carried out, but should be considered a source of error in all experiments using SDS-PAGE separation of proteins with reduction.

3.4.1 Summary

This chapter has shown that immunofluorescence is a useful method for confirming the presence of dinitrophenyl haptenation in both skin and HaCaT cells, both in terms of illustrating the extent of haptenation within a skin sample and its spatial distribution. However, the approach is prone to significant variation and reducing its usefulness as a quantitative methodology.

The radiolabelling data suggest that there may be a detection bias inherent to polyclonal antibodies for detection of haptens. However, the very long incubation period necessary to detect adducts after incubation with low concentrations of DNCB make radio-labelling impractical for use in a high-throughput workflow.

Determining a suitable dose for treating cells in culture was limited by high data variability. Though not within the further scope of this study, a more effective way to quantify adducts in epidermis and HaCaT cells would be to treat with radiolabelled DNCB (either [^{14}C] or [^{3}H] labelled), isolate protein and use scintillation counting of the lysates to quantify haptenated proteins. Similar techniques have previously been used to determine chemical penetration into skin (Weber et al., 1991). Expressing the chemical incorporation as counts per minute per mg of protein versus control could provide a more direct method to detect the presence of adducts and allow for dose comparison between skin and cell lines.

4 ASSAYING THE IMMUNOGENICITY OF DNCB MODIFIED PROTEINS EXTRACTED FROM HACAT CELLS

4.1 Introduction

Chemical sensitizers need to modify proteins within the skin to generate an immune response and trigger ACD (Kimber et al., 2002). However, it is currently unclear if specific protein modifications are responsible and if so, which proteins in particular may be involved in the process of sensitization. Looking at the properties of chemicals is an important part of elucidating the mechanisms of contact sensitivity. However, determining which proteins in skin respond to these chemicals and how the immune system responds to those modifications is just as important to understanding how sensitization occurs.

T cell assays have been used successfully in a number of studies to determine the immunogenicity of drugs and chemical haptens using the peripheral blood mononucleocytes (PBMCs) of patients allergic to certain drugs and compounds (Pichler and Tilch, 2004; Pickard et al., 2007). The PBMCs from blood samples contain around 15% monocytes which function as antigen presenting cells, enabling them to present peptides as part of MHC class II complexes (de Waal Malefyt et al., 1991; Gonwa et al., 1983; Trombetta and Mellman, 2005). This allows modified proteins to be assayed for their immunogenicity as they are endocytosed, processed and presented by monocytes. If any of the presented epitopes are recognised by T-cells specific to those antigens in the PBMCs, then these cells will become active, secrete cytokines and undergo clonal expansion (Freudenberg et al., 2009; Martin et al., 2006). Contact dermatitis to small molecular weight chemicals is mediated by protein modification, since the chemicals themselves are not generally thought to be able to interact with T-cell receptors (Martin and Weltzien, 1994; Weltzien et al., 1996). Using PBMCs from volunteers sensitized to DNCB, it is possible to assess this response using DNP haptenated proteins, modelling the *in vivo* situation by interrogating donor T-cell repertoire with monocyte-presented DNP epitopes derived from DNCB-modified proteins.

Lymphocyte proliferation assays (LPAs), often called lymphocyte transformation tests have been used in studies relating to drug allergy (Jenkins et al., 2013; Pichler and Tilch, 2004) and contact dermatitis (Kimber et al., 1990; Pickard et al., 2007). The LPA can

be used to investigate the immunogenicity of DNCB modified HaCaT proteins by incubating the PBMCs of individuals sensitized to a chemical hapten with modified proteins. Antigen-specific responses to any immunogenic proteins present within the DNCB-modified protein lysate can be determined by measuring the amount of T-cell proliferation that occurs (see chapter 2 section 2.19).

Ideally, proteins from *ex vivo* skin would be used in this study; however, there are several advantages in using a cell line as a model:

- Cell lines are more readily available than skin explants
- Cells are more easily disrupted than tissue, hence a greater range of proteins can be isolated
- Donor variation is eliminated, so the proteins extracted are more consistent and reproducible
- There are few ethical constraints to working with cell lines

These properties make cell lines a suitable primary screen for researching the tissue they are derived from. HaCaT cells are an immortalised keratinocyte cell line derived from human skin. Being derived from basal keratinocytes, these cells are phenotypically similar to keratinocytes in skin, as shown by their ability to differentiate to form skin-like tissue (Boelsma et al., 1999; Kehe et al., 1999; Schoop et al., 1999). Having previously determined the suitability of DNCB-modified HaCaT proteins as a model for their equivalent in human skin in chapter 3, it was important to determine if dinitrophenylated proteins from these cells were immunogenic. If immunogenic proteins are found within modified HaCaT cells, this would be useful information to cross-reference with future studies looking at protein modifications within skin.

4.2 Experimental design

The purpose of this work was to use protein lysate extracted from HaCaT cells treated with DNCB to stimulate T-cells in PBMCs cultured from DNCB-sensitized donors to assess whether any of the modified proteins are able to elicit a response. All volunteers were sensitized as part of a separate study conducted within the Dermatopharmacology department within the University of Southampton Clinical and Experimental Sciences division at Southampton General Hospital. No volunteers were sensitized or re-challenged with DNCB as part of this study.

Preparation of HaCaT and primary keratinocyte proteins modified with standard and / or isotopically labelled DNCB

HaCaT cells and primary keratinocytes were cultured as detailed in chapter 2 and upon reaching a confluency of between 70-80%, an equal amount of DNCB and triple deuterated DNCB (d3-DNCB) in DMSO was added to HaCaT cells at a final concentration of 30 μM DNCB. A vehicle control was also prepared by incubating HaCaT cells with DMSO with a final concentration of approximately 0.0006 % to minimise vehicle effects. This DNCB concentration was selected on the basis that it was the highest concentration where incubation for 3 hours did not cause significant cell death. After 3 hours, the cells were washed to remove free DNCB and extracted (see chapter 2 sections 2.1 & 2.3) and the pellet was stored at -20° C until required. Cells were lysed, proteins extracted (see chapter 2 section 2.16) and the detergent removed using SDS-removal columns in order to avoid stressing the PBMCs during incubation. Primary keratinocytes were treated and the proteins isolated using methods in chapter 2 sections 2.3 & 2.16.

DNCB-modified HaCaT protein lysates were separated into 12 fractions according to their isoelectric point using the OFFGEL system (see chapter 2 section 2.17). Prior to fractionation by IEF, proteins are ordinarily prepared in a buffer containing chaotropes and reducing agents to facilitate migration along the pH gradient. However, to avoid alteration of the DNP-Cys/His/Tyr adducts by thiolysis (Shaltiel, 1967), no reducing agent was included in the fractionation buffer. To reduce toxicity to lymphocytes, the fractions were dialysed 4 times against 2 litres of 50 mM ammonium bicarbonate to remove the fractionation buffer. These fractions were used to narrow the range of proteins being assayed, providing a more focussed list of which proteins which may be

immunogenic. Both 12 individual fractions and a pool of all fractions were incubated with PBMCs.

Whole cell lysates and fractions were analysed by western blot to confirm the presence of dinitrophenyl proteins. To reduce the risk of adduct removal by thiolysis as mentioned earlier, no reducing agent was added to the SDS-PAGE sample buffer.

Antigen-specific stimulation of T-cell proliferation

Isolated PBMCs in culture were stimulated with whole cell lysate from HaCaT cells treated with DNCB as well as fractions derived from DNCB-treated whole cell lysate (see chapter 2). Lysates from untreated cells were used as a control. Generic T-cell proliferation was confirmed using phytohaemagglutinin (PHA) and the presence of DNP-specific T-cells was confirmed by direct stimulation with DNCB. T-cell proliferation in response to DNCB was determined prior to experiments by treatment with 1 μM increments of DNCB from 3-9 μM, after which 3 μM was used as it gave the most consistent strong response between donors without negating proliferation with extensive cytotoxicity. Direct stimulation with DNCB was expected to generate both MHC class I and II mediated epitopes, as DNCB can penetrate into cells and modify cytosolic proteins (see chapter 3). While this wasn't directly assayed, it was expected that stimulation by DNCB would activate more T-cells than stimulation with modified proteins. Normal proliferation was measured from PBMCs without antigen and the DNP-specificity of responses to lysate from DNCB-treated HaCaT cells was confirmed by comparison with lysate from vehicle-treated HaCaT cells. To demonstrate that monocytes were able to endocytose, process and present protein antigens, human serum albumin (HSA) treated with 100 molar equivalents of DNCB for 24 hours was added to PBMCs of DNCB-sensitized donors to a concentration of 1 μM and compared with the same amount of non-treated HSA.

Proliferation was measured by pulsing with tritiated thymidine for 6 hours after 6 days of incubation with antigen followed by scintillation counting (see chapter 2).

4.3 Results

4.3.1 Lymphocyte proliferation in response to DNCB

PBMCs from volunteers sensitized to DNCB were isolated and studied. Lymphocyte proliferation assays (LPAs) were performed as described in chapter 2. A stimulation index was calculated by dividing the mean scintillation counts per minute of the antigen-treated PBMCs by the mean scintillation counts per minute from the control PBMCs. A stimulation index of above 2 was considered a weak positive response and above 3 is considered a strong response (Pichler and Tilch, 2004). In all cases of direct stimulation with 3 µM DNCB, sensitized individuals exhibited a strong response versus non-sensitized volunteers (Figs. 4.1 & 4.2).

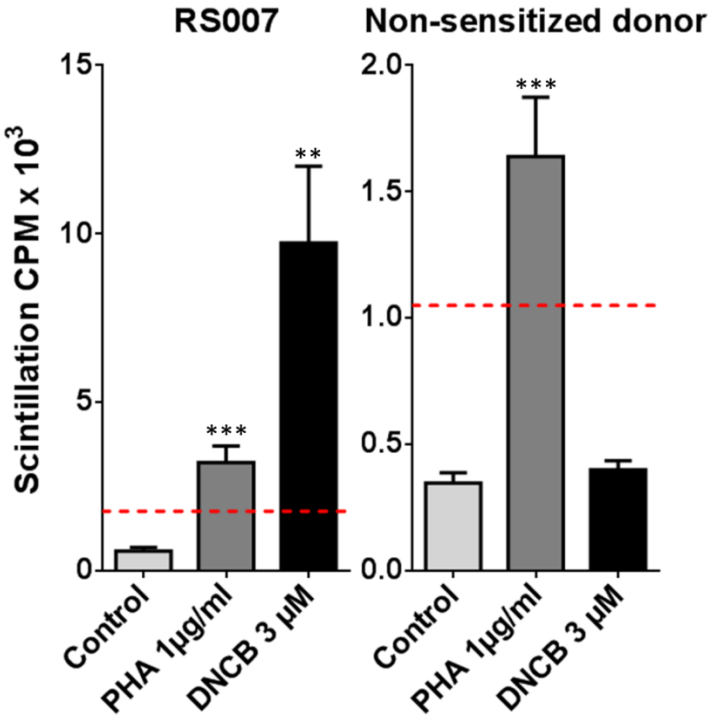

Figure 4.1. T-cell proliferation responses to positive control and DNCB

T-cell proliferation assay controls. RPMI is the negative control – the average scintillation counts per minute (CPM) from this are used to determine the SI = 3 threshold, indicated by the dotted line. PHA is the positive control.

*Student's t-test was used to determine significance – P values are as follows: * <0.05, ** < 0.005, *** < 0.001, **** < 0.0001.*

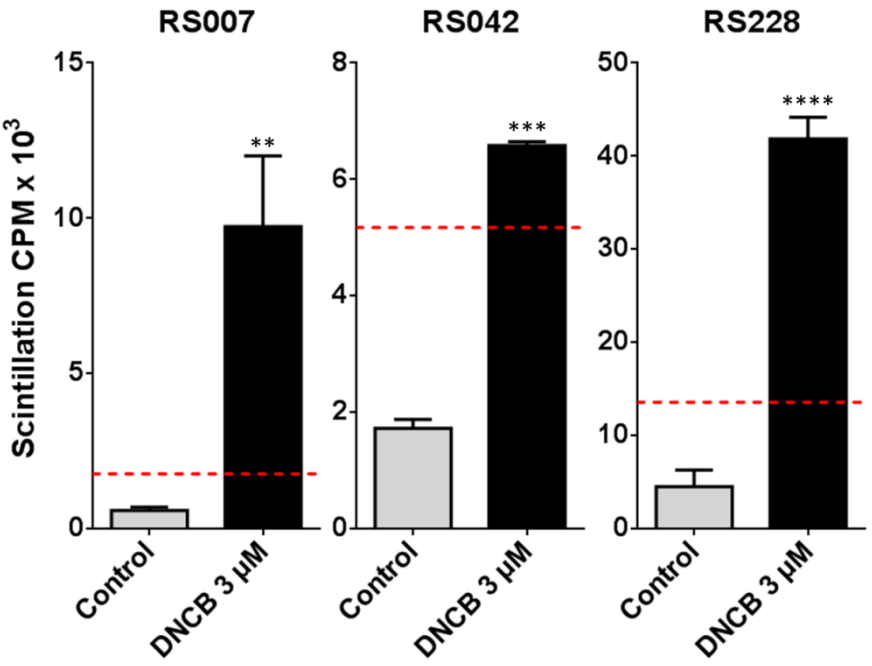

Figure 4.2. T-cell responses to direct treatment with DNCB

T-cell proliferation responses from 3 subjects in response to direct stimulation with DNCB measured by scintillation counting of incorporated tritiated thymidine. The stimulation index is indicated by a red dotted line for each subject to show that the individuals' responses were strong. RPMI medium was used as a negative control.

4.3.2 Lymphocyte proliferation in response to DNCB modified cell proteins

To investigate the immunogenicity of the DNCB haptenated HaCaT proteins, cell lysates were prepared from HaCaTs which had been incubated with 30 µM DNCB for 2 hours (see chapter 2 sections 2.2 & 2.10). To ensure that no free DNCB was present in the protein lysates, cell pellets were washed 3 times in PBS prior to lysis. DNP-modified proteins in cell lysates and cell lysate fractions were detected using western blotting prior to their use in LPA assays (Figure 4.3).

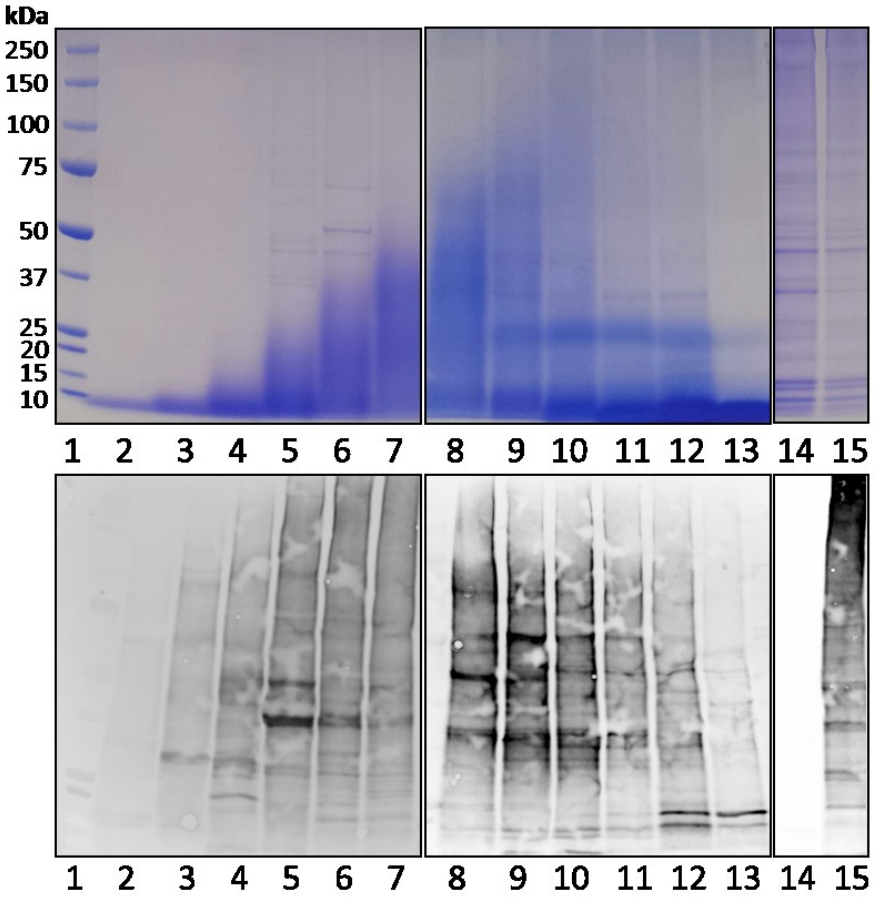

Figure 4.3. Dinitrophenylated proteins in whole cell lysates and lysate fractions from DNCB-treated HaCaTs

Coomassie blue stained SDS-PAGE (TOP) and western blots probed for DNP protein adducts using polyclonal Rb α-DNP antibodies (BOTTOM) of the following: 1) molecular weight protein standards, 2 to 13) IEF fractions 1 to 12 respectively of protein lysate from 30 µM DNCB-treated HaCaT cells, whole cell protein lysate from vehicle (14) and 30 µM DNCB-treated (15) HaCaT cells. SDS-PAGE lanes 2 to 13 show interference with the Coomassie blue staining, probably by ampholytes from the fractionation buffer not removed by dialysis which would pick up the Coomassie blue stain.

The lysates from one experiment incubating HaCaT cells with DNCB were added to the cultured PBMCs of sensitized volunteers for 6 days before proliferation was measured in the same way as the direct chemical treatment. Figure 4.4 shows that the response to proteins from DNCB-treated HaCaT cells is also above the strong reaction threshold of the stimulation index. In most cases, there was a significant reduction in proliferation in response to the control lysate, possibly due to toxicity of the lysis buffer.

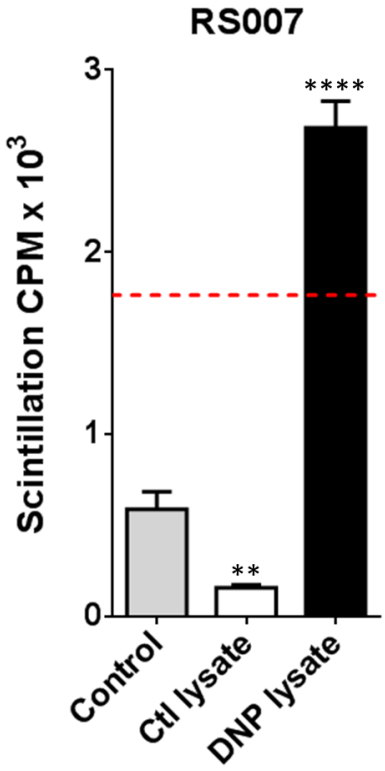

Figure 4.4. T-cell responses to dinitrophenyl HaCaT proteins

T cell proliferation responses from a DNCB-sensitized donor. T-cell proliferation as indicated by scintillation counts per minute. Results from PBMCs cultured with 20 µg/ml lysate of 36 µM DNCB-treated HaCaTs (DNP lysate) vs. 20 µg/ml of lysate of DMSO vehicle –treated HaCaTs (Ctl lysate). The red dotted line denotes where the stimulation index = 3.

Result is representative of 3 experiments.

Due to ethical consideration concerning the replicates pertaining to Figure 4.4, the experiments were repeated with a partially different cohort of donors. The donor RS007 was re-tested and new donors RS226 and RS228 were used. Protein lysate isolated from a repeat experiment incubating HaCaTs with DNCB using the same technique did not elicit a positive response in PBMC cultures and showed a significant decrease in lymphocyte proliferation in some experiments, indicating some cytotoxicity (Figure 4.5).

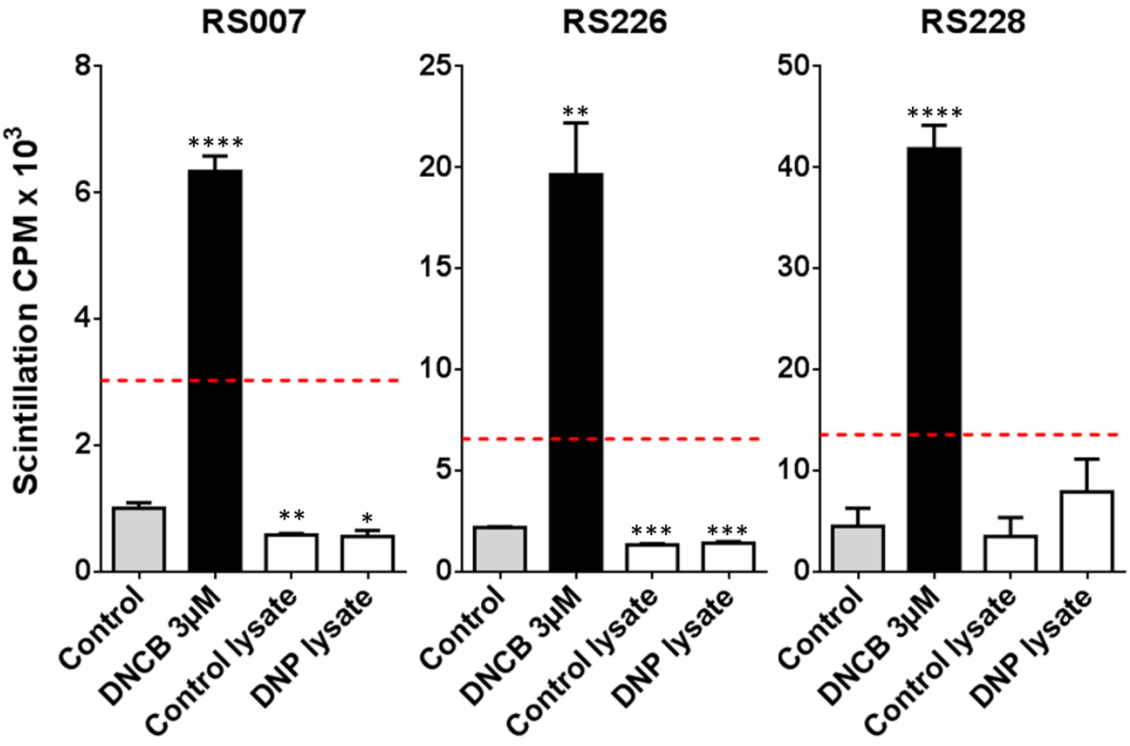

Figure 4.5. No lymphocyte proliferation responses to DNP-labelled HaCaT proteins with a repeat experiment

Donors responding to DNCB stimulation showing no proliferative response to DNP-labelled protein lysates from HaCaT cells. A negative response is observed in some experiments for the DNP-labelled and control lysates, suggesting cytotoxicity of the protein lysates.

The red dotted line denotes where the stimulation index = 3.

The whole cell lysates were fractionated using IEF and each fraction was then dialysed against 50 mM ammonium bicarbonate to remove IEF buffer. The dialysed fractions were added to LPA assays individually and a mixture of all fractions was also added for comparison. None of the 12 fractions elicited a proliferation response in PBMCs from any of 3 donors who showed a positive response to DNCB. Further to this lymphocytes treated with the fractions at a 1:100 dilution tended to show lower proliferation versus control, indicating that the fractions were cytotoxic (Figure 4.6).

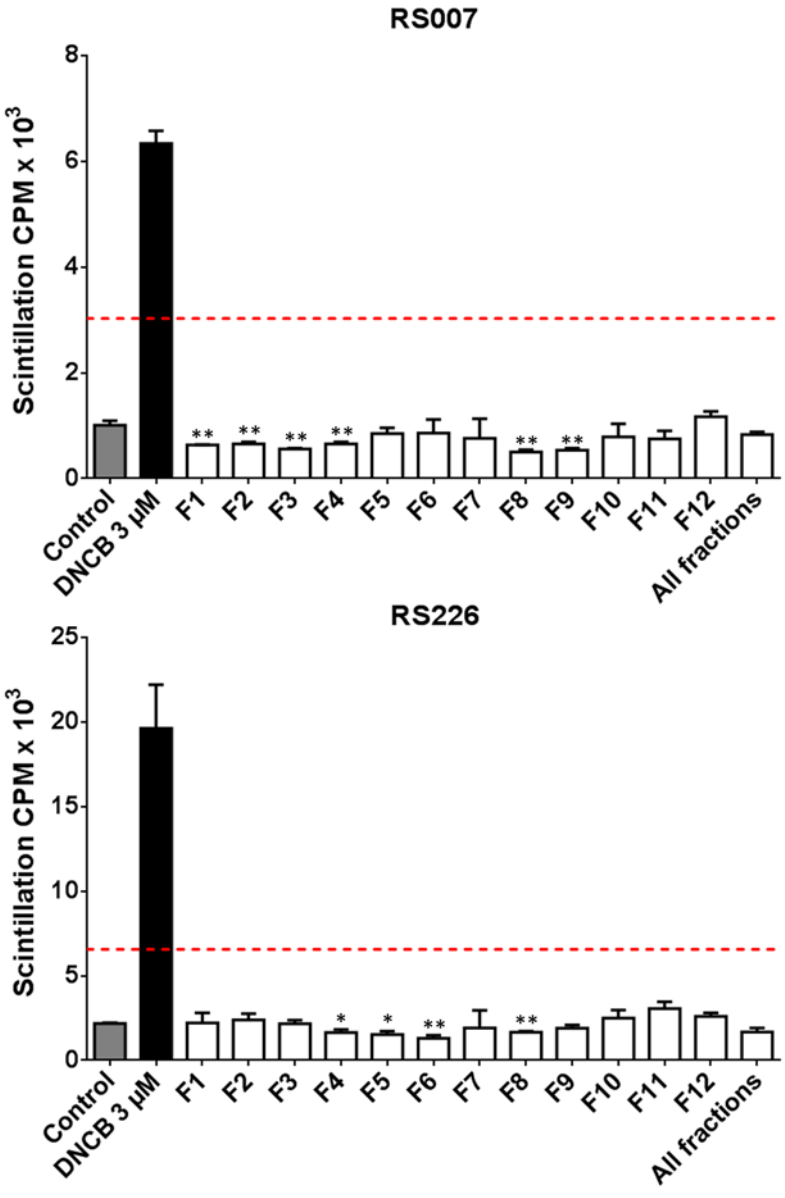

Figure 4.6. No proliferation in response to 12 DNP-HaCaT protein fractions

Proliferation responses to 3 µM DNCB, DNP-labelled HaCaT cell fractions 1-12 diluted 1:100 (F1-F12) and a pool of all 12 fractions diluted 1:100 (all fractions). Some fractions showed significantly reduced PBMC proliferation versus control.

The red dotted line denotes where the stimulation index = 3.

Incubation with dinitrophenylated human serum albumin (DNP-HSA) demonstrated that the PBMCs proliferated, albeit weakly, in response to a DNP-specific protein antigen in culture (Figure 4.7).

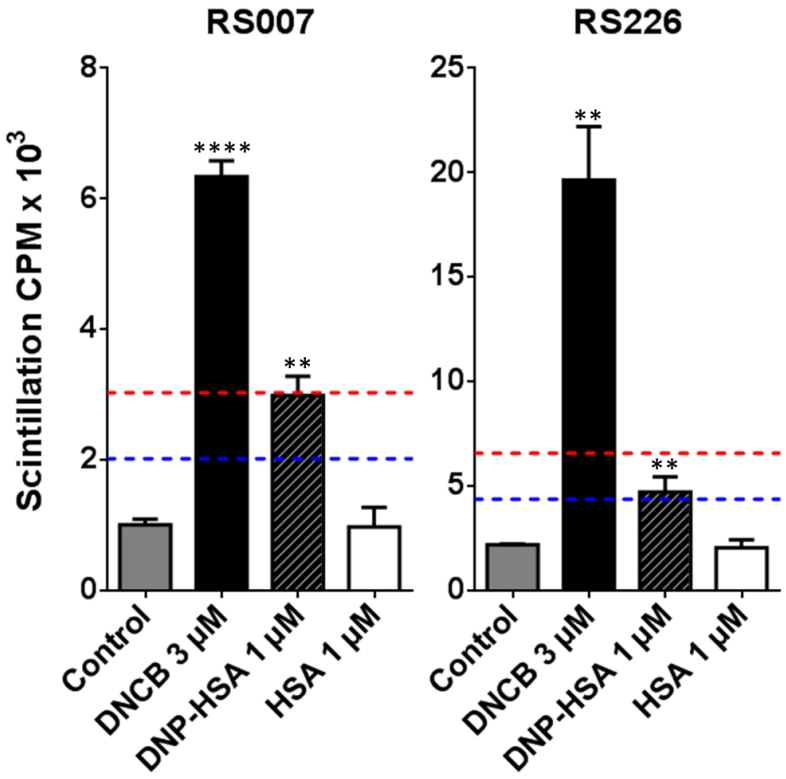

Figure 4.7. Lymphocyte responses to DNP-HSA

Antigen-specific lymphocyte proliferation in response to DNCB is demonstrated alongside a weak positive response to DNP-HSA versus non-DNP-HSA. The red and blue dotted lines denote where the stimulation index = 3 & 2 respectively.

4.3.3 Lymphocyte proliferation responses to primary keratinocytes

Primary keratinocytes extracted directly from human epidermis without transformation, are the closest cellular alternative to human skin. However, they were not used throughout this project as a model for skin due to their tendency to rapidly stop proliferating. Nonetheless, it was considered useful to compare them to HaCaT cells in these experiments to further explore the use of the latter as a suitable analogue for skin. Proteins were isolated from HPEK primary keratinocytes (CellnTec) donated by Dr Marta Polak (Dermatopharmacology, University of Southampton School of Medicine) incubated with either DMSO or 30 µM DNCB for 2 hours. Due to a limited amount of available material, responses could only be measured for two individuals. A strong positive response from PBMCs of one of the subjects (RS007) consistent with that of the dinitrophenyl HaCaT proteins was observed, however the other donor (RS042) showed a too great variation in response to reach statistical significance (Figure 4.8).

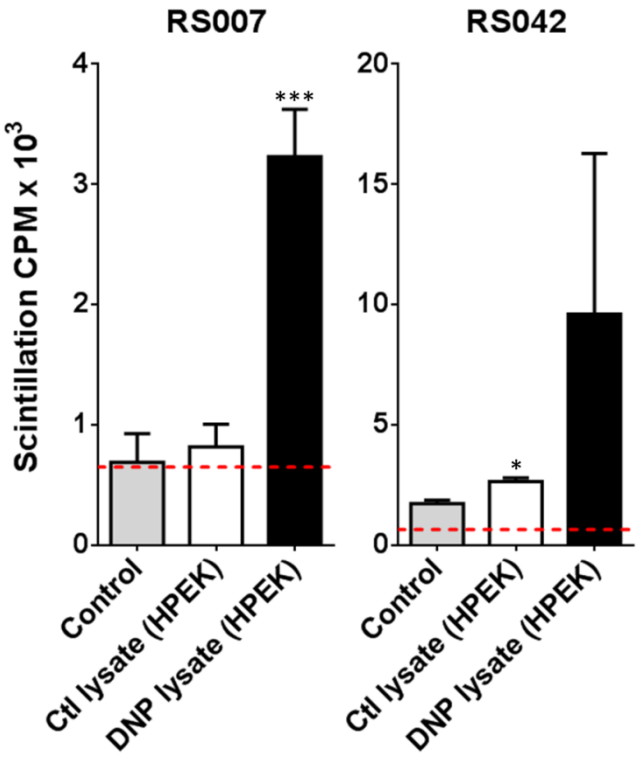

Figure 4.8. T-cell responses to dinitrophenyl primary keratinocyte proteins

T cell proliferation responses from 2 subjects RS007 and RS042. T-cell proliferation as indicated by scintillation counts per minute. Results from PBMCs cultured with RPMI medium, 3 µM DNCB, 16 µg/ml lysate of 36 µM DNCB-treated primary keratinocytes vs. 16 µg/ml of lysate of DMSO vehicle –treated HaCaTs (VTPK).

The red dotted line denotes where the stimulation index = 3.

The data shown here represent 3 positive strong (SI >3) responses to the lysates from a cohort of 7 volunteers sensitized to DNCB, 2 of which did not show responses to DNCB or modified lysates above the SI = 3 threshold (Table 4.1).

Table 4.1. Low T-cell proliferation responses

Stimulation index values for two volunteers sensitized to DNCB. Values below 3 are considered to be weak responses and values below 2 are not considered to be a significant response (Pichler and Tilch, 2004). VTL = vehicle treated HaCaT lysate, DTL = DNCB treated HaCaT lysate.

Volunteer ID	DNCB 3 μM (SI)	VTL (SI)	DTL (SI)
RS227	0.32	0.67	1.14
RS229	1.14	1.13	1.04

4.4 Discussion

The work in this chapter has demonstrated that the PBMCs from DNCB-sensitized donors can exhibit strong proliferative responses to direct stimulation with DNCB. The assay did not give consistent results to proteins extracted from HaCaT cells treated with DNCB in culture, however the strong positive response to the HaCaT lysates (Figure 4.4) indicate that modified proteins derived from these cells can provide a useful array of antigens able to provoke a strong, antigen-specific response. This is also supported by the data for modified primary keratinocyte proteins, which are a closer cellular equivalent to the keratinocytes in skin.

The western blots clearly show that both the whole cell lysates and the fractions contained DNP-labelled proteins. However, neither the second iteration of the experiments using HaCaT lysates or the 12 fractions generated from the DNP-labelled HaCaT lysates were able to elicit a proliferative response to DNP-proteins. The significantly reduced proliferation observed relative to the controls indicate that there is some cytotoxicity occurring. This could be for a number of reasons:

1) Toxicity of the cell lysis buffer

Detergent not removed from the lysis buffer by the SDS-removal columns could be toxic to lymphocytes when added to culture (Sirisattha et al., 2004). This is supported by the significant reduction of proliferation observed in PBMCs with lysates from vehicle-treated and DNCB-treated HaCaTs added. However, during the initial experiments extracting proteins from DNCB-treated HaCaTs, a lysis buffer was used which contained an anionic acid-labile surfactant (AALS, see chapter 2, section 2.16), which could be cleaved by acidification of the sample. While responsible for the initial positive results, this buffer proved highly toxic to lymphocytes during the second round of experiments. The reason for this difference may have been the decision to cease using protease inhibitors in the lysis buffer (see below). The decision to use 0.05% SDS followed by SDS-removal with resin (see chapter 2 section 2.16) was based on a comparison between this method and the AALS showing that the former was less toxic.

2) Noxious macromolecules present in the lysates

Protease inhibitors were present in the cell lysates in initial work when extracting proteins from HaCaT cells (see chapter 2 section 2.16, method 1), but were omitted from subsequent experiments to simplify intended downstream analysis by mass spectrometry. In their absence, it is possible that cellular proteases in the lysate may have been active in the PBMC cultures and affected the viability of the lymphocytes (Sarin et al., 1993). In addition to this, it is possible that there are other proteins within the cell lysate ordinarily contained within organelles such as lysosomes which could prove harmful to lymphocytes in culture.

3) Stochastic or unknown antigenic determinants

It is possible that the initial positive responses to the first batch of cell lysates was due to the chance generation of an immunogenic protein or proteins which did not occur during the follow-up experiments. It is also possible that the toxicity from the lysates, which were observed for both experiments, were offset by a proliferative response to a DNP-antigen being greater than the reduction in proliferation by any cytotoxicity. While DNP-labelled proteins were present in the cell lysates and fractions (Figure 4.3), it is not known if any of these proteins are immunogenic.

The fractions derived from the HaCaT lysates also demonstrated a lack of immunogenicity and there was also toxicity observed in response to some fractions (Figure 4.6). Since the fractions were dialysed, it seems unlikely that cell lysis agents are responsible for the toxicity, supporting the hypothesis that cellular proteases or other noxious molecules could be responsible.

These results suggest further optimisation of the methods used to generate modified proteins from HaCaT cells would be needed to generate a consistent result.

The identification of dinitrophenylated peptides from proteins within each fraction was attempted by proteolytic digestion of the fractionated proteins followed by LC-MS^E analysis. However, no DNP-proteins were identified within any of the fractions; indeed, the ProteinLynx Global Server (PLGS) analysis of the spectra produced showed a very

low number of protein identifications (data not shown). This is possibly caused by the omission of a reduction step, which was excluded to reduce the risk of thiolysis of DNP groups from cysteine (see chapter 6). The lack of reduction would result in many cysteines remaining in disulphide bridges, which would complicate the identification of proteins since these would not be alkylated by the addition of iodoacetamide (see chapter 2 section 2.20). Additionally, non-reduced protein would be prone to more missed cleavages during enzymatic digestion by Lys-C and trypsin, which would result in longer peptides which are not analysed as efficiently by mass spectrometers. Another factor in the identification process is the increase in identifying peptides as false positives if the software is configured to allow for more than 2 missed cleavages.

4.5 Summary

While variable results are an inherent issue with lymphocyte proliferation assays (Pichler and Tilch, 2004)**,** they remain useful for determining responses to chemicals and modified proteins, as demonstrated previously in drug allergy studies (Brander et al., 1995; Cavani et al., 1998; Jenkins et al., 2013; Mauri-Hellweg et al., 1995; Schnyder et al., 2000). However, results from experiments probing the immunogenicity of modified proteins with cell lysates were inconsistent. Interrogation of the literature highlights a lack of studies using these assays to identify immunogenic proteins from whole cell lysates. This could be due to use of lysates proving similarly problematic elsewhere, but also highlights the importance of optimising the methods.

5 THE EFFECTS OF DNCB CONCENTRATION AND INCUBATION TIME ON THE MODIFICATION OF HUMAN SERUM ALBUMIN

5.1 Introduction

Human serum albumin (HSA) has been used to study the covalent modification products of a range of skin sensitizers, including hexane sultones (Meschkat et al., 2000), 5-Chloro-2-methylisothiazol-3-one (MCI) (Alvarez-Sánchez et al., 2004), phenyl salicylate and DNCB (Aleksic et al., 2007), p-Phenylenediamine (PPD) (Jenkinson et al., 2010). HSA is widely utilised as a model protein due to its well characterised sequence and structure (Curry et al., 1998; He and Carter, 1992; Sugio et al., 1999) and its high abundance in human blood and tissues. HSA has a number of roles in important biological processes, including oncotic pressure regulation, pH buffering, transport of hormones, fatty acids, bilirubin and zinc (Fasano et al., 2005; Lu et al., 2008; Theodore Peters, 1995). It is synthesised in the liver as preproalbumin with the pre and pro N-terminal sequences being cleaved in the endosome and Golgi apparatus respectively to give the mature protein.

Crystal structures of HSA (Sugio et al., 1999; Wardell et al., 2002) describe it as a single chain protein with a relative molecular weight of approximately 66,500 Da and is composed of 3 homologous domains: I, II and III. The secondary structure is formed primarily of a series of alpha-helices connected by flexible loops. Each domain is made from two sub-domains denoted a and b. Sub-domains Ia, IIa and IIIa containing 6 α-helices, while Ib, IIb and IIIb contain 4. Within an HSA monomer, there are 35 cysteines, 34 of which are involved in 17 disulphide (S-S) bridges, which provide stability to the tertiary structure. There is also one unpaired cysteine at position 34 (Figure 6.1). Cysteine 34 exists *in vivo* either in a reduced state (Cys-SH) as part of mercaptalbumin (mHSA), or as albumin-Cys^{34}-S-S-Cys, where the conjugated cysteine is from another molecule (Mansoor et al., 1992). Cysteine 34 is known to bind nitric oxide, Hg^{2+} and several drugs *in vivo* (Kragh-Hansen et al., 2002), thus it is potentially available for modification by DNCB, which reacts readily with cysteine.

HSA has 2 primary binding sites which can accommodate a range of endogenous ligands, such as bilirubin, methylglyoxal, octanoate, L-tryptophan; as well as drugs, including warfarin, diazepam, ibuprofen, salicylate and many others (Kragh-Hansen et

al., 2002). These regions, referred to as Sudlow sites I and II (SUDLOW et al., 1975) are hydrophobic cavities on exposed areas of the protein *in vivo* and are of potential interest when studying haptenation by hydrophobic molecules such as DNCB.

As well as being the most abundant protein in blood, albumin is also present in high levels in the skin (Theodore Peters, 1995). Lymphocyte proliferation studies have also shown that hapten-bound HSA is able to stimulate T-cell proliferation in donors allergic to chemical sensitizers (Frew et al., 1998; Jenkinson et al., 2010). These factors combined make HSA a relevant protein to study in the context of skin sensitization.

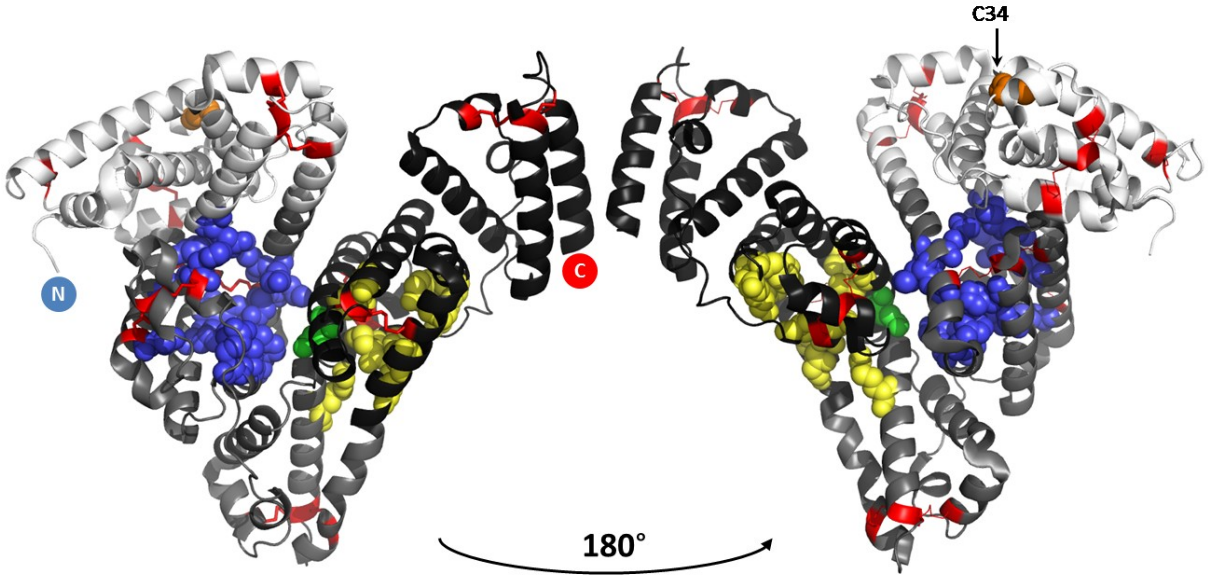

Figure 5.1. An annotated structure of HSA

A 3-dimensional crystal structure (1N5U) of a human serum albumin monomer at 1.9Å resolution with 1 hemin and 5 myristate molecules (not shown) bound. Colours denote the following: domain I (white), domain II (grey), domain III (black), Sudlow binding site I (blue), Sudlow binding site II (yellow), Glu450 found in both Sudlow sites (green), S-S bridges (red) and the free cysteine 34 (orange).

DNCB modifies the nucleophilic amino acid residues cysteine, histidine, lysine and tyrosine as well as N-terminal amines present in proteins and peptides via an electrophilic substitution reaction (Aleksic et al., 2009). There are suggestions that residues are modified by haptens in a determined, rather than stochastic fashion, influenced by the microenvironment of each residue (Chipinda et al., 2011).

Studies of dinitrophenylation of human serum albumin have previously focussed on end point analysis and the identification of modified residues with a large excess of sensitizer after a 28 day incubation (Aleksic et al., 2007). Investigating chemical modification of HSA by DNCB at different time points using a range of DNCB concentrations not only allows assessment of the relative reactivity of any residues detected as modified, but also allows an opportunity to use more advanced methods to provide a more in-depth characterisation of protein modification by DNCB compared with the combined MALDI-MS and ESI-MS/MS approach used earlier (Aleksic et al., 2007).

Previous investigation of dinitrophenyl HSA (Aleksic et al., 2007) has identified modification to lysines 195, 199 and 414 from the aforementioned binding sites, as well as the N-terminal aspartic acid, lysines 212, 225 and 351; tyrosine 140, histidine 9 and the free cysteine 34.

Using dual isotope labelled DNCB to modify HSA at different chemical concentrations and incubation times, this work aims to determine the modification kinetics of DNCB to determine which amino acid residues are the most readily modified *in vitro*.

5.2 Experimental design

DNCB modification of HSA

HSA was incubated with either DNCB or deuterated DNCB at each of 5 concentrations with molar ratios of 0.5, 1, 10, 50 & 100 DNCB to HSA as well as a vehicle control (see chapter 2). At time points of 1 hour, 6 hours, 24 hours, 8 days and 47 days, DNCB and deuterated DNCB samples from each concentration were mixed in equal amounts and the reaction stopped using separation by SDS-PAGE (see chapter 2). A zero time point for the highest DNCB concentration was also included to control for any modifications occurring during the SDS-PAGE reduction step in Laemmli sample buffer. To quantify the amount of modified protein, absorbance at 360 nm was measured for each concentration (as well as DNCB+PBS and HSA+PBS controls) at the same time points up to 8 days.

Tryptic digestion and mass spectrometric analysis of DNP-HSA

The 66 kDa protein was visualised using Coomassie blue stain, excised from the gel and digested using trypsin as described in chapter 2. The extracted peptides from each sample were then separated by reversed-phase liquid chromatography and analysed by ESI-MS^E mass spectrometry as described in chapter 2.

Assignment of modifications was performed using a dual isotope-labelling method. Here, both deuterated (d3) and standard (d0) DNCB was used to modify HSA, where peptides carrying a modification were represented as doublets separated by 3 Da per modification within the mass spectra. This enabled confident identification of modifications orthogonal to delta mass-derived modifications identified by ProteinLynx Global Server (PLGS). This technique using isotope signature in combination with MS/MS spectra was used to qualitatively determine which amino acid residues within the HSA sequence were found modified by DNCB (see chapter 2). An overview of the experimental workflow can be seen below (Figure 5.2).

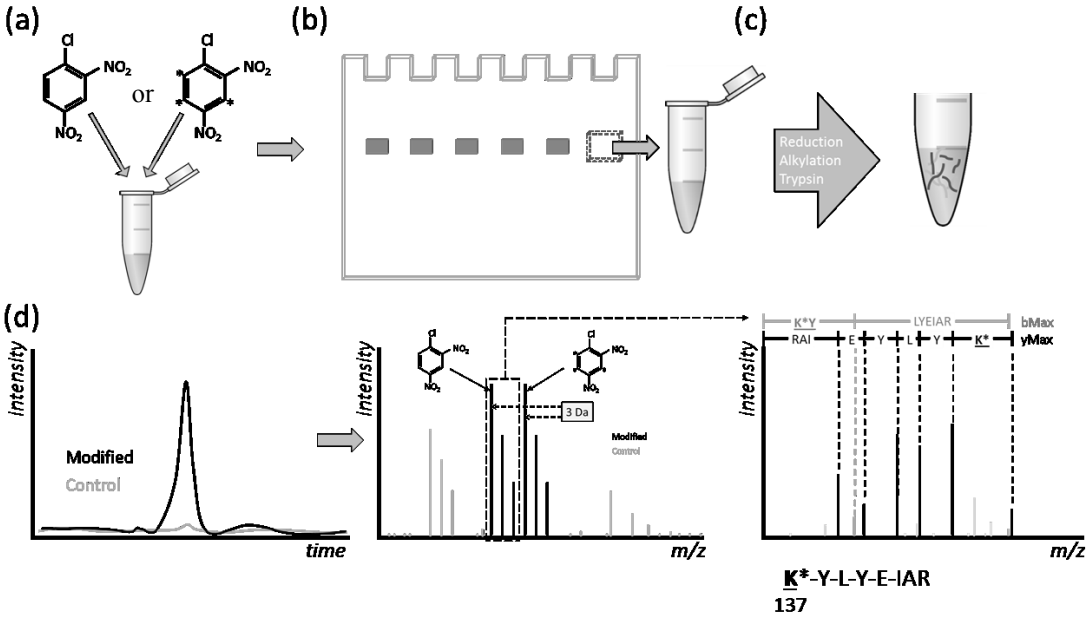

Figure 5.2. Mass spectrometric method of identifying DNP adducts in human serum using stable isotope labelled DNCB

A diagram showing the workflow used to modify HSA and determine the sites of modification: a) HSA is incubated with equal amounts of DNCB and deuterated DNCB at a range of concentrations for 4 different incubation times, b) each reaction is stopped by separation using SDS-PAGE and the protein stained using Coomassie blue and excised from the gel, c) protein within the excised gel pieces is reduced, alkylated and digested with trypsin and the peptides are extracted for mass spectrometry analysis, d) the peptides are separated and analysed using nano-LC-ESI-MS^E. Isotope doublets separated by m/z *values equivalent to 3 Da within the mass spectra were used to confirm identifications of DNP modification assigned by PLGS. The MS/MS spectra were then used to assign the modification to a specific residue with the HSA sequence.*

5.3 Results

Work carried out by Dr Richard Cubberley (Unilever Safety and Environmental Assurance Centre, Colworth, UK) determined that protein modified with DNCB shows high absorbance at 360 nm (data not published). The net absorbance was plotted for each concentration and time (Figure 5.3). While some background absorbance at this wavelength was observed in the negative controls (DNCB incubated with PBS) proportional to the DNCB concentration, this absorbance did not change over time and was subtracted as background from the absorbance values for protein modification.

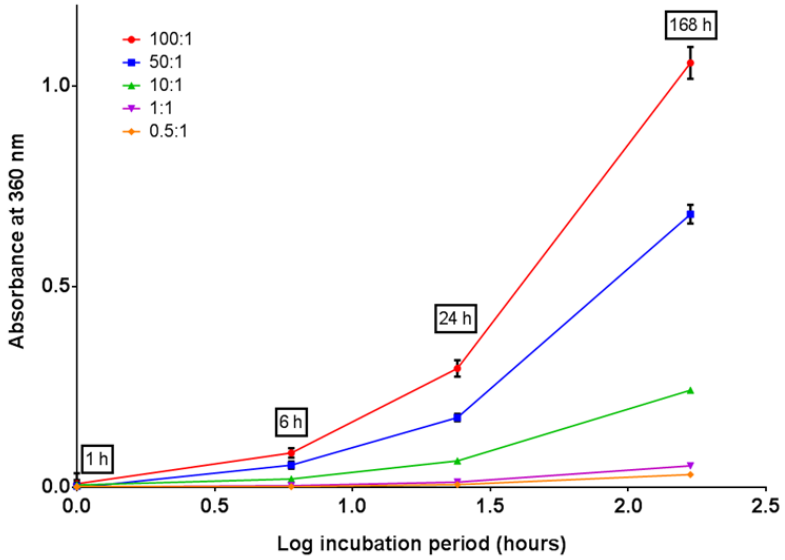

Figure 5.3. Dinitrophenylation of human serum albumin

Graph showing the rate of protein dinitrophenylation represented as an increase in absorbance at 360 nm. The 5 concentrations are shown as molar equivalents of DNCB to HSA. Data from triplicate absorbance readings are shown as the mean A360 of sample minus absorbance readings from DNCB+PBS and HSA+PBS controls.

After analysis by LC-MS^E, data was processed using PLGS software with parameters set to identify potential dinitrophenyl (DNP) adducts corresponding to a delta mass of 166.0015 Da. False positives were removed by excluding any DNP-modified peptide IDs which were also found in the vehicle control. The remaining DNP modifications identified by the software were manually accepted or rejected by checking the corresponding mass spectra for visible precursor ion peak doublets separated by the *m/z* equivalent of 3 Da per DNP adduct. For higher molecular weight peptides having more than 3 isotopic peaks, the modification was identified by a marked increase of intensity at the fourth peak denoting overlap with the deuterated moiety. Any precursor spectra

which matched with peaks found in the vehicle control at the same retention time were rejected.

A first pass of verification of the PLGS IDs yielded 57 potentially modified amino acid residues. Many of these identifications were not ideal due to low quality MS/MS data, insufficient to confidently determine which residues were modified. An ideal identification was characterised by the MS/MS showing intense fragment ions with a good signal to noise ratio and a low intensity *y max* ion indicating sufficient fragmentation, with the modified residue being distinguished from the sequence by a distinct *y* or *b* ion, or combination of *y* and *b* overlap (Figure 5.4 c). Peptides which did not have sufficient precursor ion fragmentation to identify the exact residue which was modified could still have their site of modification deduced based upon the modification being on a nucleophilic residue able to be modified by DNCB, *e.g.* cysteine, histidine, lysine & tyrosine (Aleksic et al., 2009), provided the *y* or *b* ion containing the modification in the MS/MS data did not contain more than one nucleophile (e.g. a cysteine and a histidine). For those with more than one nucleophile, both residues were noted as being potential sites of modification and rejected unless either site was confirmed by higher MS/MS data from another sample.

To definitively identify a modified amino acid residue, three criteria were used:

1. Peptide precursor spectra should be accompanied by a deuterium isotope signature proportionate to the presence of one or more d3-DNP modifications.
2. MS/MS fragmentation of the precursor peptide should be sufficient to determine its full sequence.
3. Fragmentation of the peptide should be sufficient to isolate the modified amino acid residue either by specific isolation of the modified residue or by deduction from elimination of non-nucleophilic residues.

Identifications not supported by deuterium signatures were rejected outright and those with insufficient MS/MS data to identify a specific residue modification were not retained unless supported by a confident identification for the same retention time and *m/z* in another DNCB-treated sample.

A

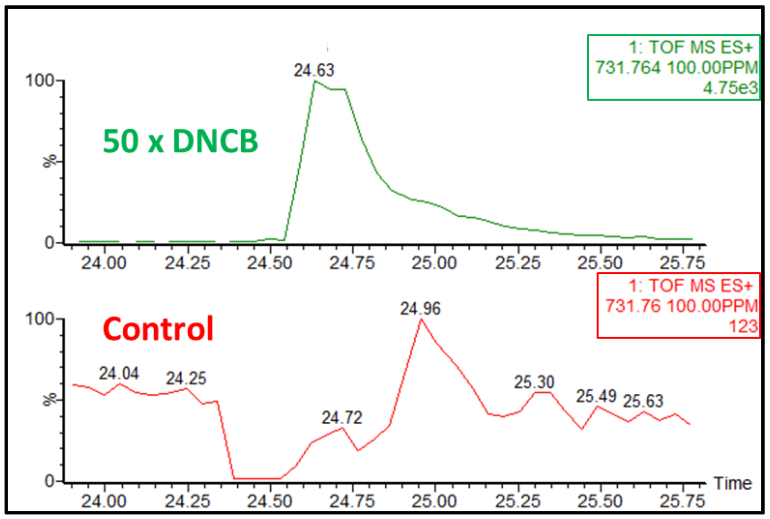

B

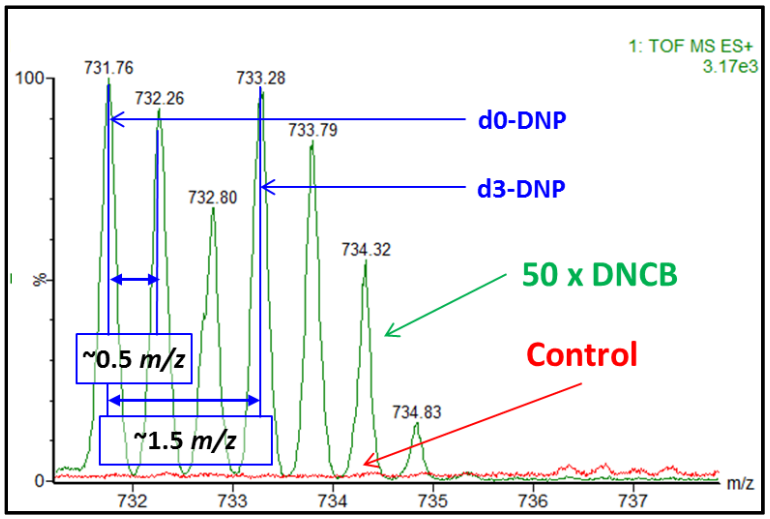

C

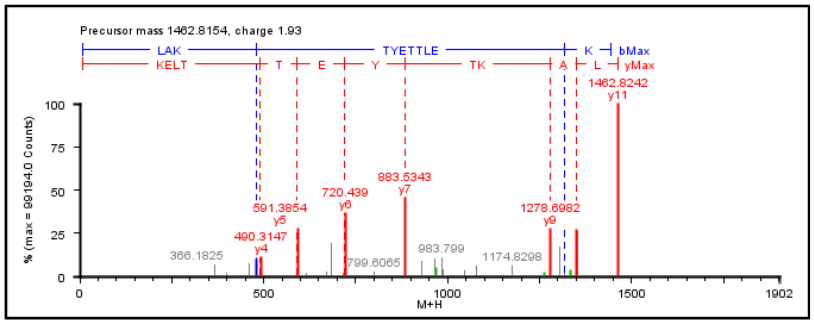

Figure 5.4. Mass spectrometric identification of amino acid residues modified by DNCB

*Representative diagrams showing the following: A) Control vs. modified extracted ion chromatogram peaks showing the elution time (x) vs. relative peak intensity (y) for precursor ion $[M+H]^{2+}$ m/z 731.76, B) Control vs. modified overlaid mass spectra showing a doubly charged peptide peak doublet beginning at m/z 731.76 $[M+H]^{+2}$ at retention time 24.635 minutes, C) b (blue) and y (red) ions generated from collision induced dissociation fragmentation of the precursor ion giving the sequence LAK*TYETTLEK (residues 349-359 of HSA).*

** - denotes the modified lysine 351.*

Some peptides which contain more than one modification would only be expected to give a doublet in the mass spectra separated by 6, rather than 3 Daltons, due to the incubations of the DNCB and deuterated DNCB being performed separately. In some cases however, a peak triplet was observed (Figure 5.5).

A

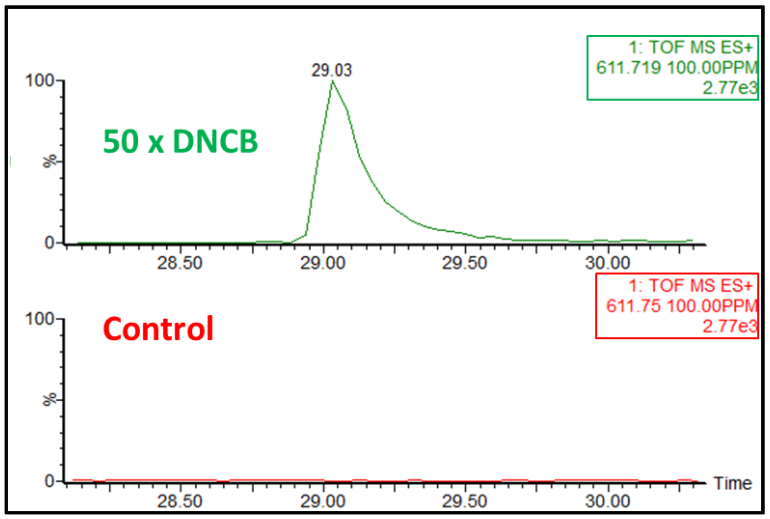

B

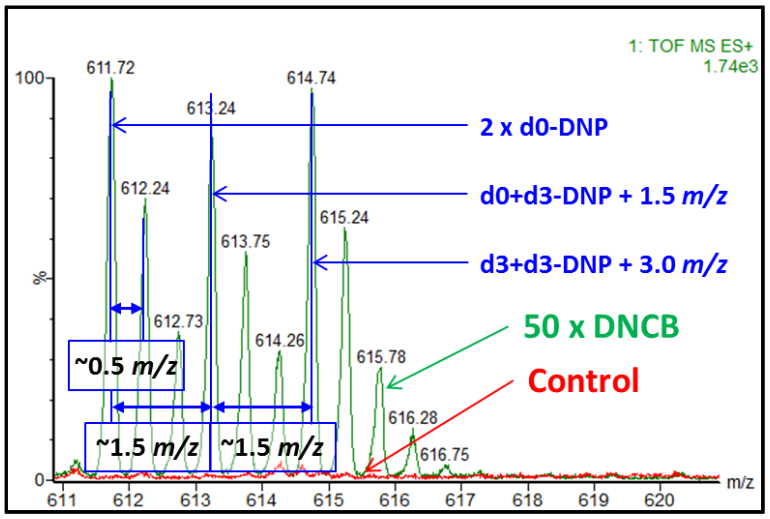

C

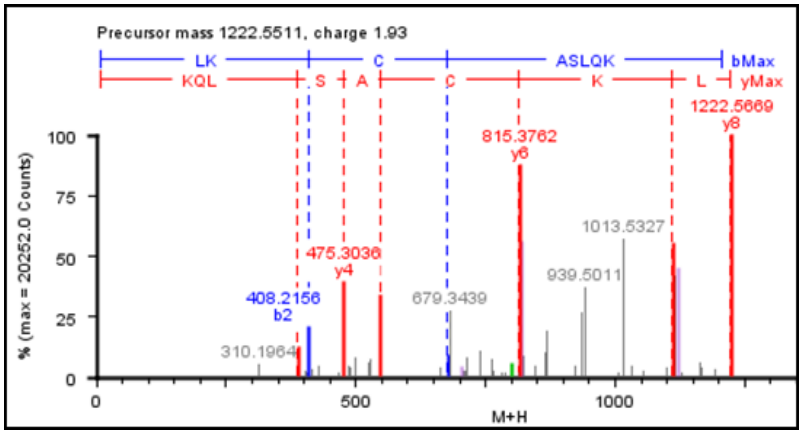

Figure 5.5. An isotope triplet showing 2 DNP modifications

*Control vs. modified overlaid chromatography and mass spectra showing a doubly charged peptide peak triplet beginning at m/z 611.70 $[M+H]^{+2}$ at retention time 28.939 minutes. The peptide detected was LK*C*ASLQK*

** denotes the modified lysine 199 and cysteine 200*

A second pass of identifications was performed by checking the mass spectra for each concentration and time for deuterium signatures corresponding to the same retention time and *m/z* as confidently identified modifications. These IDs were not supported by MS/MS data as they were not identified using PLGS, but were determined to be the same peptide as already identified, due to having the same retention time, *m/z* value and isotope doublet in the mass spectra.

Using these criteria resulted in a list of 31 distinct amino acid residues found to be modified at various concentrations and times. The definitive list of amino acids found to be modified by DNCB were plotted as a matrix corresponding to the DNCB concentrations and incubation times in which they occurred (Figure 5.6).

To determine which modifications occurred readily relative to those which did not, each modified residue was assigned a score expressed as:

((1 ÷ time (h)) x (1 ÷ concentration (μM)) x 10^6

This gave higher scores to residues which only required a short incubation time or low concentration to modify. So for example a residue found modified at 6 hours with a concentration of 750 μM DNCB (50:1 DNCB:HSA), has a score of 222.22, where one found modified at 192 hours by 750 μM DNCB would have a lower score of 6.94. The modification matrix was then sorted in order of score and separated into a top and bottom half representing scores above and below the median residue score value as a means of broadly separating the residues into the most and least readily modified (MRSV) (Figure 5.6).

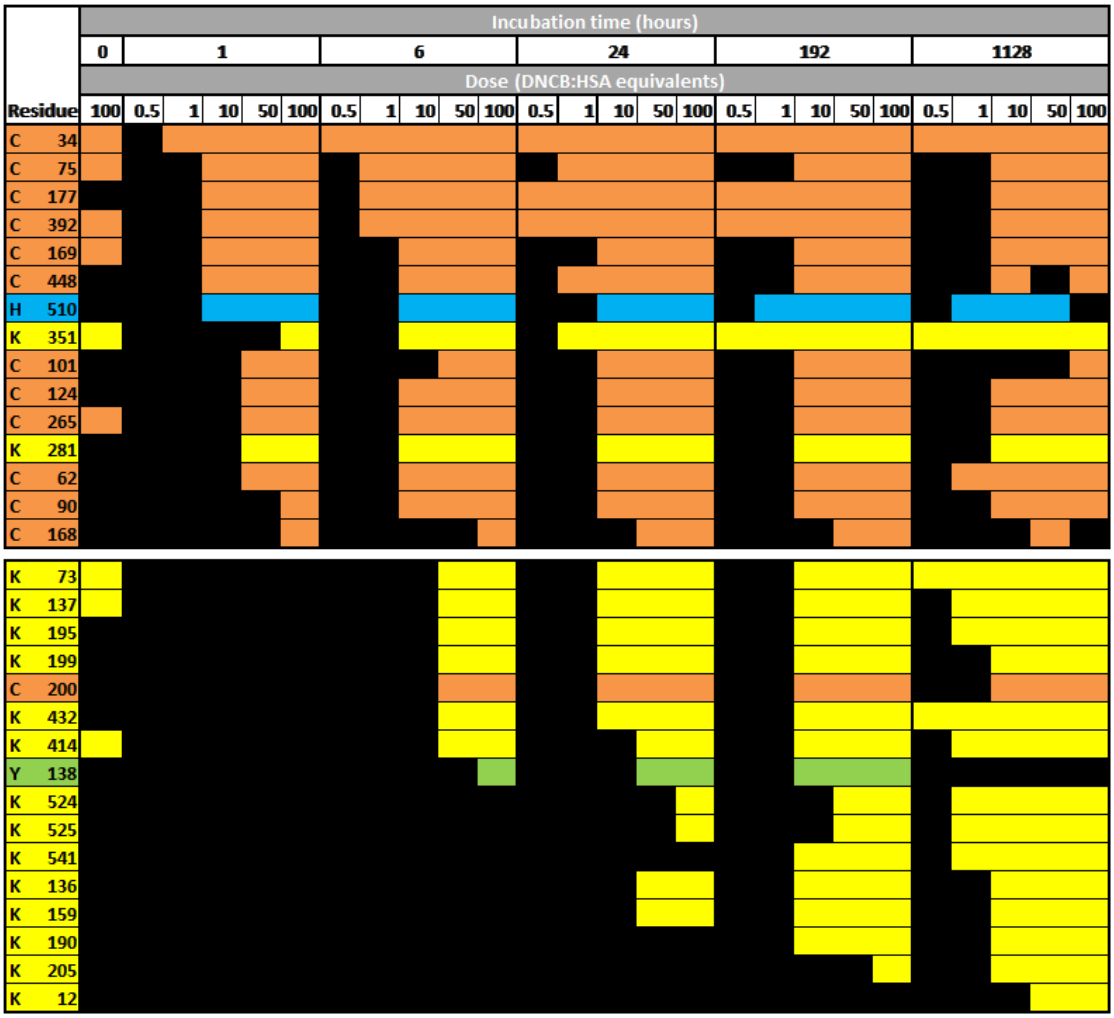

Figure 5.6. A heat map of DNP modifications to HSA

A list of identified residue modifications of HSA, mapped against incubation time and DNCB concentration. Each coloured cell corresponds to a modified amino acid residue. Amino acids are colour coded as: cysteine – orange; lysine – yellow; histidine – blue & tyrosine – green. The upper section above the break contains residues with a score above the median residue score value (MRSV) of 277.78, while the lower section contains those below the MRSV.

Modifications found at time point zero were quantified by integration of the extracted ion chromatograms for the modified precursor ions and then normalised for sample load by multiplication with the full chromatogram intensity for each sample. The values from this analysis were then plotted as a bar chart (Figure 5.7).

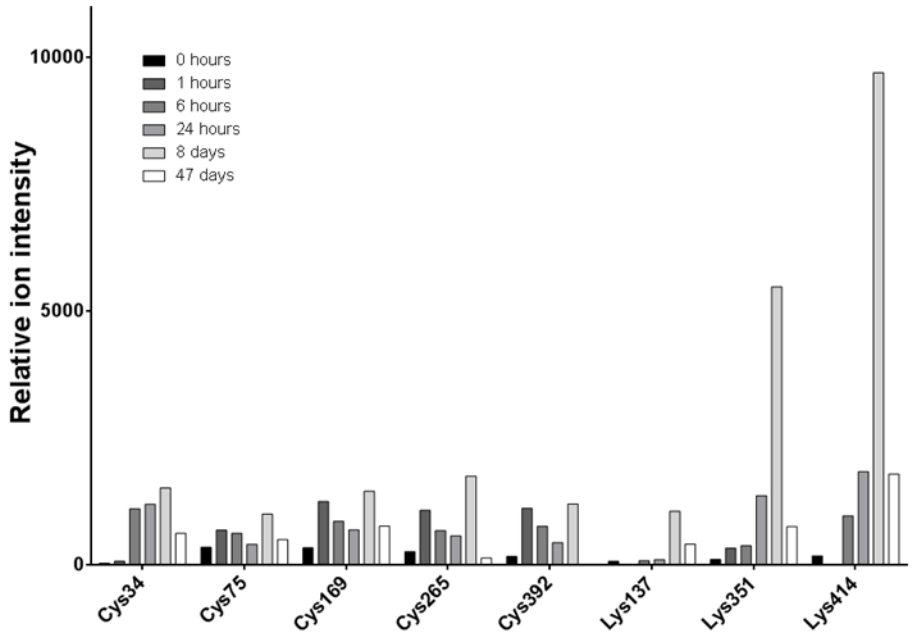

Figure 5.7. Modifications found at time zero are also influenced by incubation time
Bar chart showing the relative intensities of 8 different dinitrophenyl amino acid residues for each of 6 time points at the highest DNCB concentration of 1500 µM (100:1 DNCB:HSA).

The final list of all modified residues detected across all DNCB concentrations and incubation times was then used to create an annotated diagram of an HSA molecule taken from a crystal structure (Figure 5.8).

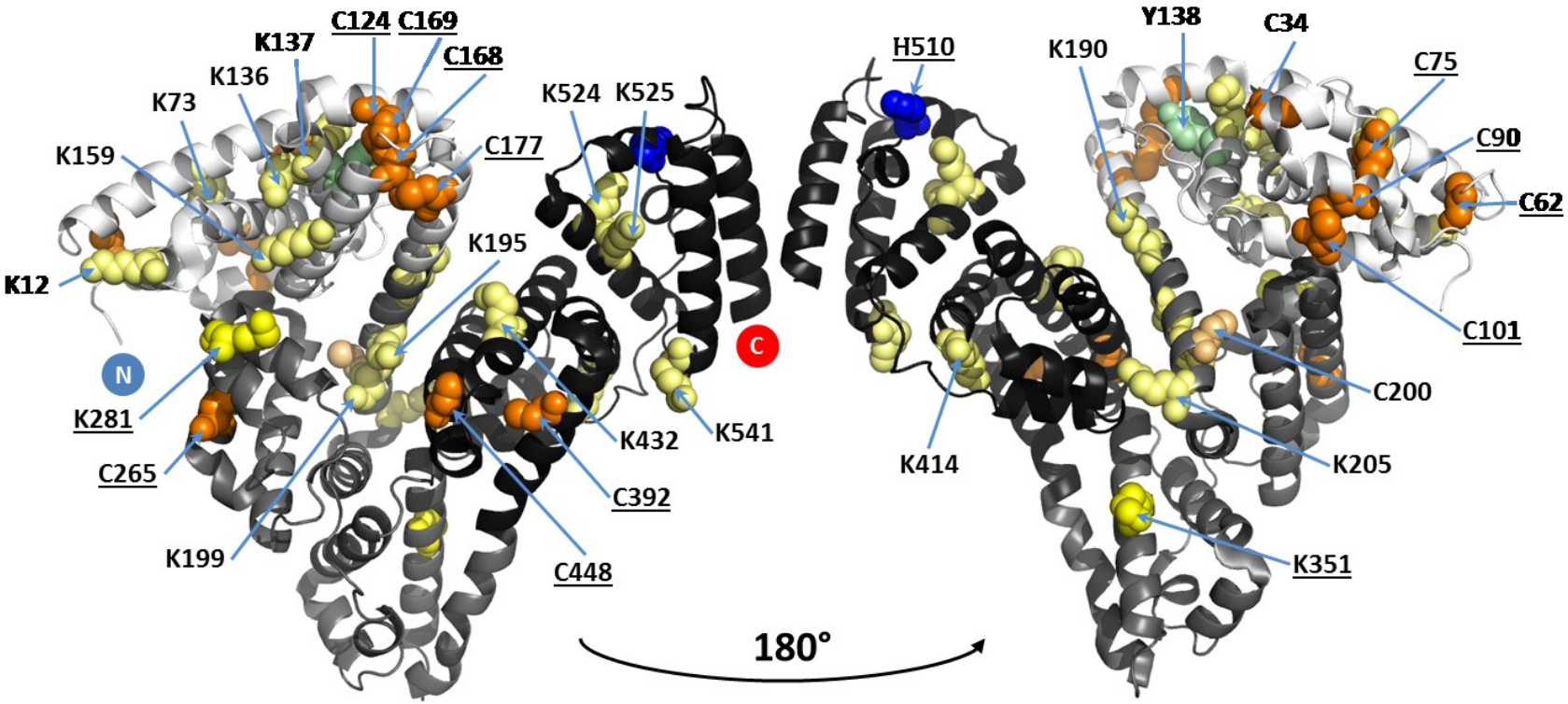

Figure 5.8. The distribution of HSA residues found modified by DNCB

A 3-dimensional crystal structure (1N5U) of a human serum albumin monomer at 1.9Å resolution with 1 hemin and 5 myristate molecules (not shown) bound. Region colours denote the following: domain I (white), domain II (grey), domain III (black). Modifications are coloured solid / pale to indicate residue scores above / below the median residue score value (MRSV) respectively: DNP-lysine (yellow / pale yellow), DNP-cysteine (orange / pale orange), DNP-histidine (blue), DNP-tyrosine (pale green). Modifications scoring above the MRSV are further highlighted by underscored labels.

A crystal structure diagram of HSA was annotated to show the position of all cysteine residues and then colour coded to show the order by score in which the cysteines were detected as modified and whether or not both cysteines in a S-S bridge were modified. The majority of cysteine modification is found within domain I of HSA with the 4 cysteines found modified within 2 S-S bridges (red-yellow) proximal to cysteine 34 in the 3-dimensional structure. Domains II and III show relatively few cysteine modifications and both areas found modified occur proximal to the C-terminus of the homologous domain (Figure 5.9). Diagrams showing the step-wise modification of cysteine in order of score can be found in the appendices (Figure 8.1).

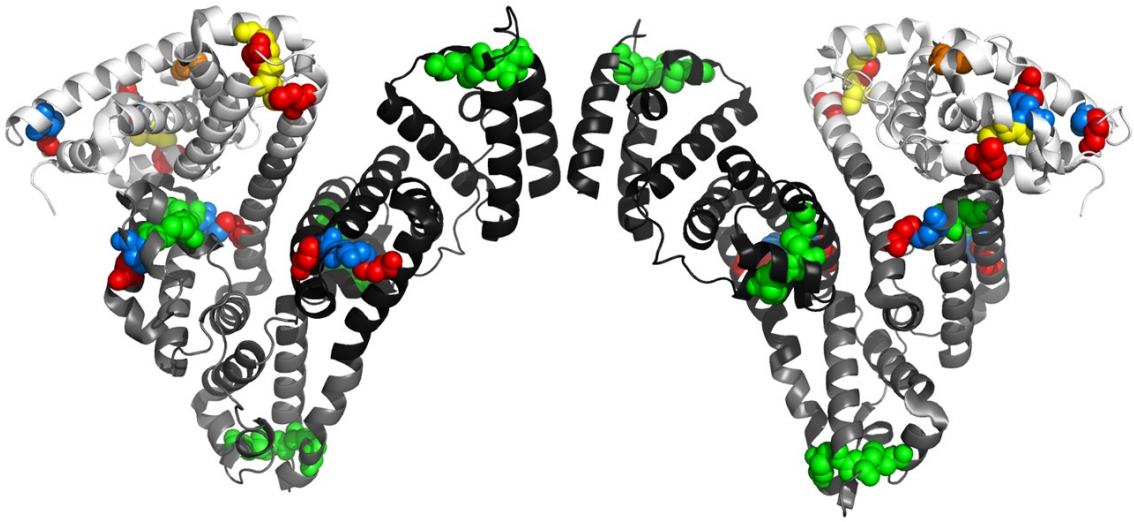

Figure 5.9. Cysteines within HSA found to be modified

Crystal structure of HSA (15NU) with domains I, II and III coloured white, grey and black respectively. All cysteines within HSA are represented as spheres and colour coded as follows: Green = non-modified cysteines forming a disulphide bridge assumed to be intact prior to reduction; Red = cysteine modified by DNCB, Yellow = cysteine modified by DNCB with a lower reactivity score than the red equivalent within the same S-S bridge; Orange = cysteine 34.

All of the modifications shown in Figure 5.6 were summed for each concentration and time point and plotted as a graph to show the change in number of sites modified over time per concentration (Figure 5.10). A two way ANOVA of the data in this graph suggest that both concentration and time had a significant effect on the number of modifications, with concentration being responsible for 74.75% of the variation ($F = 53.68$, $p < 0.0001$) and time being responsible for 19.68 % ($F = 14.13$, $p \leq 0.0001$).

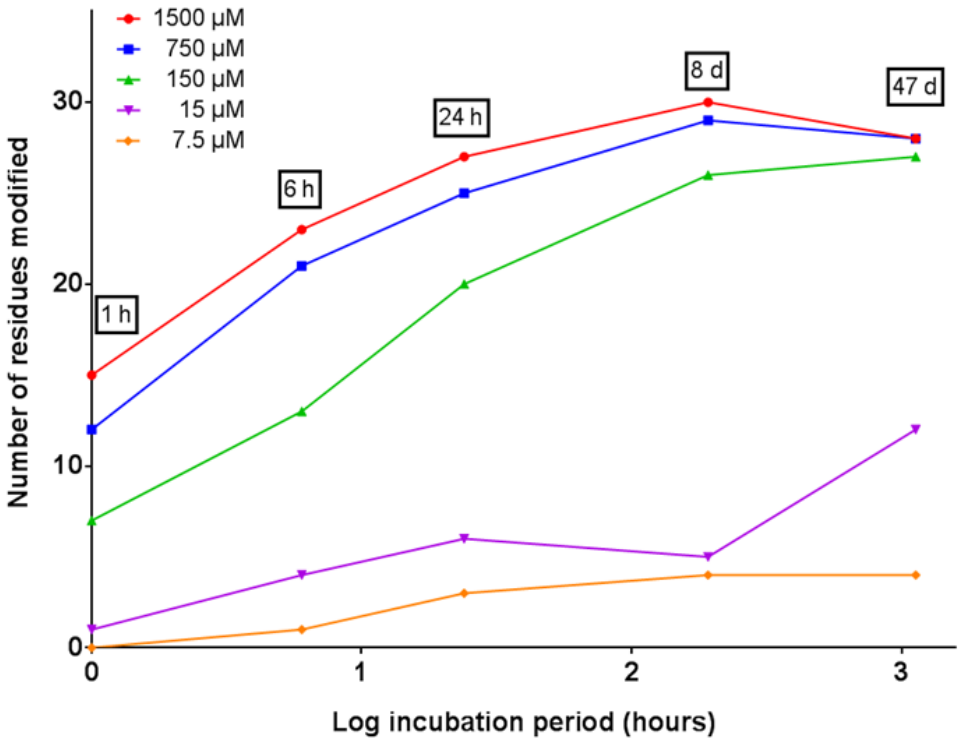

Figure 5.10. The total number of residues modified at 5 DNCB concentrations over time

A graph showing the total number of identified DNCB modifications of HSA at each incubation time point for each DNCB concentration.

Data for cysteine and lysine modifications were also plotted separately to illustrate differences in modification dynamics (Figure 5.11). Two way ANOVA analysis showed that for cysteine modifications, DNCB concentration is responsible for 86.29% of the variation ($F = 62.94$, $P < 0.0001$) and incubation time for 8.226% ($F = 6.00$, $P < 0.005$). For lysine modification, DNCB concentration explains 44.14% of variation ($F = 13.06$, $P < 0.0001$) and incubation time accounts for 42.34 % ($F = 12.52$, $P < 0.0001$).

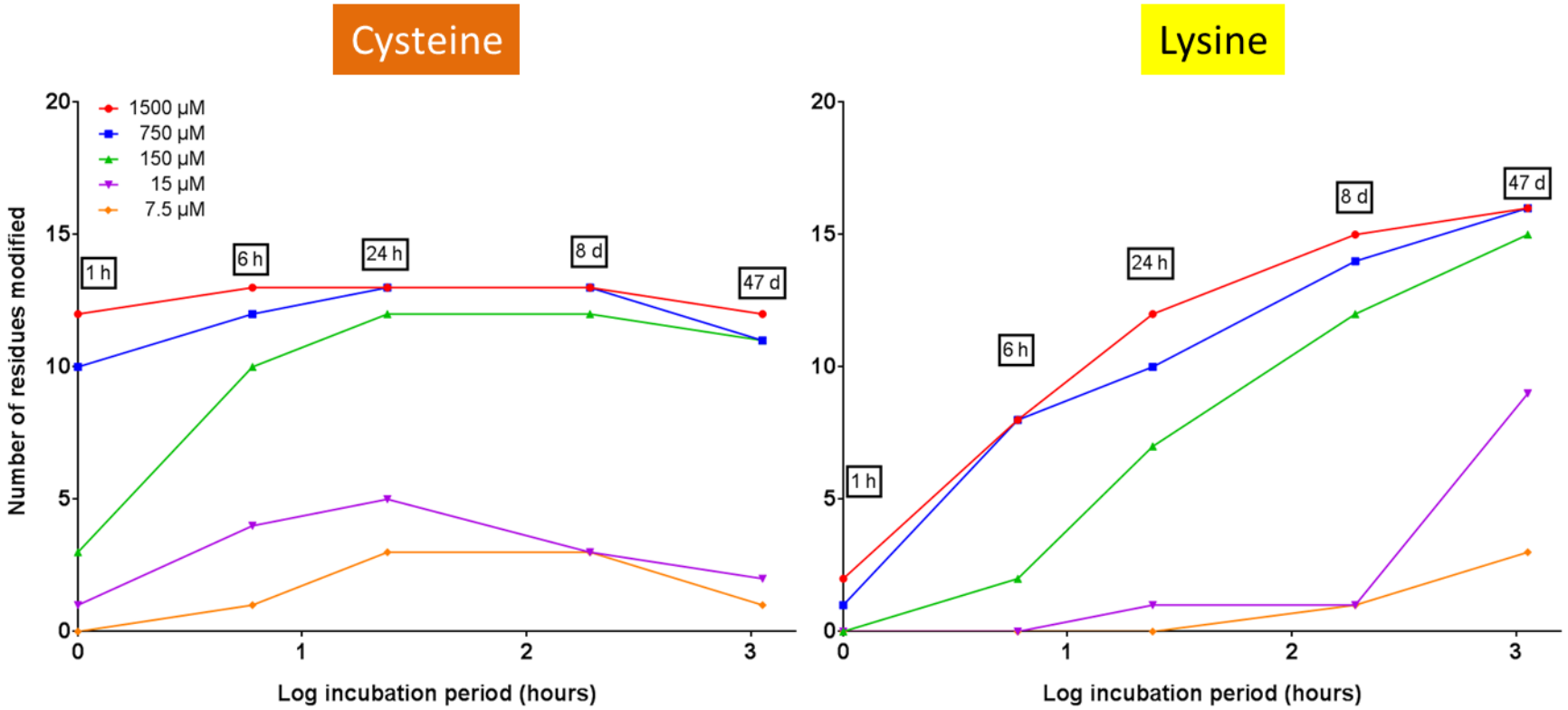

Figure 5.11. Comparing the modification kinetics of cysteine and lysine

Comparative graphs showing the change in the total cysteine (left) or lysine (right) residues found modified for each DNCB concentration and incubation time.

5.4 Discussion

These results demonstrate that both incubation time and DNCB concentration have a significant effect on both the overall amount of protein modified (Figure 5.3) and the number of different residues modified (Figs. 5.10 & 5.11). The absorbance data suggest that saturation of the protein has not occurred by 1 week (Figure 5.3). In contrast to this however, the number of sites modified remains more or less constant above a 750 μM (50:1 molar excess) concentration of DNCB or 24 hour incubation time (Figure 5.10). It is possible that the full range of site modifications is observed before modification of all of the available HSA molecules. It could be speculated that during the early stages, an HSA molecule may undergo conformational changes and have increased reactivity towards DNCB. This would explain the exponential slope and lack of a saturation point of the absorbance graph (Figure 5.1) and the relatively fast leveling off of the number of sites modified in higher DNCB concentration incubations revealed by mass spectrometry (Figure 5.10). This is partly supported by earlier studies on the effect of ligand binding and covalent modification to HSA inducing changes in conformation (Anraku et al., 2001; Bertucci and Domenici, 2002; Jacobsen, 1972; Narazaki et al., 1997). However, this is contradicted by the lower number of amino acid residues found modified after 47 days. This decrease could be due the length of the incubation time allowing the protein to be modified in other ways such as by water loss, methylation or oxidation. Over time, this could alter the stoichiometry of the modified peptides and suppress their detection at their hypothetical *m/z* values by lowering the intensity ratio of the DNP-modified peptide relative to those with additional modifications. Another explanation could be that additional lysine modifications incurred over the extended incubation time have caused additional missed trypsin cleavages, resulting in peptides which are too large to ionize and travel in the mass spectrometer correctly, or are excluded from the PLGS search which only factors in up to 2 missed cleavages. For example, the peptide **Y**LYEIAR which shows tyrosine 138 modified (underlined), is preceded by a lysine, which is also found modified elsewhere. If the proportion of lysine 137 modifications were to increase over time, the detection of tyrosine 138 would decrease proportionately.

Various studies of the folding properties of HSA have suggested that the secondary and tertiary structure of the protein changes in response to temperature (Flora et al., 1998; Wetzel et al., 1980), pH (Dockal et al., 2000; Lee et al., 2000), ligand binding (Bertucci and Domenici, 2002; Narazaki et al., 1997) and covalent modification by chemicals

(Anraku et al., 2001; Jacobsen, 1972), which supports a hypothesis that perhaps initial DNCB modifications of HSA perhaps altering its conformation to open up more reactive sites over time. This could also provide some explanation for the disruption of the basement membrane observed in the immunofluorescence images of skin treated with high concentration DNCB (Figure 3.1), as a chemically induced disruption of protein structure could be expected to weaken structural proteins and cause tissue to weaken. However, this needs to be explored further empirically, perhaps by nuclear magnetic resonance detection of hydrogen-deuterium exchange fluorescence energy resonance transfer labelling in HSA during modification by DNCB at similar concentration and time points.

The distribution of sites found (Figure 5.6) is broad in terms of relative reactivity of amino acid residues. The data either side of the MRSV splits the sites almost completely into cysteines and lysines, with a few exceptions (Lys 281, 351; Cys 200). This is reflected in the graphs comparing the modification rates of cysteine and lysine (Figure 2.10), which demonstrates that cysteine is much more rapidly modified than lysine. This could be due to the incubation pH (7.4) being more favourable to cysteine reactivity, since lysines tend to be more reactive at higher pH (Gerberick et al., 2004b; Leavell et al., 2004). Based on these data, histidine and tyrosine would appear to be less readily modified than either cysteine or lysine overall, however histidine 510 is far more readily modified than tyrosine 138. It is known that DNCB can react with the side chains of cysteine, lysine, histidine and tyrosine as well as the N-terminal amine group. Human serum albumin contains 59 lysines, 35 cysteines, 18 tyrosines and 16 histidines. Of these, the percentages of each found modified were 27.12, 37.14, 5.56 & 6.25% respectively. While variations in reactivity probably exist due to differences in the microenvironment in which each residue resides, it can be broadly interpreted that cysteine and lysine are modified readily, with cysteine being modified far more rapidly than lysine.

These findings are interesting as 34 of the 35 cysteines within HSA are ordinarily involved in S-S bonds and should be inaccessible to modification by chemicals in solution. It is not known why DNCB was able to modify these cysteines, however other experiments using similar techniques have shown cysteines 75, 124, 177 and 392 modified by DNCB but no cysteines were identified as having been modified by the chemical sensitizers 5-chloro-2-methylisothiazol-3-one (MCI), cinnamic aldehyde or 6-

methylcoumarin (personal comms. Dr Erika Parkinson). This indicates that DNCB in particular is able to modify cysteines within S-S bonds. One possibility is that DNCB is capable of breaking the bond; however, experimental data shows that DNCB is not able to reduce S-S bridges in bodipy-FL-cysteine during one hour at a range of concentrations (Figure 5.12).

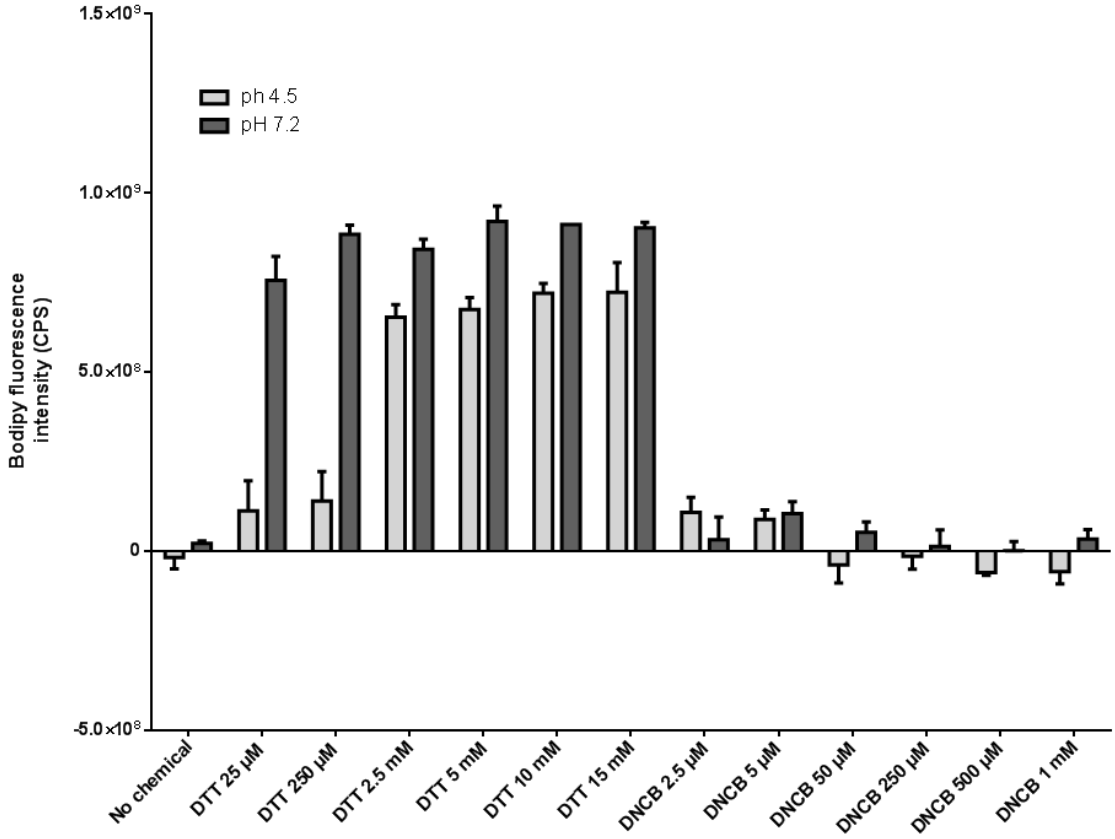

Figure 5.12. DNCB is not able to reduce disulphide bonds in bodipy-FL-cysteine
A bar graph showing fluorescence intensity as counts per second for the S-S bridged self-inhibiting fluorophore bodipy-FL-cysteine incubated for 1 hour with a range of concentrations of DNCB and DTT and two different pH values. DNCB does not show any ability to reduce S-S bonds.

It remains possible that DNCB is interfering with S-S bonds indirectly. Perhaps the initial modification of HSA alters the conformation of the protein such that S-S bonds are stressed or weakened. An interesting aspect of the distribution of cysteine modifications on HSA (Figure 5.9) is that the majority of the modifications occur on domain I in the proximity of cysteine 34. Since the non-covalent binding of fatty acids to Sudlow's site I is linked allosterically to the relative position of cysteine 34 (Fasano et al., 2005), it could be hypothesised that the covalent modification of cysteine 34

influences the protein's local reactivity to DNCB. Another interesting observation is that the modified cysteines which do not occur within domain I are located adjacent to Sudlow's sites I & II. This could either mean that the domains and binding sites influence the reactivity of cysteines in S-S bonds to DNCB or it could simply be that modifications are taking place during reduction steps in the sample preparation and that those sites are preferentially reactive during reduction. It is important to note that the annotated crystal structure used to illustrate this is not representative of the conformation of HSA during the experiments. There was some minor modification taking place during the reduction step prior to SDS-PAGE, as the dithiothreitol in the sample buffer reduces S-S bonds, making them available for modification. However, this does not account for the extensive modifications of cysteine in these experiments and shows a clear effect of incubation time with DNCB in the intensity of the modifications detected by mass spectrometry (Figure 5.7).

Another explanation for the modification of cysteines could be due to the process of thiolysis (see chapter 6) removing DNP groups from cysteine (and potentially histidine and tyrosine (Shaltiel, 1967)) followed by transfer of DNP haptens from cysteine 34 to other cysteines during the reduction step of the in-gel protein digestion (see chapter 2 section 2.24). This could explain the presence of DNP-cysteines proportionate to DNCB concentration and incubation time as the extent of cysteine 34 modification could allow the protein to 'carry' more DNP at higher DNCB concentrations to transfer to other cysteines during this reduction step. This would also explain the presence of isotope triplets in some modifications, since simultaneous modification of a peptide with both d0 and d3 DNCB should not be possible when incubated separately (see chapter 2 section 2.23) meaning that the triplet signatures detected (Figure 5.5) may originate from one of the sample preparation steps after the mixing together of the d0 and d3 DNCB treatments. Determining if this is the case would be complicated, since removing the reduction step from protein digestion would reduce the efficiency of trypsin digestion, resulting in more missed cleavages. It would also confound identification of peptides from the mass spectra by creating a mixture of cysteines with and without alkylation by iodoacetamide, so the disappearance of the triplets could not be confidently attributed to the elimination of thiolytic reduction steps.

Cysteine 34 was found modified in 25 out of 26 incubations and scored most highly for relative reactivity, suggesting that this residue is preferentially modified by DNCB.

This is consistent with studies on the structure of HSA and the reactivity of cysteine 34 with a range of chemical agents, including DNCB (Aleksic et al., 2007; Jenkinson et al., 2010; Peng et al., 2012). It should also be noted that cysteine 34 has an unusually low pK_{SH} of 5 compared with the ordinary value of 8.5 for cysteine (Pedersen and Jacobsen, 1980). Since cysteine 34 accounts for the majority of free cysteine in the blood and is heavily conserved between species, it is likely that this residue's availability and high reactivity are crucial to protein function (Carter and Ho, 1994). Indeed, cysteine 34 is thought to be allosterically linked to Sudlow's binding site I (Fasano et al., 2005) and may be responsible for much of the nitric oxide transport in the blood (Stamler et al., 1992).

Of the 7 nucleophilic residues located in the 2 binding sites, only 3 were identified in this study (Lys 414, 195 and 199). As well as these drug binding sites, there are also sites which accommodate the binding of fatty acids (Curry et al., 1998). Within these sites, lysines 159 and 351 were found to be modified. In total, 5 of the 31 identified modifications (16.13%) reside in characterised ligand binding sites. While it may be useful to map the remaining identified modifications against the crystal structure used (1N5U) in order to determine their proximity to the solvent interface, the structure of HSA *in vivo* is subject to significant conformational change (Carter and Ho, 1994; Dockal et al., 2000; Ferrer et al., 2001; Wetzel et al., 1980). Crystallography studies rely on very specific and stable molecular states in order to give a crystal structure which will allow high resolution structural information, but are not fully representative of the structure in solution. One such example is that cysteine 34 is characterised as being occluded in some crystal structure studies (Sugio et al., 1999), but this has not prevented modification by DNCB. Instead, it may be more useful to repeat this work using e.g. de-lipidated HSA to determine if conformational changes have a consistent effect on the availability of residues for DNCB modification. It has been suggested elsewhere that the binding of fatty acids may lead to cysteine 34 being exposed to the solvent interface (Narazaki et al., 1997).

In contrast to previous studies of DNCB modification of HSA (Aleksic et al., 2007), an additional 25 potential modifications have been identified, however the N-terminal aspartic acid residue identified by previous studies, as well as histidine 9 and lysines 212 and 225 were not detected. It can be surmised that an increase in the number of detected adducts is largely due to the use of more sophisticated mass spectrometry and

liquid chromatography techniques, particularly the use of MS^E allowing all precursor ions to undergo analysis, as well as the use of stable isotopes to increase identification confidence and allow the inclusion of low abundance species. However, the 4 residues found by the former study and missing from these data could also be explained by differences in incubation conditions. In particular, the Aleksic study used a high proportion of organic solvent in the incubation buffer, which could have effects on the conformation of the protein and potentially the reactivity of the DNCB (De Vleeschouwer et al., 2012). Though none of the missing four residues are present in any of the identified binding sites, the difference in HSA preparation could have an effect on the conformation of the HSA resulting in some regions of the protein having different propensities for modification. The HSA used here, for example, was pooled from plasma and purified without treatment, whereas the HSA used in the Aleksic study was de-lipidated, which would result in an altered tertiary structure (Curry et al., 1998) as well reducing the initial availability of cysteine 34 (Narazaki et al., 1997).

5.4.1 Summary

The range of DNCB modifications to HSA which are possible is far broader than previously thought (Aleksic et al., 2007), and varies greatly in response to concentration and also to a lesser extent, time. Of the cysteines detected, 12 were thought to be unavailable for modification due to involvement in S-S bridges, which opens interesting avenues of future research. There is a marked difference in the reactivity of cysteine and lysine with DNCB in the conditions used, suggesting that cysteines are overall more reactive, despite most of the cysteine in HSA being involved in S-S bridges. This warrants further investigation of the preparation techniques used, but also, pending ongoing work, raises questions about potential lability of the disulphides in HSA, as well as the potential reactivity of DNCB towards S-S bridges.

In relation to the study of allergic contact dermatitis, the residues modified at low concentrations and early time points (e.g. cysteine 34, histidine 510 and lysine 351 if studying different amino acids) could be considered of interest with regards to the mechanism of haptenation of proteins by chemicals. Although the environment *in vivo* is likely to be very different to *in vitro*, it is likely that residues which are more easily modified carry a higher probability of being presented to the immune system during sensitization.

6 A NOVEL PROCESS OF HAPTEN TRANSFER IN MEDIATING IMMUNOGECITY TO DNCB

6.1 Introduction

For contact allergy to occur, chemical sensitizers must generate an immunogenic epitope through protein modification. This leads to T-cell activation when a modified protein is degraded in antigen presenting cells (APCs), and modified peptides derived from the protein are loaded onto an MHC molecule for presentation to the T-cell receptor (TCR) of a naïve T-cell in the local lymph node (Freudenberg et al., 2009; Lepoittevin and Leblond, 1997; Martin and Weltzien, 1994). The current consensus is that the immunogenic modified peptides are derived directly from the protein modified by the chemical when it penetrates into the skin (Kaplan et al., 2012; Vocanson et al., 2009). However, there is also evidence that sensitizers modify MHC-bound peptides at the cell surface (Martin et al., 1992; Martin et al., 1993; Martin, 2004; Ortmann et al., 1992; Padovan et al., 1997; Padovan et al., 1996). The principle factor in activation of naïve T-cells is a peptide-MHC complex binding to a T-cell receptor with a strong enough affinity to activate the T-cell (Grakoui et al., 1999).

Antigen processing and presentation typically occurs in one of two ways:

1. The MHC class I pathway

Proteins within the cytosol are constitutively digested in the proteasomes and the peptides generated are transported into the endoplasmic reticulum before being loaded on to MHC class I molecules by protein chaperones and trimmed by peptidases. The peptide-MHC complex is then transported via vesicles to the cell surface where it is presented on the outside of the cell. This allows cells to display a sample of their protein content at all times, which permits immune recognition of cells infected by pathogens (Neefjes et al., 2011; Vyas et al., 2008). Peptides presented on MHC class I molecules are able to activate $CD8^+$ naïve T-cells, leading to the generation of cytotoxic T lymphocytes (CTLs), which induce apoptosis in cells presenting an MHC-I peptide complex which corresponds to their T-cell receptor.

2. The MHC class II pathway

Proteins endocytosed by cells which express MHC class II, are enzymatically degraded by reduction and proteolysis in lysosomes and endosomes and loaded on to MHC class II molecules with the aid of the protein chaperone HLA-DM. The peptide-MHC complexes are then transported via vesicles to the cell surface. Only professional antigen presenting cells such as dendritic cells, macrophages and B cells tend to express MHC class II. Cells expressing MHC class II are present throughout most tissues and present a continuous sample of the ambient extracellular protein environment, allowing immune surveillance of invading pathogens which remain outside of cells. Immunogenic peptides bound to MHC class II are able to stimulate $CD4^+$ T-cells which differentiate to generate helper (T_H) and regulatory (T_{REG}) T-cells (Neefjes et al., 2011).

There has not been any definitive identification of specific peptide modifications which lead to the activation of T-cells, although several studies have shown that peptides can be used to sensitize and elicit an allergic response in mice (Weltzien et al., 1996). Using keratinocyte-derived cell lines as a model for human skin (see chapter 3) my aim was to generate a range of DNCB-modified proteins analogous to that generated during a sensitization event. Using these modified proteins to elicit T-cell proliferation from lymphocytes isolated from DNCB-sensitive donors (see chapter 4) demonstrates the possibility that some of these proteins are indeed relevant to the process. However, there is no evidence that the proteins which are eliciting the response do so because of similarities in sequence and modification loci to the proteins which caused the initial sensitization.

In endosomes and lysosomes within the endocytic pathway, the enzyme gamma interferon-inducible lysosomal thiol reductase (GILT) plays a role in reducing disulphide bonds in proteins and facilitates the presentation of peptides in MHC class II molecules (Maric et al., 2001; Phan et al., 2000). While GILT has no homologues, its active site contains a conserved $C^{46}XXC^{49}$ motif, which is similar to thioredoxin, a cytosolic protein catalysing the reduction and oxidation of proteins (Arnér and Holmgren, 2000). The proposed mechanism of GILT's action is that reducing agents within the endosome, possibly L-cysteine, act as an agent to interrupt the disulphide bond in the active site of GILT. Once free, cysteine 46 within the active site attacks disulphide bridges and forms a mixed disulphide bond with a sulphur atom from the

target protein. Cysteine 49 then displaces the target protein from cysteine 46 of GILT by re-forming the initial disulphide bridge with cysteine 46, returning GILT to its original state, ready to be activated once more (Figure 6.1)(Hastings and Cresswell, 2011).

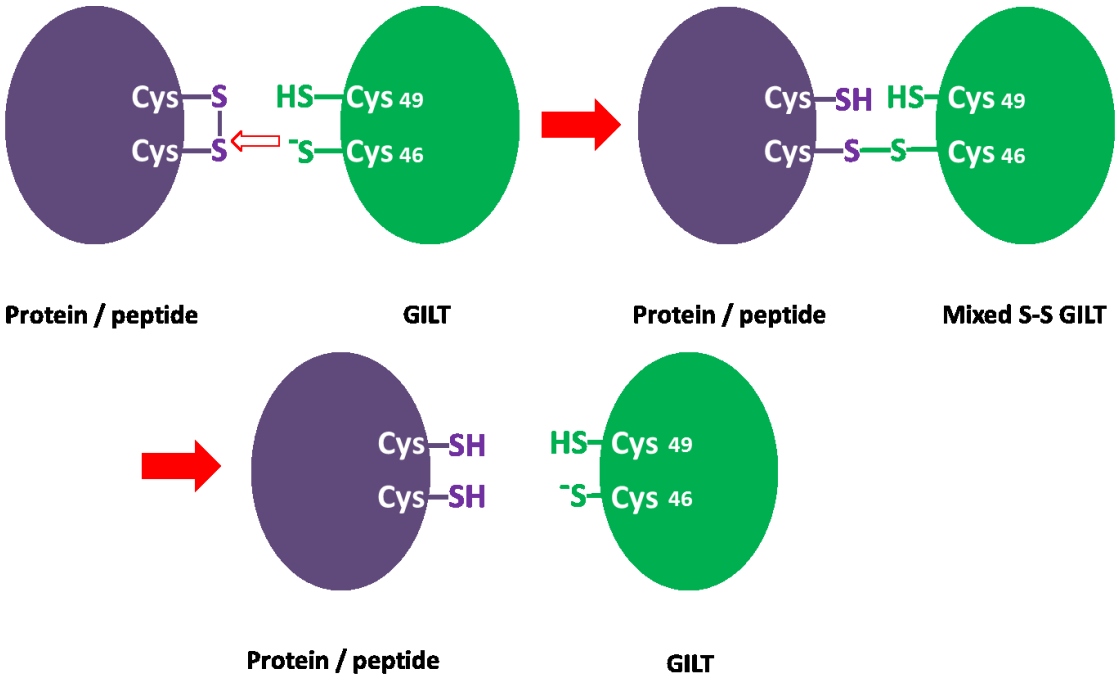

Figure 6.1. The reduction of disulphide bridges in proteins by GILT

The proposed mechanism for disulphide bond reduction in proteins by GILT in vivo. Initially, GILT must be activated by a reducing agent, which in the endosome is presumed to be free cysteine or similar. Reduced GILT then interrupts disulphide bridges by forming a mixed disulphide with the protein, before releasing the protein when the other cysteine in the GILT active site competes to form a disulphide bridge, ending with the active site in an oxidised state, ready to be re-activated.

It may also be reasonable to expect that a thiol reductase could be capable of removing DNP-Cys/Tyr/His adducts in a similar way to a reducing agent (Shaltiel, 1967) during MHC class II antigen processing. If this is the case, it would raise interesting questions about the role of protein modification in the mechanism of contact allergy.

The epidermis contains many cysteine-rich proteins such as keratins. Prior analysis of DNCB modified HSA has identified that cysteine is more readily modified than other nucleophilic amino acid residues and in particular that cysteine 34 is the most reactive residue of HSA. However, the results additionally show that cysteine residues involved in disulphide bridges may also be modified by DNCB (see chapter 5). As the pH of the

epidermis ranges from 4.5 to 6.8 (Ohman and Vahlquist, 1994) and the modification of cysteine tends to occur more readily than lysine, histidine and tyrosine in this pH range (Gerberick et al., 2004b; Leavell et al., 2004), it can therefore be expected that DNCB will generate cysteinyl haptens in the epidermis. Further, recent work has shown cysteine modification in reconstructed human epidermis when treated with chemical sensitizers (Elbayed et al., 2013). The reactivity of chemicals to cysteine residues in synthetic peptides correlates significantly to sensitizer potency values from the murine local lymph node assay (LLNA), a stronger correlation being observed with reactivity to glutathione (Gerberick et al., 2004a). Indeed, glutathione depletion shows a strong relationship to sensitizer potency (Schmidt and Chung, 1992, 1993). Glutathione is also of relevance to endocytic antigen acquisition as it is secreted from cells after conjugation to xenobiotic molecules (Ishikawa, 1992; Lee et al., 2000). Since glutathione expression is up-regulated in response to the oxidative stress generated by xenobiotics, including DNCB (Hirai et al., 1997) and because glutathione is expressed in high quantities in keratinocytes (Leccia et al., 1998; Lee et al., 2000) it is reasonable to expect that DNP-glutathione will be part of the extracellular milieu during sensitization and will therefore enter into the endocytic pathway.

The aim of the work in this chapter is to determine if a relationship exists between the immunogenicity of DNP-cysteine haptens and an intracellular process of thiolysis during antigen processing.

To investigate this potential relationship, synthetic peptides containing DNP-cysteine and DNP-lysine were compared using the following methods:

- Proliferation assays using lymphocytes from DNCB-sensitized donors to determine if DNP-cysteine is more immunogenic than DNP-lysine.
- DNP immuno-labelling of protein lysates extracted from human monocytes incubated with the peptides to see if DNP groups are transferred to other proteins
- Comparison of DNP removal by reduction between DNP-cysteine and DNP-lysine peptides
- Investigation of a candidate protein GILT for the ability to remove DNP groups from cysteine.

6.2 Experimental design

Synthetic dinitrophenyl peptides for the immunogenic comparison of cysteine to lysine

Two peptides were synthesised by Peptide Protein Research (Southampton, UK) based on an 8 amino acid sequence from human serum albumin (HSA), beginning at residue 30 and ending at residue 37 with residue 34 carrying a dinitrophenyl (DNP) group on the side chain. To demonstrate a differential immunogenicity between DNP-cysteine and DNP-lysine, the DNP-modified residue corresponds to cysteine 34 of HSA in one peptide, but is replaced with a DNP-lysine in the other. Cysteine 34 was chosen since it is the most readily modified residue in human serum albumin (see chapter 5) and being a common adduct found in other published studies (Aldini et al., 2006; Aleksic et al., 2007; Jenkinson et al., 2010).

The sequences are as follows:

Peptide 1: Tyr-Leu-Gln-Gln-**DNP*Cys**-Pro-Phe-Glu (YLQQ**C***PFE)

Peptide 2: Tyr-Leu-Gln-Gln-**DNP*Lys**-Pro-Phe-Glu (YLQQ**K***PFE)

To examine the role of MHC class II presentation in peptide immunogenicity, DNP-glutathione (DNP-GHS, Santa Cruz, Dallas, Texas, US) was used as a control, since glutathione is only 3 amino acids in length (Glu-**DNP*Cys**-Gly) and would not be expected to interact with the MHC class II binding groove.

Lymphocyte proliferation assays to compare the immunogenicity of synthetic DNP-peptides

Peripheral blood mononucleocytes (PBMCs) were isolated from blood obtained from DNCB sensitized volunteers (see chapter 2). Lymphocyte proliferation assays (LPAs, see chapter 2 section 2.19) were performed to determine the immunogenicity of each synthetic peptide. Controls were used to demonstrate background proliferation (culture medium), general proliferation (PHA), DNCB-specific proliferation (3 μM DNCB) and MHC class II-independent hapten-peptide stimulation (DNP-GSH). Proliferation was measured by the addition of tritiated thymidine for 6 hours after 6 days of incubation and scintillation counting of harvested cells (see chapter 2).

Monocyte processing of synthetic peptides and western blot detection of indirect protein adducts

Monocytes isolated from human blood were incubated overnight with DNP peptides and controls (see chapter 2 sections 2.26 & 2.27). The DNP-C, DNP-K and DNP-GSH peptides described earlier were incubated by themselves, with chloroquine (which accumulates within endosomes, raising the pH of the endosome) or with interferon-γ. The latter activates monocytes and should upregulate the expression of GILT (Arunachalam et al., 2000) as well as influencing the differentiation of monocytes into macrophages (Delneste et al., 2003). After incubation, protein lysates were separated using SDS-PAGE without reduction and then transferred to PVDF membranes and detected using immunoblotting (see chapter 2 section 2.13). This was used to determine whether adducts were being transferred to other proteins during the incubation.

Thiolysis of DNP groups from a cysteinyl peptide using DTT

The reducing capability of DTT at pH 4.5 (endosomal pH) and pH 7.4 (physiological pH) was compared using a Bodipy-FL-cysteine (BFLC) assay (see chapter 2).

Each of the DNP-C and DNP-K synthetic peptides were incubated for 1.5, 2.5 and 4.5 hours at either pH 4.5 or 7.4 with a molar excess of 5, 12.5, 25, 50 or 100 DTT versus a control without DTT. The experiment was quenched by the addition of a 5 x molar excess of iodoacetamide to DTT, raising the pH to 8.0 and incubating for 30 minutes to allow alkylation of any free cysteine side chains (Figure 6.2). Peptides were then centrifuged through a 10 kDa molecular weight cut-off filter, de-salted using C18 solid phase extraction and then analysed using LC-MS^{E} (see chapter 2). The degree of DNP thiolysis was determined by generating extracted ion chromatograms for each relevant peptide ion in the mass spectra and integrated within the software package MassLynx (Waters, Manchester, UK) (see chapter 2 section 2.29). Intensity values for peptides with altered mass indicating loss of DNP were divided by the intensity values for peptides whose delta mass indicated presence of the DNP group + those without to give a value for the percentage of peptide which has lost the DNP.

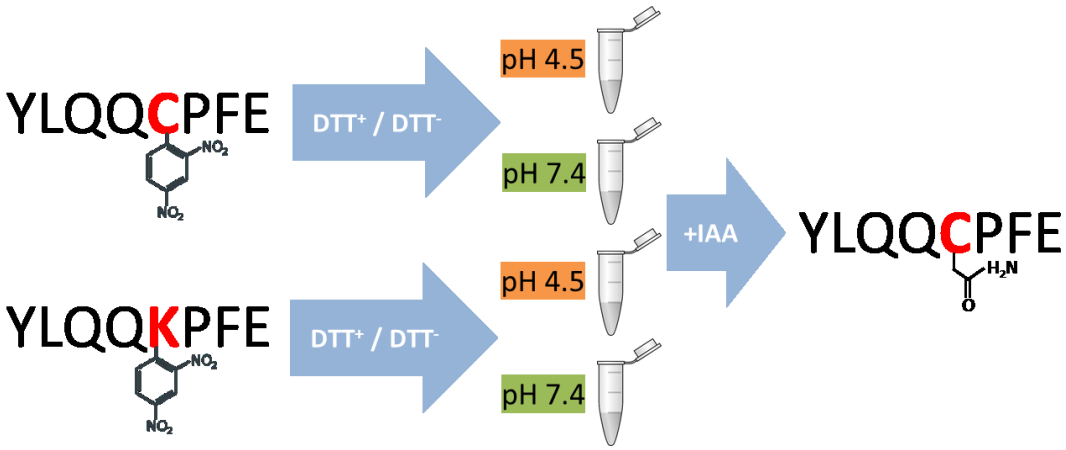

Figure 6.2. Thiolysis of DNP from synthetic peptides

A diagram showing a generalised workflow of a DTT thiolysis experiment. Peptides with either a DNP-Cys or DNP-Lys were incubated with various concentrations of DTT versus control at mildly acidic(pH 4.5) and neutral pH (pH 7.4). After different incubation periods, the reactions were stopped by alkylation of the free cysteines to give a non-reversible carbamidomethyl adduct.

Determination of rM GILT activity and incubation of rM GILT with DNP peptides

Recombinant mouse GILT was kindly provided by Professor Peter Cresswell and Laura Ciaccia West (Department of Immunobiology, Yale University, New Haven, Connecticut). As with DTT, the BFLC assay was used to assess reducing activity. Assays were performed (see chapter 2) using halving serial dilutions of GILT from 1000 ng/well to 31.25 ng/well. Controls used were GILT without the addition of 25 μM DTT, 25 μM DTT alone at pH 4.5 and 7.4 and incubation of GILT with each synthetic peptide for one hour prior to the addition of BFLC.

Synthetic DNP peptides were incubated at a 2.3:1 ratio (5 μM peptide, 1.79 μM GILT) with DTT activated GILT. These concentrations kept the peptide concentration in solution the same as for the DTT thiolysis, which were optimised and used the highest concentration of GILT possibly by using the undiluted stock of GILT. Incubations were performed at pH 4.5 to ensure optimal GILT activity while avoiding significant thiolysis by the DTT used to activate the enzyme. The reaction was quenched by the addition of 5:1 IAA:DTT and increasing the pH to 8.0. The peptides were separated from the GILT by centrifugation through a 10 kDa molecular weight cut-off filter column and then de-salted by solid phase extraction with C18 silica. The peptides were then analysed by LC-MS to determine if thiolysis had taken place. The specific effects of GILT were determined by comparison to DTT at pH 4.5 (see chapter 2).

6.3 Results

6.3.1 Differences in immunogenicity and antigen processing between DNP-Cys and DNP-Lys

T cell proliferation in culture was measured after incubation with the synthetic peptides. A strong lymphocyte response indicated by a stimulation index (SI) value greater than 3 was observed in response to the DNP-C peptide and the DNP-GSH (Figure 6.3.). No response to the DNP-K peptide was observed compared to the negative control. This was observed in 4 out of 5 DNCB-sensitized donors.

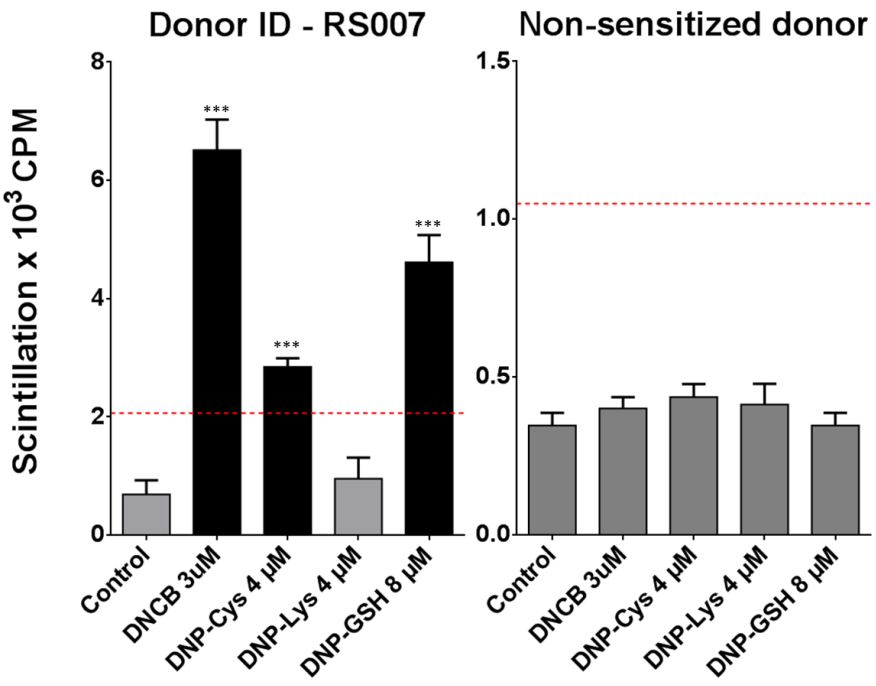

Figure 6.3. DNP-cysteine stimulates T-cell proliferation non-specifically

*Graphs showing lymphocyte proliferation responses in a DNCB-sensitized volunteer versus a non-sensitized donor. Responses to DNP antigen control (3 µM DNCB), synthetic peptides: YLQQC*PFE (DNP-Cys), YLQQK*PFE (DNP-Lys) and DNP-glutathione (DNP-GSH) are shown. The red dotted line denotes where the stimulation index = 3.*

*Student's t-test was used to determine significant difference from control: *** = P <0.001*

A positive response to 3 µM DNCB corresponded to a positive response to DNP-C and DNP-GSH in every case. PBMCs isolated from donors not sensitized to DNCB showed no significant response to any of the peptides or DNCB.

Western blot detection of DNP proteins in the lysate of monocytes incubated with the DNP peptides showed that the cysteinyl peptide and DNP-GSH donates DNP groups to other proteins during incubation (Figure 6.4).

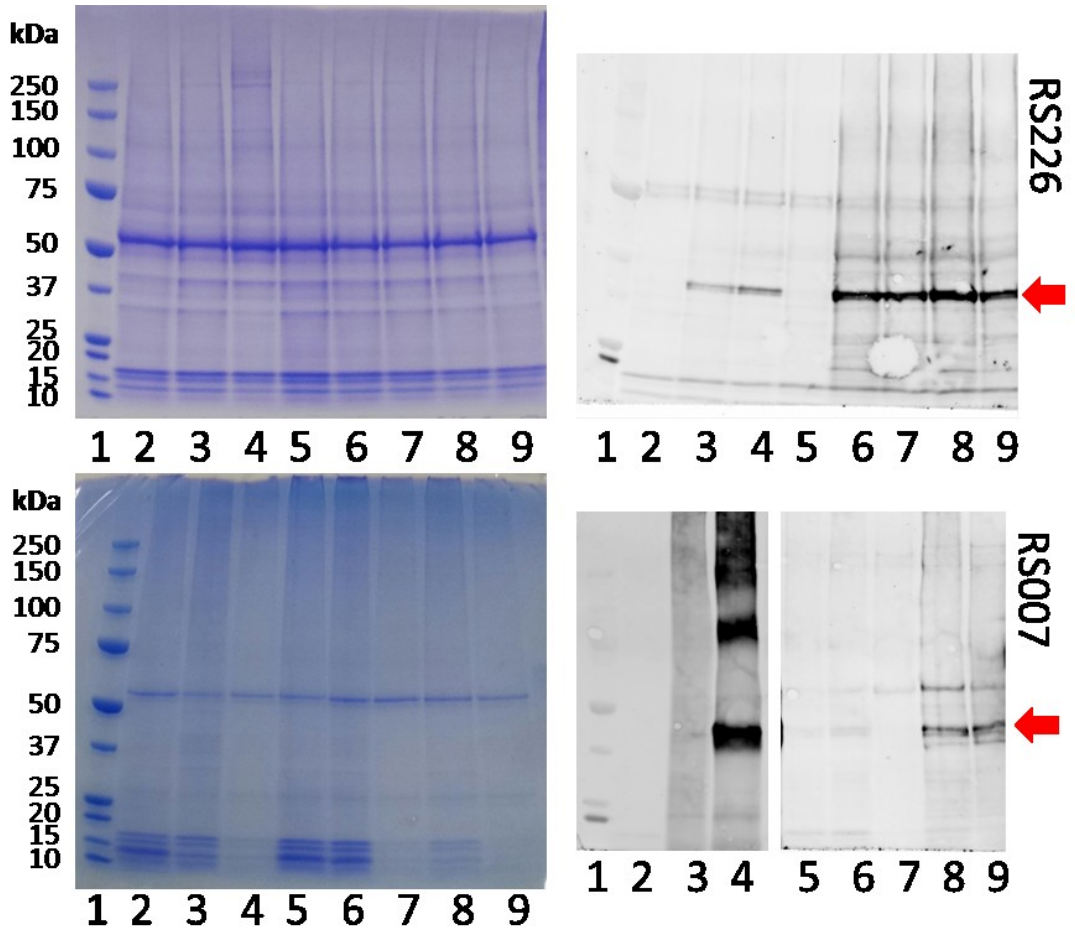

Figure 6.4. The transfer of haptens from DNP-Cys to proteins within monocytes in culture
Non-reducing SDS-PAGE and western blot for DNP adducts in the lysate of monocytes cultured with:
TOP (donor RS226)*: 2) No peptide,3) DNP-Cys, 4) DNP-Cys + 50 µM chloroquine, 5) DNP-Lys, 6) DNP-GSH, 7) DNP-GSH + 50 µM chloroquine, 8) DNP-GSH + 100 µM chloroquine, 9) DNP-GSH + 1000 UI/ml IFN-γ.*
BOTTOM (donor RS007): *2) No peptide, 3) 20 µg protein lysate of 30 µM DNCB-treated HaCaT cells, 4) ~1 µM DNP human serum albumin, 5) DNP-Cys, 6) DNP-Cys + 50 µM chloroquine, 7) DNP-Lys, 8) DNP-GSH, 9) DNP-GSH + 50 µM chloroquine*
All peptides were used at 8 µM. Molecular weight standards in lane 1. The red arrows indicate a dominant modified protein at ~37-50 kDa.

Chloroquine is a weak base which accumulates within endosomes and lysosomes, increasing their pH and interfering with antigen processing (Deduve et al., 1974; Gonzaleznoriega et al., 1980; Ziegler and Unaue, 1982). Cultures incubated overnight

with 50 μM or 100 μM chloroquine as well as the DNP peptides do not show any difference in the amount of proteins found modified. Incubation with IFN-γ, which activates monocytes causing them to up-regulate antigen processing enzymes, including GILT (Arunachalam et al., 2000; Farrar and Schreiber, 1993); also did not induce any detectable changes in the transfer for DNP groups to other proteins.

6.3.2 The buffer pH has a pronounced effect on the reduction properties of dithiothreitol (DTT)

The mean fluorescence values for non-reduced Bodipy-FL-cysteine (BFLC) at each pH were subtracted from the residual values for DTT to compensate for background fluorescence. The reducing activity of DTT is attenuated at pH 4.5 until there are between 50 and 500 equivalents of DTT per BFLC molecule (Figure6.5).

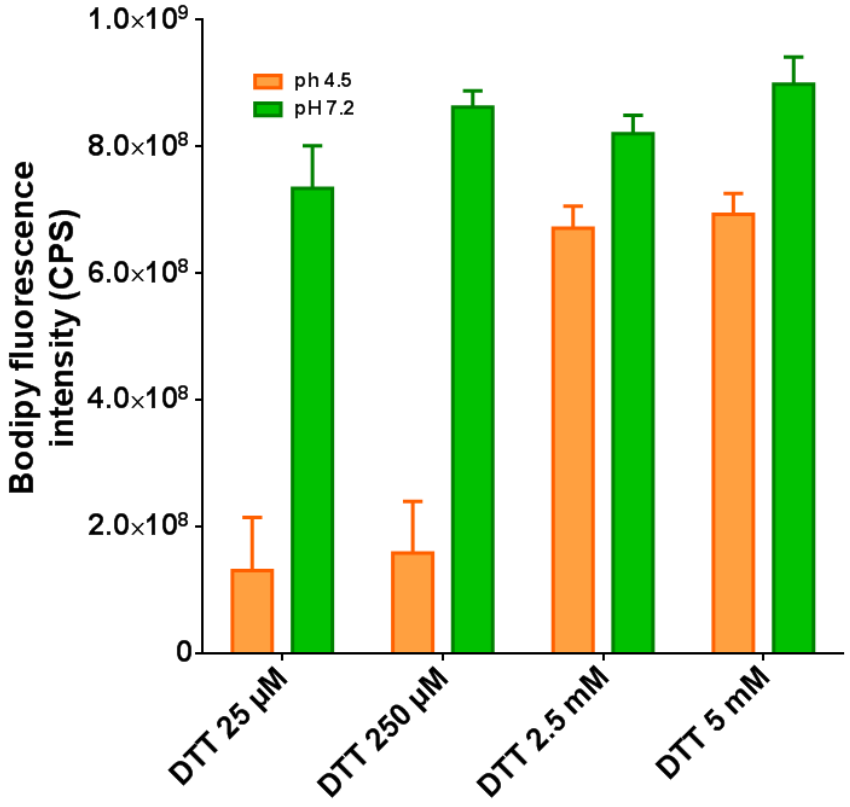

Figure 6.5. DTT shows reduced activity at low pH

Graph showing the reduction of BFLC by DTT at 5, 50, 500 and 5000 molar equivalents at pH 4.5 and 7.4 as measured by fluorescence (excitation λ 485 nm, emission λ 530 nm). Reduction is expressed as average triplicate values of bodipy fluorescence.

6.3.3 Exploring the removal of DNP groups from DNP-Cys using DTT and GILT

Liquid chromatography coupled with mass spectrometry was used to determine DNP removal from a DNP-labelled peptide by DTT thiolysis. Changes in peptide mass were predicted based on the loss of a DNP group (-166.0015 Da) offset by a gain of a carbamidomethyl group (+57.022 Da), resulting in a mass shift of -108.980 Da. To

assess the completion of the reaction, spectra were also interrogated for ions corresponding to a loss of DNP with no carbamidomethyl adduct (Figure 6.6).

Mass spectra and chromatograms of the DNP-labelled synthetic peptides incubated with DTT and controls were manually interrogated for ions with *m/z* values corresponding to peptides with delta mass values pertaining to loss of DNP and alkylation by iodoacetamide.

The cysteinyl peptide with a DNP group has a theoretical mass of 1193.450 Da, 1027.448 without the DNP and 1084.470 where the DNP is replaced with a carbamidomethyl group (Figure 6.6).

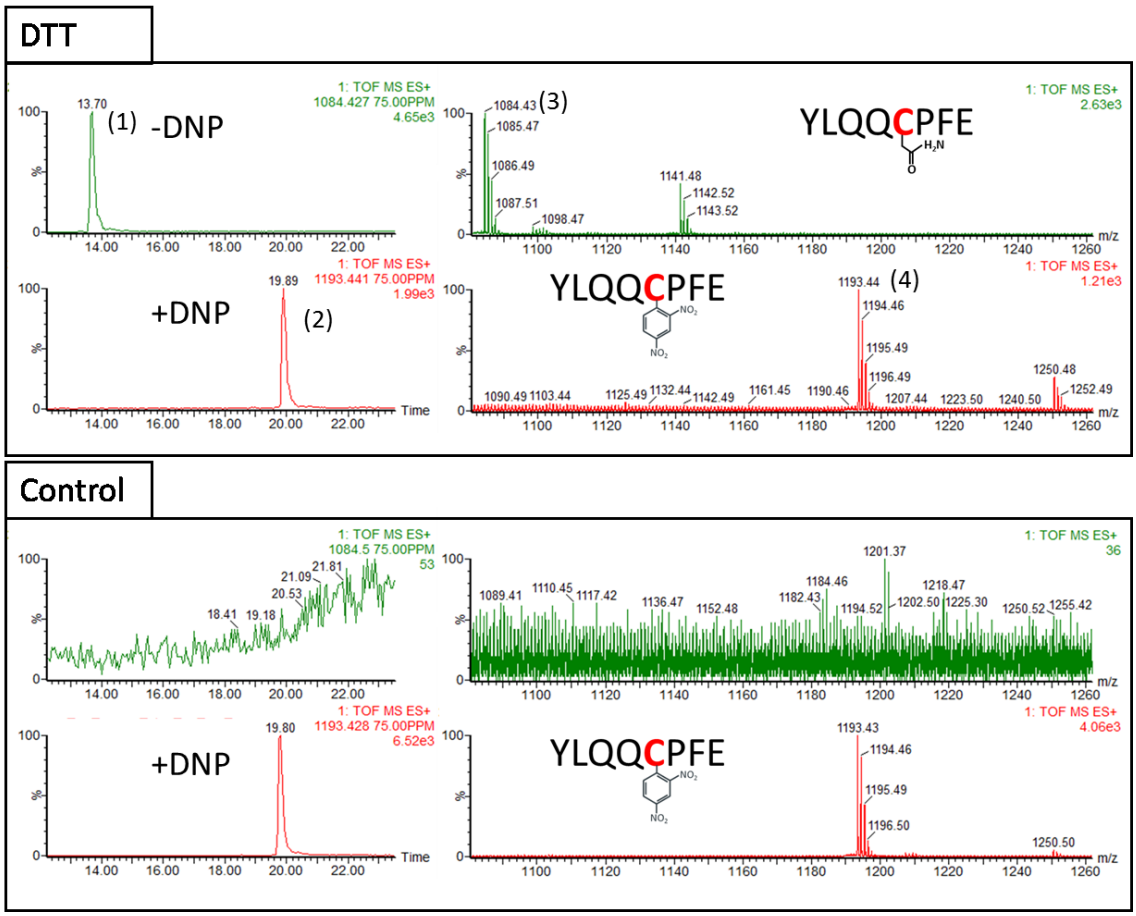

Figure 6.6. DTT removes the DNP group from the cysteinyl peptide

Top: [DTT thiolysis] *Chromatograms (left) and mass spectra (right) showing the presence of carbamidomethyl (1 & 3) and dinitrophenyl (2 & 4) species of the synthetic cysteinyl peptide YLQQC*PFE after incubation with a 100-fold molar excess of DTT.*

Bottom: [Control] *Chromatograms (left) and mass spectra (right) showing the presence of only the dinitrophenyl (2 & 4) peptides when incubated without DTT.*

The lysinyl peptide has a theoretical mass of 1218.535 Da with a DNP group, 1052.534 without the DNP and 1109.556 without the DNP and with a carbamidomethyl group. No ions corresponding to any predicted loss of DNP were found for the lysinyl peptide at any concentration of DTT or either of the pH's tested (Figure 6.7).

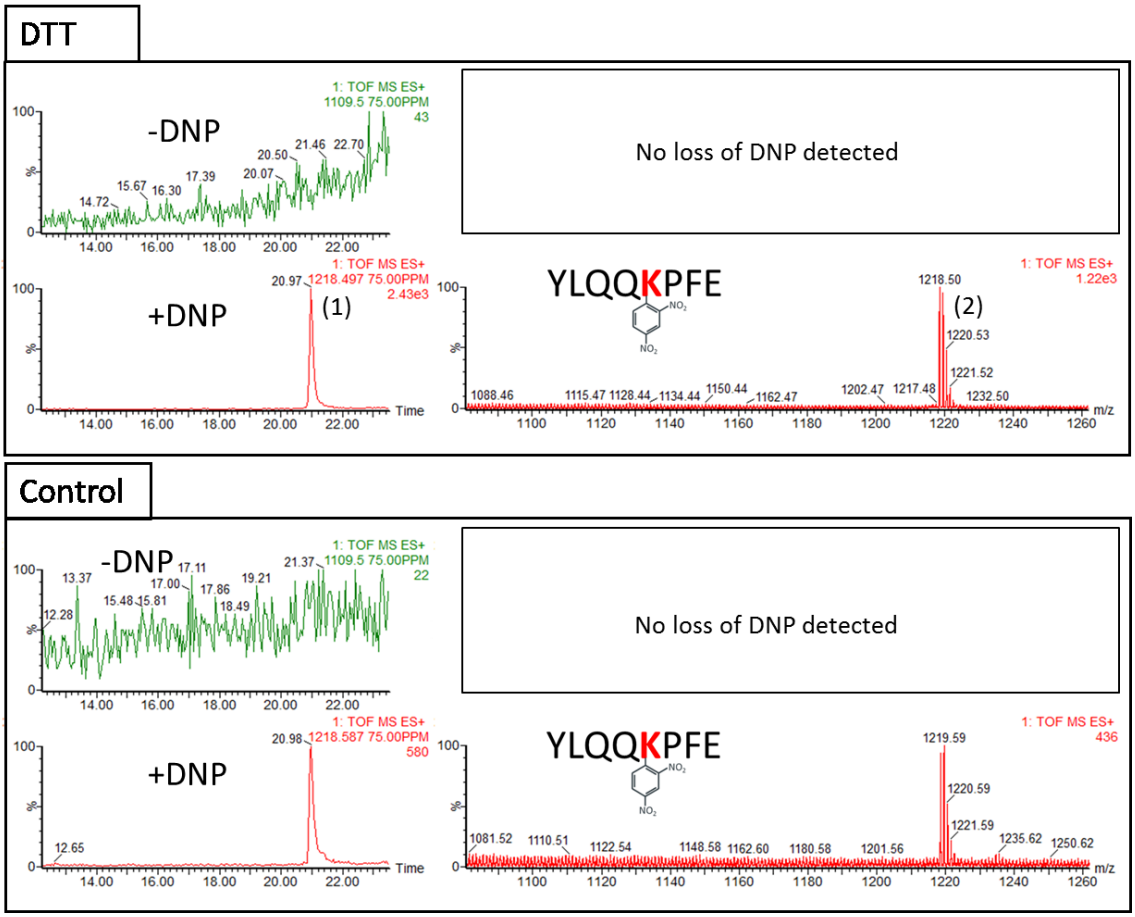

Figure 6.7. DTT does not affect the DNP group on the lysinyl peptide

Top: [DTT] *Chromatograms (left) and mass spectra (right) showing the presence of dinitrophenyl species of the synthetic lysinyl peptide YLQQK*PFE (1, 2) after incubation with a 100-fold molar excess of DTT.*

Bottom: [Control] *Chromatograms (left) and mass spectra (right) showing the presence of only the dinitrophenyl (1, 2) peptides after incubation without DTT.*

Peptides were quantified by generating extracted ion chromatograms for each relevant ion in the mass spectra and integrated within MassLynx across the 40 minute gradient (see chapter 2 section 2.29). Intensity values for peptides with a delta mass corresponding to the loss of DNP were divided by the intensity values for peptides whose mass indicated presence of a DNP group + those without to give a value for the percentage of peptide which had lost the DNP (Table 6.1).

Table 6.1. Peptide ions denoting the presence or absence of the DNP group

The theoretical m/z values used to identify the DNP-labelled peptides group and the replacement of DNP with a carbamidomethyl group on the cysteinyl peptide.

Peptide	DNP	Carbamidomethyl	*m/z*
YLQQ**C***PFE	+	-	1193.450
YLQQ**C***PFE	-	+	1084.470
YLQQ**K***PFE	+	-	1218.535

The removal of DNP groups from the cysteinyl peptide by DTT occurred consistently at pH 7.4 and shows a clear response to concentration and incubation time. No DNP removal from cysteine was observed in control samples or samples containing 5:1 DTT:peptide. No DNP loss was observed for the lysinyl peptide at any pH, time point or concentration of DTT. A relatively low amount of DNP removal from the DNP-cys peptide occurred at pH 4.5 and showed a clear effect of DTT concentration and incubation period (Figure 6.8).

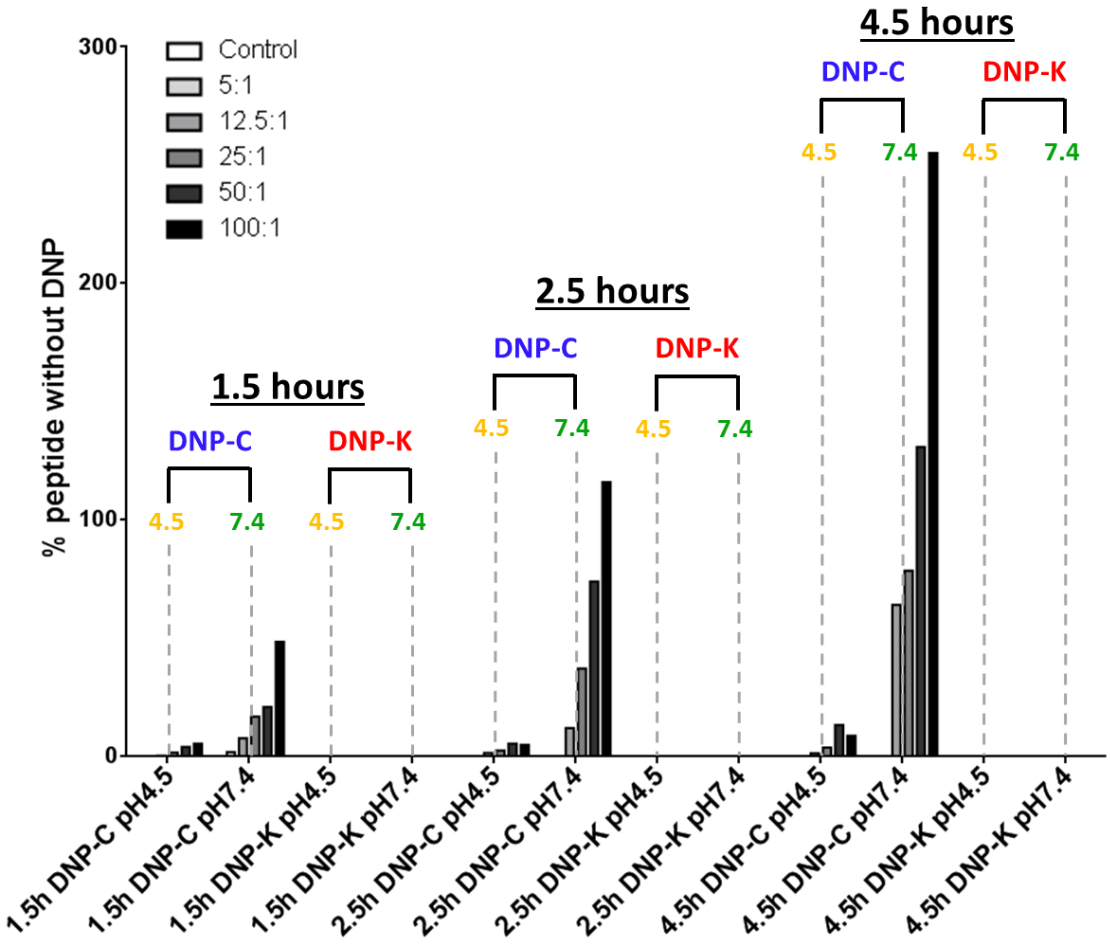

Figure 6.8. DTT thiolysis of DNP from a DNP-Cys peptide by DTT concentration, pH and incubation period

A graph showing the percentage of peptide ions identified by LC-MS as having lost the DNP group. Values are shown for each of the DNP-C and DNP-K peptide (indicated by x axis labels) for each of three time points at pH 4.5 or 7.4 (indicated by graph labels).

The reducing activity of GILT was compared to that of DTT at both pH 4.5 and 7.4, since GILT is most active in the endosome at pH 4.5 while DTT is active at physiological pH. The mean background fluorescence of the BFLC for either pH was subtracted from the residuals for the relevant pH in order to show just the reducing effect. As well as showing the reduction from the GILT the values are also shown corrected for the effect of DTT, achieved by subtracting the mean DTT values from the GILT residuals. This illustrates a difference between the effectiveness of GILT between pH 4.5 and 7.4 which is not otherwise apparent (Figure 6.9). While no reduction was observed to occur in the presence of 25 µM DTT at pH 4.5 in this experiment and a later one (Figure 6.11), a small amount has been observed previously (Figure 6.5). The cause of this difference is unknown but could be due to experimental error. This is supported by the larger range of deviation from the mean between the replicates.

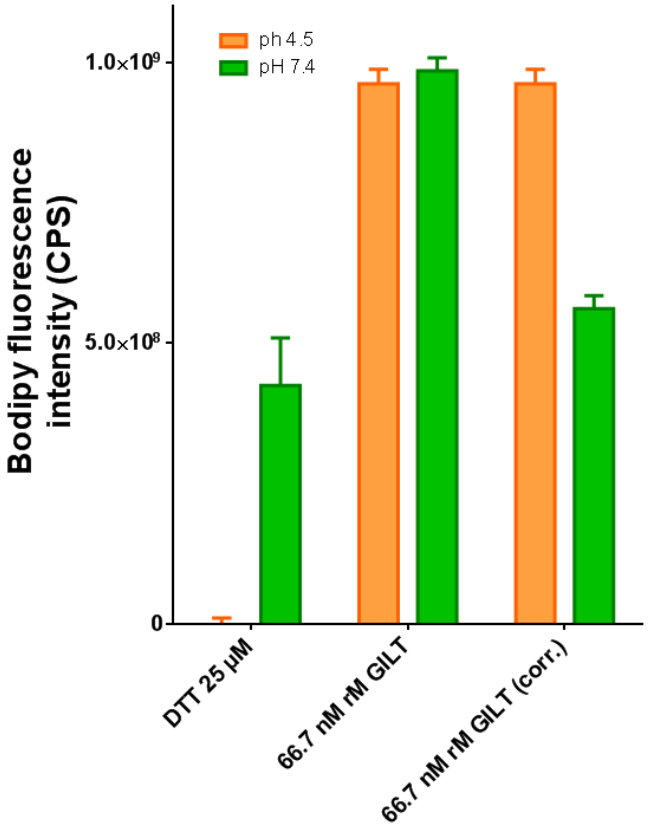

Figure 6.9. rM GILT is a powerful reducing agent at pH 4.5

Graph showing the reduction activity of DTT and rM GILT as fluorescence (excitation λ 485 nm, emission λ 530 nm) from reduced BFLC. BFLC was incubated for 1 hour at pH 4.5 and pH 7.4 with 25 µM DTT or 66.7 nM GILT + 25 µM DTT.

The reduction seen with the DTT and GILT samples are approximately similar at their respective optimal pH and highlights the efficiency of the GILT enzyme which is present at 0.0026 the molar concentration of DTT.

Based on the results of the GILT reduction of BFLC and the outcomes of the DTT thiolysis of the DNP peptides, GILT activated with 100 fold DTT was used to test the hypothesis that GILT could remove DNP groups from a peptide. Although there is evidence that some thiolysis may have occurred at around 1.5 hours, the same effect was not observed at 4.5 hours (Figure 6.10). However, more replicates are needed to establish an effect. It was not possible to repeat the experiments due to the small amount of the enzyme available and time constraints.

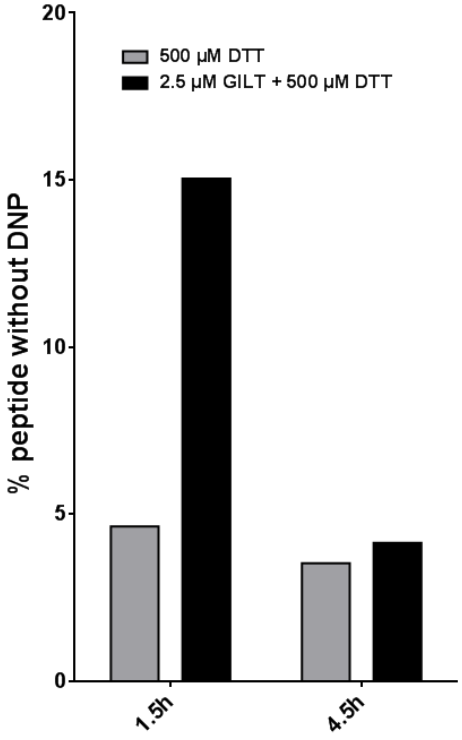

Figure 6.10. GILT thiolysis of DNP-C at two time points

The percentage removal of DNP groups from 5µM DNP-Cys after incubation with 500 µM DTT or 2.5 µM GILT + 500 µM DTT. The cysteinyl peptide was incubated at pH 4.5 with either 500 µM DTT or 2.5 µM GILT + 500 µM DTT.

One possibility for the result seen at 4.5 hours is that GILT's activity was being lost during the reaction, however, incubation of DTT-activated GILT with each of the synthetic DNP peptides for 1 hour prior to the addition of BFLC did not affect the reducing activity of GILT significantly (Student's t-test: DNP-C – t = 0.704, P > 0.05; DNP-K – t = 1.609, P > 0.05). Further, neither of the peptides has any direct effect on BFLC itself, GILT shows no reducing capability without activation by 25 µM DTT and 25 µM DTT has no effect by itself at pH 4.5 (Figure 6.11).

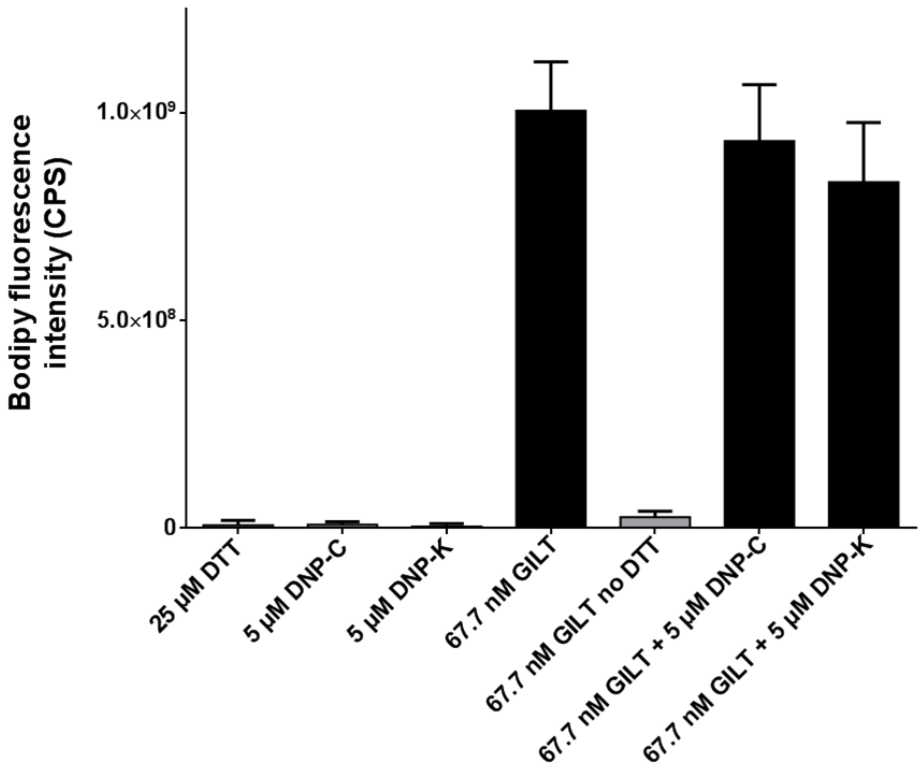

Figure 6.11. GILT reduction is dependent on DTT activation and is not affected by prior incubation with the DNP-peptides

BFLC was incubated at pH 4.5 with 25 µM DTT, 5 µM of each of the DNP-peptides, 67.7 nM GILT both with and without the addition of 25 µM DTT. The final two bars show an experiment where GILT was activated with 25µM DTT and then incubated for 1 hour with each peptide before BFLC was added for 1 hour.

6.4 Discussion

Ordinarily, generation of an immunological response from a peptide would require the use of a synthetic peptide whose sequence is designed to interact with the MHC binding groove. This is due to the MHC molecules using specificity pockets in the binding cleft to anchor peptides with the appropriate sequence affinity, rather than simply binding to any peptide of a suitable length (Yaneva 2010). Curated databases (SYFPEITHI, SNEP, IEDB) containing known MHC compatible peptides can be used for predicting the peptides presented or designing peptides for presentation on MHC class I and II molecules (Rammensee et al., 1999; Schuler et al., 2007; Sette et al., 2005). The requirement for a peptide to be tailored to fit into the MHC groove suggests that any immunogenic response from the synthetic peptide sequences used in this work and derived from HSA should be considered unlikely through orthodox processing of the peptide. Indeed, the SYFPEITHI, SNEP and IEDB online epitope prediction databases did not predict any affinity for the peptides used for this study in any class or restriction of MHC molecule (data not shown).

The strong T-cell proliferation observed in response to addition of the cysteinyl peptide, but not the lysinyl peptide (Figure 6.3) suggests that the former has been presented via MHC loading and the lysinyl peptide has not. It could also be that both peptides have been presented, but only the DNP-cysteine epitope stimulates T-cell receptors. While the peptides are not designed to interface with the MHC binding clefts, either idea can still be considered in the absence of a better explanation. However, the strong response to the trimer DNP-GSH demonstrates clearly that there is DNP-specific proliferation that is not mediated by ordinary MHC-peptide presentation to T-cells, since the minimum length peptide found to be associated with either class of MHC molecule is 8 amino acids (Neefjes et al., 2011). The common factor between the positive responses appears to be DNP-cysteine. Given that we show that DNP groups can be removed by thiolysis (Shaltiel, 1967) from cysteine by a reducing agent, it is possible that the DNP group is removed during antigen processing and that this may be responsible for the response. Whether this is due to DNP groups being transferred to other proteins or by some other mechanism in unclear. This supposition is reinforced by the results of the immunoblotting experiments, which clearly show the presence of several DNP-modified proteins in the lysate of monocytes incubated with the cysteinyl peptide, but not the lysinyl peptide. The addition of 50 μM chloroquine was added, increasing the pH of the endosomes (Seglen et al., 1979) with the intention of attenuating the transfer

of DNP groups to other proteins. This was based on the idea that the thiol reductase GILT, a strong candidate protein for the role of removing DNP groups, is optimally active at pH 4.5 (Phan et al., 2000) (also see Figure 6.9). Contrary to expectations, the addition of chloroquine had no discernible effect. Similarly, the activation of monocytes with IFN-γ was used to try to increase the transfer of haptens by up-regulating GILT expression and increasing the hapten transfer effect and no effect was observed. While this could mean that GILT is not responsible for the hapten transfer, another explanation is that the increase in pH, while reducing GILT's effectiveness (see Figure 6.9), is not sufficient to stop it from transferring DNP groups. It is also possible that GILT's activity is reduced, but free DNP groups generated by GILT thiolysis react more readily with nucleophilic amino acid side chains, since fewer of these groups will be protonated at higher pH and will be more reactive towards a free electrophile. This could offset any attenuation of GILT activity. If this hapten-transfer process were to happen continually during antigen processing, one would expect a gradual reduction in the number of cysteine modifications and an increase in the number of lysine modifications, since the latter are presumably stable and not affected by reduction. Determining if a cellular process of thiolysis alters the ratio of haptenated cysteine versus lysine over time would be an interesting course of further study of this topic.

The reducing activity of DTT is strongly affected by pH (Figure 6.5) and does not occur at pH 4.5 until a significant excess of DTT over substrate is present. This is also reflected in the removal of DNP groups from the cysteinyl peptides (Figure 6.8) which only occurs at low levels with a maximum of ~10% of the peptide observed without DNP groups after 4 hours. At pH 7.4, the removal of DNP groups from the cysteinyl peptide shows a strong response to both DTT concentration and incubation time, with almost 80% of the observed peptide having the DNP group replaced with a carbamidomethyl group. This demonstrates that the DNP group on cysteine of the HSA-derived peptide is susceptible to removal via reduction and that this relationship is affected by both the DTT concentration and the length of the incubation period. In contrast, the modification is consistently stable on lysine under all reducing conditions.

One possible mechanism of the thiolysis reaction could be attributed to the sulphur on cysteine acting as an electron-withdrawing group. At physiological pH, the sulphydryl group of DTT is nucleophilic allowing attack on the bond between the DNP and the sulphur of the cysteine. This occurs due to the combined electron-withdrawing

properties of the two nitro groups and the sulphur leaving the bond open to nucleophilic attack, so long as the DTT is in high excess (Figure 6.12). The amine group of lysine however would tend to push electrons into the bond, leaving it stable and not prone to attack by DTT (personal comms. Dr Jennifer Hiscock, University of Southampton).

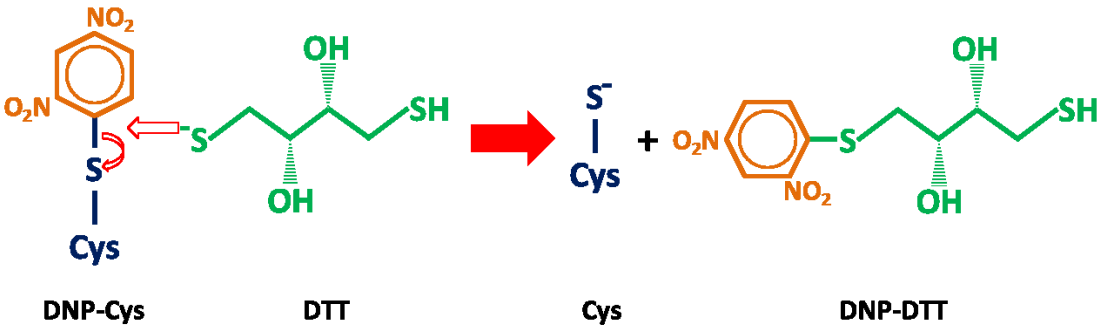

Figure 6.12. A proposed reaction schema for DTT thiolysis of DNP groups from cysteine
At neutral pH, the de-protonated sulphydryl group of DTT (green) is able to attack the bond between the sulphur of a cysteine (blue) and a DNP group (orange) due to the combined electron withdrawal of the nitro (NO_2) groups and the sulphur of the cysteine. The product of this reaction is a reduced cysteine and dinitrophenyl DTT.

When adjusting for background reduction by DTT, GILT was shown to have approximately 60% of the reducing strength at pH 7.4 than at pH 4.5, which agrees with previous studies (Phan et al., 2000). Studying HSA as a model protein in solution (chapter 5) demonstrated a high tendency for modification of cysteine by DNCB, particularly cysteine 34. Knowing that approximately 80% of DNP can be easily removed from cysteine at pH 7.4 by 100 equivalents of DTT and considering that GILT at pH 4.5 acts as a far stronger reducing agent, it is reasonable to hypothesise that GILT should be capable of removing the DNP from the cysteinyl peptide. However, the experimental ratio of 2.3:1 peptide:GILT does not allow similar DNP-removal as observed with DTT. This may suggest that either GILT does not reduce off the DNP groups by the same mechanism as DTT, or that the assay is not fully optimised for GILT. Although interesting, further investigation is required since a strong thiol reductase present in the endocytic pathway may explain both the immunogenicity of the cysteinyl peptide and DNP-GSH as well as the hapten transfer observed in our immunoblotting results. The results show some suggestion of the DNP being removed by GILT in the 1.5 hour incubation (Figure 6.10), but this effect was absent in the 4.5 hour incubation. One possibility is that an initial de-haptenation is subsequently reversed. The fact that the BFLC reducing assay shows results within a 1 hour supports

GILT being capable of having an effect in this time frame. One initial concern was that if DNP groups were removed from the peptide, they might bind to the active site of GILT and inhibit the action of the enzyme (Figure 6.13).

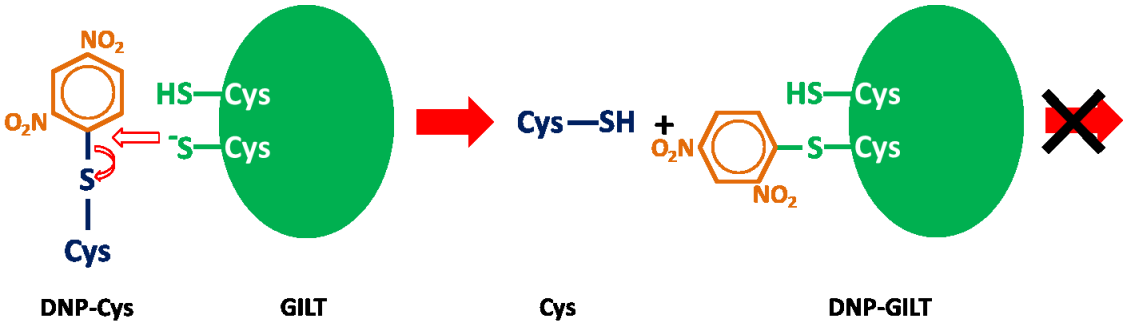

Figure 6.13. Proposed reaction of DNP thiolysis leading to GILT inhibition

GILT could be inactivated by transfer of the DNP group into the active site. The disulphide bond in the active site of GILT is reduced experimentally by the presence of 25 µM DTT which might allow the now de-protonated sulphydryl group to attack the bond between the cysteinyl sulphur and the aromatic ring of the DNP.

However, experiments incubating GILT with the peptides for 1 hour prior to the addition of BFLC showed no significant difference from the standard incubation of GILT with BFLC (Figure 6.11). Additionally, if the DNP groups were being removed and binding to GILT, one could expect the percentage of thiolysed peptides to persist between incubation times, rather than there being a reversal.

It is also possible that the GILT may remove DNP groups by forming a mixed disulphide with the cysteine from the peptides (Figure 6.14).

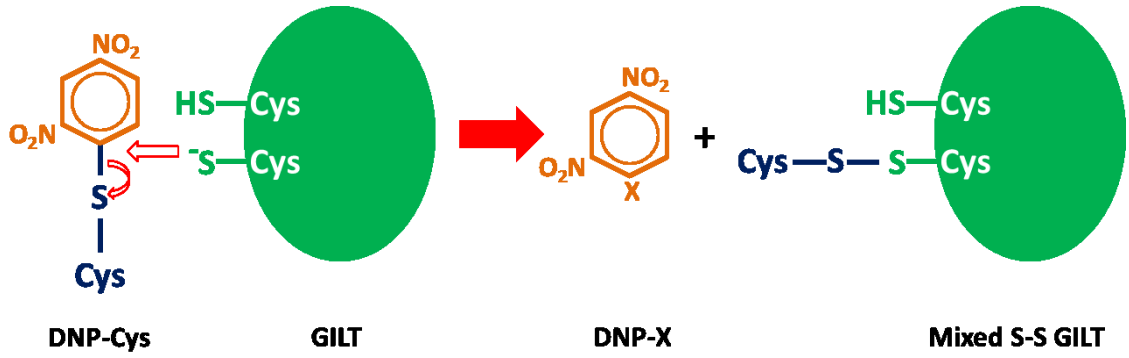

Figure 6.14. Proposed reaction of GILT thiolysis leading to a mixed disulphide GILT
A diagram showing a proposed alternative mechanism to that shown in Figure 6.13 whereby the DNP group leaves the reaction, with GILT forming a mixed disulphide intermediate with the cysteinyl peptide.

In theory, this reaction could lead to GILT being re-activated by DTT and leaving the cysteine free to be modified by IAA in the reaction, which could explain the thiolysed moieties seen.

There are several possibilities which need to be explored:

1 – The DTT used to activate the GILT is depleted over time by binding to free DNP generated during thiolysis allowing the reaction to reverse.

This would fit with the reaction proposed in Figure 6.14 and could be confirmed by incubating DTT-activated GILT with the peptides for 4.5 hours prior to the addition of BFLC to see if the reducing capacity of GILT is inhibited by DNP transfer to its active site over a longer time period. This could be addressed by adding L-cysteine to the incubation of GILT, DTT and DNP-peptide. The cysteine would assist in the activation of the GILT and be able to capture free DNP preventing depletion of GILT's activation factor.

2 – Unknown co-factors are required for GILT to remove DNP groups from cysteines, or the peptide is simply the wrong conformation or size for GILT activity.

Such co-factors are observed for other reductases such as thioredoxin, which requires both thioredoxin reductase and NADPH to remain active in the cystosol. While it is thought that GILT reduces proteins in solution in the late endosome prior to their digestion by cathepsins (Hastings and Cresswell, 2011), the mechanism cannot be assumed for DNP thiolysis. The DTT experiments and BFLC assays point towards the possibility of GILT being able to cleave DNP groups, but both DTT and BFLC are comparatively small substrate molecules, so the results might not directly translate to a DNP-labelled 8mer peptide. However a method would need to be optimised to achieve this. Incubating GILT with DNP-GSH and looking for thiolysis could determine if this is the case. If GSH shows a greater loss of DNP versus the DNP-cys peptide, this would support molecule size being a factor and may point towards there being a co-factor necessary for the reaction. The western blot experiments in this chapter show a greater degree of hapten transfer from DNP-GSH versus a DNP-labelled cysteine within an 8-mer peptide. This could be due to GILT being more effective at removing DNP from smaller peptides.

3 – GILT is not involved in the removal of DNP from cysteines.

The null hypothesis must be considered. The role of GILT could be investigated by reducing GILT in human monocytes or a monocyte-like cells (e.g. THP-1 cells) with specific siRNAs (Fontana et al., 2007; Liu et al., 2007), or using murine IFI30$^{-/-}$ cells (Hastings et al., 2006). The immunoblotting experiments seen earlier could be repeated using B cells from GILT knockout mice to determine if hapten transfer still occurs. Such experiments should be a priority for further work.

The ability for a DNP-cysteinyl peptide not designed for MHC interaction to stimulate a positive immune response from lymphocytes taken from DNCB-sensitized volunteers is unexpected. The response from the tri-peptide DNP-GSH is even more remarkable, since this strongly indicates a non MHC-mediated method of immune stimulation by DNP-cysteinyl proteins and peptides. The immunogenicity of DNP-GSH is also interesting as DNP-GSH is an expected bi-product of detoxification of DNP within the skin and as such could be contributing to the immunogenic response. The immunoblotting experiments show that the DNP group can be removed from the

peptides and transferred to other protein targets during incubation with monocytes and that this response is more pronounced with DNP-GSH. Experiments with DTT show conclusively that while DNP-cysteine is extremely susceptible to removal by thiolysis, DNP-lysine is not. This result mirrors the evidence that the DNP-lysinyl peptide is not able to stimulate T-cell proliferation and shows no redistribution of haptens during monocyte incubations. Combined, these findings convincingly point to the lability of DNP-cysteine as a factor in its immunogenicity. One study has shown that adducts generated by the extreme skin sensitizer oxazolone have been observed spontaneously coming off of cysteine residues and forming stable adducts on lysine residues (Natsch et al., 2010). The same group have also shown that chemical sensitizers which modify proteins by the SN2 reaction are more strongly correlated with sensitizing potential than those which modify by Michael addition (Natsch et al., 2011a). While a mechanism for this difference is suggested in the article, it would be interesting if the effect was also linked to SN2-derived adducts being more labile from cysteine residues. The role of GILT, a powerful thiol reductase which resides within the endocytic pathway is as yet unclear, but a clear route to determining its involvement is presented.

6.4.1 Summary

The immunogenicity of modified cysteine may not be dependent on traditional antigen processing and presentation mechanisms, instead being linked to a removal of the hapten during antigen processing and transfer to other protein targets. If a significant amount of DNCB modifications in the epidermis are present on cysteine residues, then these modifications could be re-distributed to other proteins during antigen processing for presentation, by direct modification of presented peptides or even the MHC molecule itself. Whether this is a mechanism shared by other sensitizers and whether it determines their potency remains to be seen.

7 GENERAL DISCUSSION AND FUTURE WORK

7.1 Summary of experimental work and results

The antibody labelling in chapter 3 was shown to have more use as a qualitative rather than quantitative method for detection of DNP-proteins. The immunofluorescence results showed that the extent of DNCB modification of proteins within the epidermis varies between individual donors (Figs. 3.2 and 3.3) and that a sufficiently high dose can damage the dermal-epidermal junction and potentially allowing the chemical to reach the dermis (Figure 4.1). The distribution of modified proteins in epidermis seems to be widespread, while there appears to be association with structures in the cytosol of HaCaT cells. Both this and the autoradiography suggest that the range of proteins modified by DNCB is broad rather than specific. Differences between the antibody-labelling and autoradiography highlight a limitation of the former in detecting the full range of adducts.

DNCB-modified HaCaT proteins are able to generate an antigen-specific response in the PBMCs of DNCB-sensitized donors which is comparable with that of modified proteins from primary keratinocytes and to DNCB itself. These results imply that some modified HaCaT proteins may contain epitopes which share similarities with those involved in the sensitization of the donors, since a detectable lymphocyte proliferation response within 6 days suggests the stimulation of antigen-specific memory T-cells by a protein or proteins within the lysates. However this effect was not able to be reproduced, suggesting a need for methodological optimisation. While fractionation of the DNCB-treated HaCaT cell lysates were shown to contain detectable DNP adducts (Figure 4.3), the fractions were not able to elicit T-cell proliferation in PBMCs. Additionally it was not possible to identify specific DNP peptides by mass spectrometric analysis of enzymatic digests of the proteins. This was possibly due to the methodological limitation of omitting protein reduction prior to digestion and analysis.

The modification of human serum albumin by DNCB has been quantified broadly using spectrophotometry and is shown to increase logarithmically over time at all doses with no end point having been reached at after 1 week (Figure 5.3). Using mass spectrometric analysis, many novel sites of HSA modification were detected at different combinations of DNCB dose and incubation time. The total number of modifications was shown to increase more strongly in response to dose than time, but still

significantly for both, which supports the spectrophotometry findings, which showed no end point after 7 days. In contrast to this, the total number of mass spectrometry detected modifications reached its apex after around 24 hours. The majority of the modifications found were on cysteine or lysine residues; however cysteines were shown to be modified much more readily at lower DNCB concentrations and shorter incubation times than lysines. Cysteine 34 was demonstrated to be the most readily modified residue within HSA. The use of isotope-labelled sensitizers with UPLC-MS^E provides a robust method of detecting the amino acid residues modified on HSA by DNCB. Interestingly, most of the cysteines modified were thought to be unavailable due to their involvement in S-S bonds. The ability of DNCB to reduce S-S bonds was ruled out experimentally. This suggests either that the DNCB modification of HSA is somehow able to weaken S-S bonds, or it is also possible that some of the haptens are being transferred from cysteine 34, which was found heavily modified, to the other cysteines made available during reduction, as DNP groups can be removed from cysteines in the presence of a reducing agent.

The thiolysis work has used DNP-specific lymphocyte proliferation to demonstrate that a DNP-cysteine modification is immunogenic whereas the DNP-lysine equivalent is not. Further, the immunogenicity of DNP-GSH highlights a mechanism of immunogenicity which does not require loading of the modified peptide into MHC molecules. This has been linked to a process of hapten-transfer shown by anti-DNP western blot to occur within monocytes which affects DNP-cysteine modifications, particularly DNP-GSH, but not the lysinyl equivalent. My work shows that DNP-cysteine modifications are labile under reducing conditions and can be removed by incubation with dithiothreitol. By contrast, DNP-lysine modifications remain stable and are not affected by reduction. The enzyme GILT, which is present within endosomes and reduces proteins prior to enzymatic degradation during antigen processing is presented as a candidate for the *in vivo* hapten transfer of DNP groups by thiolysis. However, the results do not conclusively show the role of GILT in this process.

7.2 Can models be used to determine sensitizers?

The core purpose of this work is to investigate the mechanisms of protein modification using *in vitro* model systems and determine which modifications in particular confer immunogenicity. The usefulness of model systems in reducing sample variation and allowing for higher throughput work is offset against their differences from the *in vivo* systems they model. Previously, animal models have been favoured for assessing chemical sensitizers, most notably the guinea pig maximisation test and its successor, the local lymph node assay (Basketter and Scholes, 1992; Landsteiner and Chase, 1937). However the recent EU ban on animal testing for cosmetics and toiletries necessitates the development of alternative methods for screening novel chemicals. To date, a method has not yet been developed which identifies chemical sensitizers as well as the LLNA. The LLNA is used as a comparison for *in vitro* assays to determine their effectiveness (Johansson et al., 2013; Nukada et al., 2012; Ouwehand et al., 2010a). Though the LLNA is considered the default test for chemicals, it incorrectly identifies SDS as a sensitizer rather than an irritant and fails to identify nickel or its salts as a sensitizer (Basketter et al., 1999). It should be noted that nickel is a somewhat special case due to its reliance on binding to conserved histidine residues specific to human toll-like receptor 4 (TLR4). Without this interaction, nickel is unable to trigger the innate response necessary for inducing sensitization (Schmidt et al., 2010).

The work within this project does not set out to develop a single assay, but to investigate the properties of the model sensitizer DNCB through the way it interacts with proteins and in turn how those proteins interact with the acquired immune system. It is hoped that some of the results can be used to further characterise sensitizers and inform the prediction of sensitizing chemicals other than DNCB. The current consensus is that chemicals must be able to do the following in order to be an effective sensitizer:

1. Penetrate through the *stratum corneum* into the epidermis
2. Trigger an innate immune response, generating pro-inflammatory signals
3. Modify proteins in the skin to confer an immunogenic epitope

The use of HaCaT cells as a model can be justified initially since they are derived from basal keratinocytes from histologically normal skin and can be maintained in culture indefinitely (Boukamp et al., 1988). Gene expression analysis has also showed similarities between HaCaT cells and keratinocytes *in vivo* (Lemaître et al., 2004). It

can be argued that the results of chapters 3 and 4 support this further by exhibiting similarities in protein modification profiles between HaCaT cells and *ex vivo* skin and the stimulation of DNP-specific T-cell proliferation in lymphocyte proliferation assays. The use of the lymphocyte proliferation data to specifically add weight to the argument of HaCaT cells being similar to epidermis would be further supported by refining the experiments to give reproducible proliferative responses with less toxicity and extending the work using a cell line which is phenotypically disparate from skin. Any significant differences in similarity of modification profile or T-cell proliferation would strengthen the case for a keratinocyte cell-line being useful as a model for skin. Without a noticeable effect attributable to keratinocytes specifically, it could be argued that the protein modifications involved in sensitization are related to common or ubiquitously expressed proteins, such as actin, rather than anything specific to keratinocytes.

7.3 Is DNCB immunogenicity driven by specific or generic protein modifications?

The thiolysis work demonstrating the immunogenicity of DNP-GSH and DNP-Cys versus DNP-Lys is compelling evidence for a DNP adduct mediated immune response which does not rely on MHC presentation of the DNP-peptide (Figure 6.3). This mirrors the results of the western blot (Figure 6.4) and peptide LC-MS (Figure 6.8) experiments to make a convincing case for the immunogenicity of DNP-Cys being linked to a cellular process of thiolysis, which occurs after endocytosis of the peptides. The thiol reductase GILT is a suitable candidate for being able to remove DNP groups *in vivo*, as shown by its strong reducing activity when coupled with DTT (Figure 6.9). However the latter may remove DNP groups and it is not yet certain whether GILT is capable of removing them and as such, its role in the process remains speculative (Figure 6.10).

With or without evidence to determine the precise biological mechanism of hapten transfer within monocytes, the work raises some compelling questions about the nature of protein modifications in allergic contact dermatitis. The current consensus is that studies of protein modification should serve to identify the hapten-mediated peptide epitopes which are presented by antigen-presenting cells to the naïve T-cell repertoire within lymph nodes (Vocanson et al., 2013). If these initial modifications are able to be transferred during antigen processing however, then the role of many of the initial

modification events may be generic rather than specific, with cysteinyl modifications (and possibly tyrosine and histidine (Shaltiel, 1967)) acting as carriers for certain haptens rather than a specific determinant of immunogenicity. This makes the HSA results in chapter 5 potentially more interesting as modifications appear to occur far more readily on cysteines than other amino acid residues. In particular, cysteine 34 has been shown by a number of published studies to be modified by a range of chemicals (Aleksic et al., 2007; Dietz et al., 2010; Jenkinson et al., 2010). However, it is important to consider the possibility that some of these modifications were generated by reduction during the protein preparation steps.

This work should be extended to other sensitizers as a high priority to determine if thiolysis is relevant to all electrophilic sensitizers, just nitrohalobenzenes, or perhaps just those sensitizers which modify proteins by an SN_2 mechanism. The ability to modify proteins both directly and after bioactivation is known to contribute to a sensitizer's potency, but reactivity assays have yet to show a comprehensive agreement with the more established LLNA (Gerberick et al., 2008). However some work has identified a correlation between different mechanisms of modification and sensitizer potency (Natsch et al., 2011b). Could this process of hapten transfer apply to other chemical sensitizers and perhaps go some way to explaining some of the discrepancies between protein reactivity and ability to cause allergic contact dermatitis?

There is good reason to suppose that this novel process may play a part in contact allergies. The following hypothetical mechanisms can be proposed:

1) Hapten transfer to MHC-bound peptides increases immunogenicity

Modified proteins are endocytosed by APCs and any cysteine, histidine or tyrosine residues with DNP modifications may lose that modification within the MHC class II processing pathway. If this occurs within the endosome, it may be possible that MCH II bound peptides are modified by reactive DNP moieties liberated by GILT thiolysis. This could increase the probability of DNCB generating MHC-presented DNP-peptides, thus increasing immunogenicity.

2) Hapten transfer to MHC molecules

It is also possible that thiolysed DNP groups attach to the MHC molecules themselves. This could create immunogenic epitopes by eccentric binding of ordinary peptides to the MHC molecule. This could be by the DNP binding to the MHC binding groove itself or by altering the MHC binding groove allosterically by modifying a distal part of the molecule.

Both of these possibilities are supported by the lymphocyte proliferation in response to DNP-Cys and DNP-GSH – immunogenic responses are being observed and are unlikely to be due to direct presentation of the peptides.

Lastly, this work has shown that when analysing DNCB adducts, it is extremely important to consider the experimental preparation and the chemicals used prior to analysis. It is not appropriate to use a reducing agent if the adduct is to be considered remaining intact. Hence for proteomic analysis, the reduction of disulphide bonds should not be carried out as this is likely to perturb the modifications generated during the initial incubations. However, retaining disulphide bonds produces difficulties. For example, enzymatic digestion of proteins which still contain disulphide bonds is inefficient, resulting in many peptides that are too large to ionise and travel through a mass spectrometer. Mass spectrometric analysis of proteins which have not been reduced increases the complexity of database searching, since carbamidomethylation of cysteines using iodoacetamide will be incomplete.

Additionally, thiolysis could have important implications for the role of polyclonal antibodies in detecting DNP adducts, since e.g. DNP-HSA is used to generate anti-DNP antibodies in a host species, the immunogenic epitopes which drive antigen production may be largely different from the conformational epitopes in DNP-HSA, which would be used to affinity purify the resulting immunoglobulin fraction. This would mean that anti-DNP antibodies may be specific only to epitopes which resemble those originating in DNP-HSA and that many other useful antibodies which do not recognise DNP-HSA are being discarded.

It is therefore necessary to work on the optimisation of existing techniques and perhaps development of novel methods for the analysis of adducts which are sensitive to removal by reducing agents.

7.4 Summary

The findings relating to thiolysis and hapten-transfer during antigen processing have interesting implications on the other work involved in this study. If reduction can remove DNP groups, then how can we confidently interpret the results of proteomics experiments which include reduction steps during sample preparation? If the proteins modified within the epidermis are only acting as carriers for the DNP group, then is it possible to determine which peptides are immunogenic by analysing modified HaCaT lysates?

The results of the work undertaken here have shown that DNCB as a sensitizer can modify a great range of proteins in tissue and cell lines and that these modifications are significantly immunogenic. The way that DNCB modifies a single protein target has been shown to be both comprehensive in terms of the number of modifications found and paradoxical due to the presence of DNP-cysteines where one would expect to find disulphide bridges, despite DNCB showing no reducing ability. There remains the question of how this process occurs within cells, and the thiol reductase GILT has been suggested as a possible candidate for future work in this area.

7.5 Further work

The inability to derive a relevant experimental DNCB dose for cells by comparing antibody labels between skin and HaCaTs requires that a different technique be considered. The approach should be reconsidered by a combination of a viability assay, combined with the use of radioisotope-labelled DNCB treatment of skin at the clinical dose of 50 $\mu g/cm^2$ and HaCaT cells at a range of doses which do not seriously affect viability. The lysates derived from the skin and HaCaT cells could be quantified in terms of DNCB modification by comparing scintillation counting of the lysates.

The results of the lymphocyte proliferation assays with HaCaT lysates were variable. It would be useful to repeat them using protease inhibited lysates extracted from untreated HaCaT cells incubated with 100-fold molar excess of DNCB and assayed for their immunogenicity. This would allow for a more definitive idea of the presence of immunogenic proteins derived from these cells.

The study of proteins is typically assisted by reduction of S-S bonds during sample preparation to simplify analyses by removing secondary and tertiary structure; however in future this analysis should be carried out without a reducing step. The inclusion of reducing agents will arguably show the effects of thiolysis rather than solely the effects of incubation with the chemical as intended. Further study is required to determine the extent to which this undermines the results from previous work; however a re-appraisal of methodology is needed to allow the unbiased analyses of DNCB modifications to proteins. A methodology should be devised to improve the enzymatic digestion and identification of non-reduced proteins by LC-MS^E. If successful, this could be applied to immunogenic HaCaT lysates and fractions and the DNP-HSA experiments could be repeated without reduction to determine if a significant amount of the modification has been affected by thiolysis.

Protein prepared from each of the DNCB dose and incubation time points of the HSA work, or perhaps a selection of them, could be added to LPA assays to see what effect the different states of modification have on the immunogenicity of the protein. Additionally, these DNP-HSA samples could be exposed to a strong reducing buffer for 24 hours before being washed with buffer by retention in centrifuge filters and then assayed for immunogenicity. Any loss of immunogenicity linked to the removal of

DNP from cysteine, histidine and tyrosine would provide useful information to the immunogenic properties of DNCB.

The role of thiolysis in the generation of immunogenic peptides should be further explored using a second set of non-DNP synthetic peptides to act as acceptors for any reactive DNP groups generated by DNP thiolysis. This will determine if the DNP groups can be conferred to new acceptors by thiolysis. Perhaps most importantly, the thiolysis experiments should be repeated with other haptens to determine which modifications in particular this effect applies to.

It would be interesting to see which DNP-positive peptides are complexed with MHC molecules by antigen-presenting cells. If DNP-GSH could be synthesised with both non-labelled and deuterated DNP groups, then APCs could be incubated with DNP-GSH overnight, MHC groups could be isolated by immune pull-down and the presented peptides analysed by mass spectrometry. This could provide a great insight into the specific immunogenicity of DNCB, since any non-GSH peptides shown to carry a modification must be the result of a hapten transfer.

8 Appendix

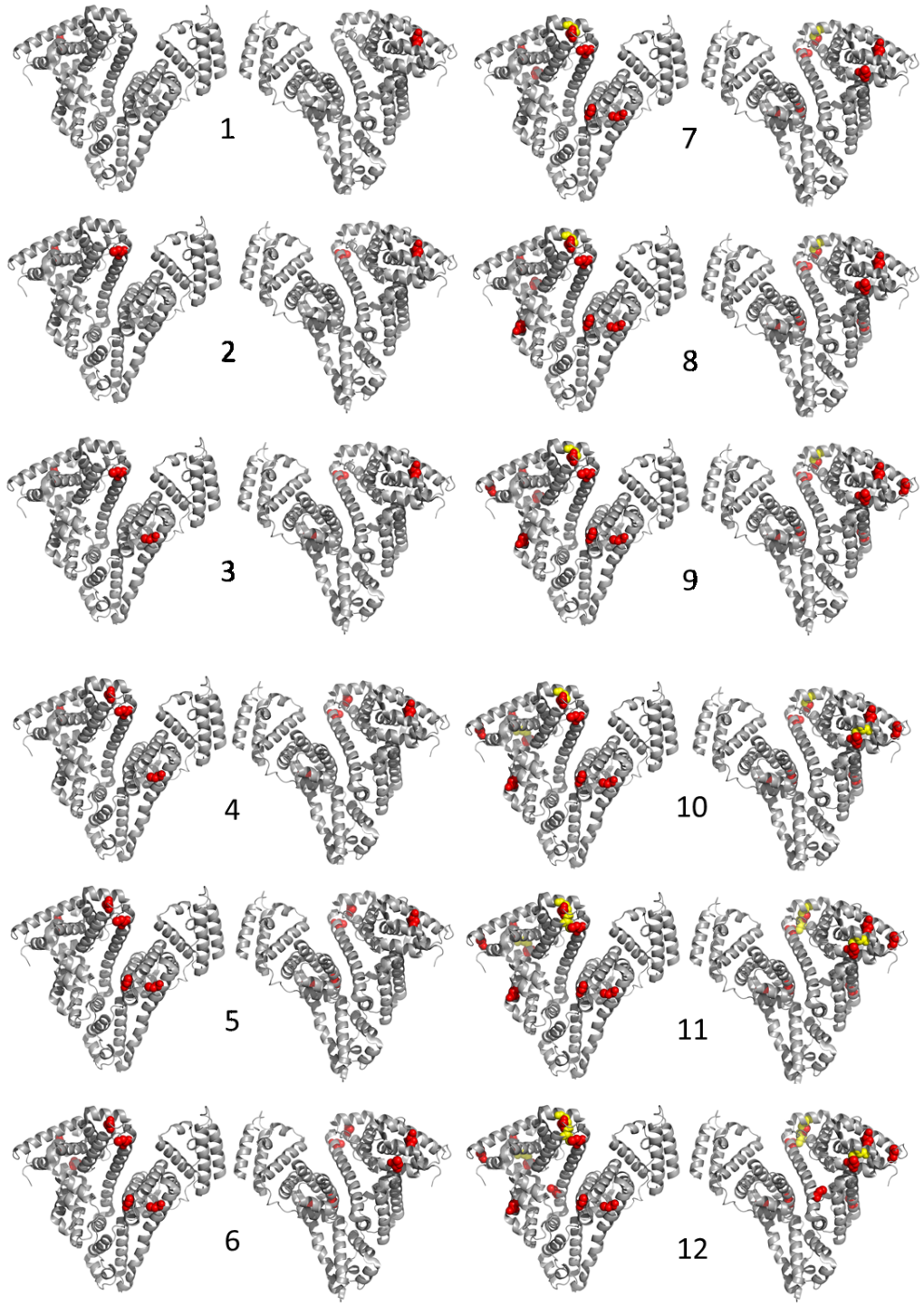

Figure 8.1. Progressive modifications of disulphide bond cysteines within HSA

A crystal structure (1ŠNU) of human serum albumin annotated to show the modification of cysteines ordinarily within disulphide bonds in order to reactivity score (see chapter 5). Cysteines are colour coded as follows: Green = non-modified cysteines forming a disulphide bridge assumed to be intact prior to reduction; Red = cysteine modified by DNCB, Yellow = cysteine modified by DNCB with a lower reactivity score than the red equivalent within the same S-S bridge.

9 REFERENCES

Abraham, M.H., Chadha, H.S., and Mitchell, R.C. (1995). The Factors That Influence Skin Penetration of Solutes. J Pharm Pharmacol *47*, 8-16.

Aebersold, R., and Mann, M. (2003). Mass spectrometry-based proteomics. Nature *422*, 198-207.

Aldini, G., Gamberoni, L., Orioli, M., Beretta, G., Regazzoni, L., Maffei Facino, R., and Carini, M. (2006). Mass spectrometric characterization of covalent modification of human serum albumin by 4-hydroxy-trans-2-nonenal. Journal of Mass Spectrometry *41*, 1149-1161.

Aleksic, M., Pease, C.K., Basketter, D.A., Panico, M., Morris, H.R., and Dell, A. (2007). Investigating protein haptenation mechanisms of skin sensitisers using human serum albumin as a model protein. Toxicology in Vitro *21*, 723-733.

Aleksic, M., Pease, C.K., Basketter, D.A., Panico, M., Morris, H.R., and Dell, A. (2008). Mass spectrometric identification of covalent adducts of the skin allergen 2,4-dinitro-1-chlorobenzene and model skin proteins. Toxicology in Vitro *22*, 1169-1176.

Aleksic, M., Thain, E., Roger, D., Saib, O., Davies, M., Li, J., Aptula, A., and Zazzeroni, R. (2009). Reactivity profiling: covalent modification of single nucleophile peptides for skin sensitization risk assessment. Toxicological sciences : an official journal of the Society of Toxicology *108*, 401-411.

Allan, R.S., Smith, C.M., Belz, G.T., van Lint, A.L., Wakim, L.M., Heath, W.R., and Carbone, F.R. (2003). Epidermal viral immunity induced by CD8alpha+ dendritic cells but not by Langerhans cells. Science *301*, 1925-1928.

Alvarez-Sánchez, R., Divkovic, M., Basketter, D., Pease, C., Panico, M., Dell, A., Morris, H., and Lepoittevin, J.-P. (2004). Effect of Glutathione on the Covalent Binding of the 13C-Labeled Skin Sensitizer 5-Chloro-2-methylisothiazol-3-one to Human Serum Albumin: Identification of Adducts by Nuclear Magnetic Resonance, Matrix-Assisted Laser Desorption/Ionization Mass Spectrometry, and Nanoelectrospray Tandem Mass Spectrometry. Chemical Research in Toxicology *17*, 1280-1288.

Anraku, M., Yamasaki, K., Maruyama, T., Kragh-Hansen, U., and Otagiri, M. (2001). Effect of oxidative stress on the structure and function of human serum albumin. Pharmaceut Res *18*, 632-639.

Arnér, E.S.J., and Holmgren, A. (2000). Physiological functions of thioredoxin and thioredoxin reductase. European Journal of Biochemistry *267*, 6102-6109.

Arunachalam, B., Phan, U.T., Geuze, H.J., and Cresswell, P. (2000). Enzymatic reduction of disulfide bonds in lysosomes: characterization of a gamma-interferon-inducible lysosomal thiol reductase (GILT). Proceedings of the National Academy of Sciences of the United States of America *97*, 745-750.

Basketter, D.A., Blaikie, L., Dearman, R.J., Kimber, I., Ryan, C.A., Gerberick, G.F., Harvey, P., Evans, P., White, I.R., and Rycroft, R.J.G. (2000). Use of the local lymph node assay for the estimation of relative contact allergenic potency. Contact Dermatitis *42*, 344-348.

Basketter, D.A., Lea, L.J., Cooper, K.J., Ryan, C.A., Gerberick, G.F., Dearman, R.J., and Kimber, I. (1999). Identification of metal allergens in the local lymph node assay. American journal of contact dermatitis : official journal of the American Contact Dermatitis Society *10*, 207-212.

Basketter, D.A., and Scholes, E.W. (1992). Comparison of the local lymph node assay with the guinea-pig maximization test for the detection of a range of contact allergens.

Food and chemical toxicology : an international journal published for the British Industrial Biological Research Association *30*, 65-69.

Bauer, B., Andersson, S.I., Stenfeldt, A.-L., Simonsson, C., Bergström, J.r., Ericson, M.B., Jonsson, C.A., and Broo, K.S. (2011). Modification and Expulsion of Keratins by Human Epidermal Keratinocytes upon Hapten Exposure in Vitro. Chemical Research in Toxicology *24*, 737-743.

Bennett, C.L., Noordegraaf, M., Martina, C.A., and Clausen, B.E. (2007). Langerhans cells are required for efficient presentation of topically applied hapten to T cells. J Immunol *179*, 6830-6835.

Berard, F., Marty, J.P., and Nicolas, J.F. (2003). Allergen penetration through the skin. European Journal of Dermatology *13*, 324-330.

Bertucci, C., and Domenici, E. (2002). Reversible and Covalent Binding of Drugs to Human Serum Albumin: Methodological Approaches and Physiological Relevance. Current Medicinal Chemistry *9*, 1463-1481.

Bleumink, E., Mitchell, J.C., Geissman, T.A., and Towers, G.H.N. (1976). Contact hypersensitivity to sesquiterpene lactones inChrysanthemumdermatitis. Contact Dermatitis *2*, 81-88.

Boelsma, E., Verhoeven, M.C., and Ponec, M. (1999). Reconstruction of a human skin equivalent using a spontaneously transformed keratinocyte cell line (HaCaT). The Journal of investigative dermatology *112*, 489-498.

Boukamp, P., Petrussevska, R.T., Breitkreutz, D., Hornung, J., Markham, A., and Fusenig, N.E. (1988). Normal Keratinization in a Spontaneously Immortalized Aneuploid Human Keratinocyte Cell-Line. J Cell Biol *106*, 761-771.

Brand, C.U., Hunziker, T., and Braathen, L.R. (1992). Studies on Human Skin Lymph Containing Langerhans Cells from Sodium Lauryl Sulfate Contact-Dermatitis. Journal of Investigative Dermatology *99*, S109-S110.

Brander, C., Mauri-Hellweg, D., Bettens, F., Rolli, H., Goldman, M., and Pichler, W.J. (1995). Heterogeneous T cell responses to beta-lactam-modified self-structures are observed in penicillin-allergic individuals. The Journal of Immunology *155*, 2670-2678.

Brown, S.J., and McLean, W.H.I. (2009). Eczema Genetics: Current State of Knowledge and Future Goals. The Journal of investigative dermatology *129*, 543-552.

Buchanan, M.V., and Hettich, R.L. (1993). Fourier transform mass spectrometry of high-mass biomolecules. Analytical chemistry *65*, 245A-259A.

Carr, M.M., Botham, P.A., Gawkrodger, D.J., Mcvittie, E., Ross, J.A., and Hunter, J.A.A. (1983). Early Cellular Events in Contact Sensitivity Induced by Dinitrochlorobenzene. Brit J Dermatol *109*, 691-691.

Carr, M.M., Botham, P.A., Gawkrodger, D.J., Mcvittie, E., Ross, J.A., Stewart, I.C., and Hunter, J.A.A. (1984). Early Cellular Reactions Induced by Dinitrochlorobenzene in Sensitized Human-Skin. Brit J Dermatol *110*, 637-641.

Carter, D.C., and Ho, J.X. (1994). Structure of Serum-Albumin. Adv Protein Chem *45*, 153-203.

Cavani, A., Mei, D., Guerra, E., Corinti, S., Giani, M., Pirrotta, L., Puddu, P., and Girolomoni, G. (1998). Patients with Allergic Contact Dermatitis to Nickel and Nonallergic Individuals Display Different Nickel-Specific T Cell Responses. Evidence for the Presence of Effector CD8+ and Regulatory CD4+ T Cells. *111*, 621-628.

Cerio, R., Griffiths, C.E.M., Cooper, K.D., Nickoloff, B.J., and Headington, J.T. (1989). Characterization of factor XIIIa positive dermal dendritic cells in normal and inflamed skin. Brit J Dermatol *121*, 421-431.

Chang, H.T., Yergey, A.L., and Chrambach, A. (2001). Electroelution of proteins from bands in gel electrophoresis without gel sectioning for the purpose of protein transfer into mass spectrometry: Elements of a new procedure. Electrophoresis *22*, 394-398.

Chen, E.I., Hewel, J., Felding-Habermann, B., and Yates, J.R. (2006). Large Scale Protein Profiling by Combination of Protein Fractionation and Multidimensional Protein Identification Technology (MudPIT). Molecular & Cellular Proteomics *5*, 53-56.

Chipinda, I., Hettick, J.M., and Siegel, P.D. (2011). Haptenation: chemical reactivity and protein binding. Journal of allergy *2011*, 839682.

Coenraads, P.J., and Goncalo, M. (2007). Skin diseases with high public health impact. Contact dermatitis. European journal of dermatology : EJD *17*, 564-565.

Coombs, G. (1975). Classification of allergic reactions for clinical hypersensitivity and disease. In Clinical Aspects of Immunology, C.R.R.A. Gell P G H, Lachman R, ed. (London: Blackwell Scientific), pp. 761-781.

Coquette, A., Berna, N., Vandenbosch, A., Rosdy, M., and Poumay, Y. (1999). Differential expression and release of cytokines by an in vitro reconstructed human epidermis following exposure to skin irritant and sensitizing chemicals. Toxicology in Vitro *13*, 867-877.

Cox, J.r., Neuhauser, N., Michalski, A., Scheltema, R.A., Olsen, J.V., and Mann, M. (2011). Andromeda: A Peptide Search Engine Integrated into the MaxQuant Environment. Journal of proteome research *10*, 1794-1805.

Craig, R., and Beavis, R.C. (2004). TANDEM: matching proteins with tandem mass spectra. Bioinformatics *20*, 1466-1467.

Cumberbatch, M., Dearman, R.J., Griffiths, C.E.M., and Kimber, I. (2000). Langerhans cell migration. Clin Exp Dermatol *25*, 413-418.

Curry, S., Mandelkow, H., Brick, P., and Franks, N. (1998). Crystal structure of human serum albumin complexed with fatty acid reveals an asymmetric distribution of binding sites. Nature structural biology *5*, 827-835.

de Hoffmann, E.a.S., V (2007). Mass spectrometry: Principles and applications., 3rd edn (Chichester: Wiley).

de Jong, M.A., Vriend, L.E., Theelen, B., Taylor, M.E., Fluitsma, D., Boekhout, T., and Geijtenbeek, T.B. (2010). C-type lectin Langerin is a beta-glucan receptor on human Langerhans cells that recognizes opportunistic and pathogenic fungi. Molecular immunology *47*, 1216-1225.

De Vleeschouwer, F., Geerlings, P., and De Proft, F. (2012). Radical electrophilicities in solvent. Theor Chem Acc *131*.

de Waal Malefyt, R., Haanen, J., Spits, H., Roncarolo, M.G., te Velde, A., Figdor, C., Johnson, K., Kastelein, R., Yssel, H., and de Vries, J.E. (1991). Interleukin 10 (IL-10) and viral IL-10 strongly reduce antigen-specific human T cell proliferation by diminishing the antigen-presenting capacity of monocytes via downregulation of class II major histocompatibility complex expression. The Journal of Experimental Medicine *174*, 915-924.

Dearman, R.J., and Kimber, I. (1991). Differential stimulation of immune function by respiratory and contact chemical allergens. Immunology *72*, 563-570.

Deduve, C., Debarsy, T., Poole, B., Trouet, A., Tulkens, P., and Vanhoof, F. (1974). Lysosomotropic Agents. Biochemical pharmacology *23*, 2495-&.

Delneste, Y., Charbonnier, P., Herbault, N., Magistrelli, G., Caron, G., Bonnefoy, J.-Y., and Jeannin, P. (2003). Interferon-γ switches monocyte differentiation from dendritic cells to macrophages. Blood *101*, 143-150.

Deshmukh, G.R., Kumar, K.H., Reddy, P.V.S., and Rao, B.S. (2012). In vitro skin corrosion: Human skin model test – A validation study. Toxicology in Vitro *26*, 1072-1074.

Dietz, L., Esser, P.R., Schmucker, S.S., Goette, I., Richter, A., Schnölzer, M., Martin, S.F., and Thierse, H.-J. (2010). Tracking Human Contact Allergens: From Mass Spectrometric Identification of Peptide-Bound Reactive Small Chemicals to Chemical-Specific Naive Human T-Cell Priming. Toxicological Sciences *117*, 336-347.

Dinkova-Kostova, A.T., Holtzclaw, W.D., Cole, R.N., Itoh, K., Wakabayashi, N., Katoh, Y., Yamamoto, M., and Talalay, P. (2002). Direct evidence that sulfhydryl groups of Keap1 are the sensors regulating induction of phase 2 enzymes that protect against carcinogens and oxidants. Proceedings of the National Academy of Sciences of the United States of America *99*, 11908-11913.

Divkovic, M., Pease, C.K., Gerberick, G.F., and Basketter, D.A. (2005). Hapten-protein binding: from theory to practical application in the in vitro prediction of skin sensitization. Contact Dermatitis *53*, 189-200.

Dockal, M., Carter, D.C., and Rüker, F. (2000). Conformational Transitions of the Three Recombinant Domains of Human Serum Albumin Depending on pH. J Biol Chem *275*, 3042-3050.

EC (2003). Directive 2003/15/EC of the European Parliament and of the Council of 27 February 2003 Amending Council Directive 76/768/EEC on the Approximation of the

Laws of the Member States Relating to Cosmetic Products. Official Journal of the European Union *66*, 9.

Elahi, E.N., Wright, Z., Hinselwood, D., Hotchkiss, S.A.M., Basketter, D.A., and Smith Pease, C.K. (2004). Protein Binding and Metabolism Influence the Relative Skin Sensitization Potential of Cinnamic Compounds. Chemical Research in Toxicology *17*, 301-310.

Elbayed, K., Berl, V., Debeuckelaere, C., Moussallieh, F.-M., Piotto, M., Namer, I.-J., and Lepoittevin, J.-P. (2013). HR-MAS NMR Spectroscopy of Reconstructed Human Epidermis: Potential for the in Situ Investigation of the Chemical Interactions between Skin Allergens and Nucleophilic Amino Acids. Chemical Research in Toxicology *26*, 136-145.

Elortza, F., Nühse, T.S., Foster, L.J., Stensballe, A., Peck, S.C., and Jensen, O.N. (2003). Proteomic Analysis of Glycosylphosphatidylinositol-anchored Membrane Proteins. Molecular & Cellular Proteomics *2*, 1261-1270.

Eng, J.K., Martin, D.B., and Aebersold, R. (2004). Tandem mass spectrometry database searching. In Encyclopedia of Genetics, Genomics, Proteomics and Bioinformatics (John Wiley & Sons, Ltd).

Evans, C.C., and Fleming, J.D. (2008). Allergic Contact Dermatitis from a Henna Tattoo. New England Journal of Medicine *359*, 627-627.

Farrar, M.A., and Schreiber, R.D. (1993). The Molecular Cell Biology of Interferon-Gamma and Its Receptor. Annual review of immunology *11*, 571-611.

Fasano, M., Curry, S., Terreno, E., Galliano, M., Fanali, G., Narciso, P., Notari, S., and Ascenzi, P. (2005). The extraordinary ligand binding properties of human serum albumin. IUBMB Life *57*, 787-796.

Ferrer, M.L., Duchowicz, R., Carrasco, B., de la Torre, J.G., and Acuna, A.U. (2001). The conformation of serum albumin in solution: a combined phosphorescence depolarization-hydrodynamic modeling study. Biophysical journal *80*, 2422-2430.

Fleischmajer, R., Schechter, A., Bruns, M., Perlish, J.S., Macdonald, E.D., Pan, T.C., Timpl, R., and Chu, M.L. (1995). Skin fibroblasts are the only source of nidogen during early basal lamina formation in vitro. The Journal of investigative dermatology *105*, 597-601.

Flora, K., Brennan, J.D., Baker, G.A., Doody, M.A., and Bright, F.V. (1998). Unfolding of acrylodan-labeled human serum albumin probed by steady-state and time-resolved fluorescence methods. Biophysical journal *75*, 1084-1096.

Fontana, L., Pelosi, E., Greco, P., Racanicchi, S., Testa, U., Liuzzi, F., Croce, C.M., Brunetti, E., Grignani, F., and Peschle, C. (2007). MicroRNAs 17-5p-20a-106a control monocytopoiesis through AML1 targeting and M-CSF receptor upregulation. Nat Cell Biol *9*, 775-787.

Freudenberg, M.A., Esser, P.R., Jakob, T., Galanos, C., and Martin, S.F. (2009). Innate and adaptive immune responses in contact dermatitis: analogy with infections. Giornale italiano di dermatologia e venereologia : organo ufficiale, Societa italiana di dermatologia e sifilografia *144*, 173-185.

Frew, A., Chang, J.H., Chan, H., Quirce, S., Noertjojo, K., Keown, P., and Chan-Yeung, M. (1998). T-lymphocyte responses to plicatic acid–human serum albumin conjugate in occupational asthma caused by western red cedar. J Allergy Clin Immun *101*, 841-847.

Friedmann, P.S. (1990). The immunology of allergic contact dermatitis: the DNCB story. Advances in dermatology *5*, 175-196.

Friedmann, P.S. (2006). Contact sensitisation and allergic contact dermatitis: Immunobiological mechanisms. Toxicol Lett *162*, 49-54.

Friedmann, P.S., and Gilchrest, B.A. (1987). Ultraviolet radiation directly induces pigment production by cultured human melanocytes. J Cell Physiol *133*, 88-94.

Fuchs, E. (1995). Keratins and the skin. Annu Rev Cell Dev Bi *11*, 123-153.

Fuchs, E. (2008). Skin stem cells: rising to the surface. The Journal of Cell Biology *180*, 273-284.

Fukunaga, A., Khaskhely, N.M., Sreevidya, C.S., Byrne, S.N., and Ullrich, S.E. (2008). Dermal dendritic cells, and not Langerhans cells, play an essential role in inducing an immune response. J Immunol *180*, 3057-3064.

Gallucci, S., and Matzinger, P. (2001). Danger signals: SOS to the immune system. Curr Opin Immunol *13*, 114-119.

Gerberick, F., Aleksic, M., Basketter, D., Casati, S., Karlberg, A.T., Kern, P., Kimber, I., Lepoittevin, J.P., Natsch, A., Ovigne, J.M*., et al.* (2008). Chemical reactivity measurement and the predicitve identification of skin sensitisers. The report and recommendations of ECVAM Workshop 64. Alternatives to laboratory animals : ATLA *36*, 215-242.

Gerberick, G.F., Vassallo, J.D., Bailey, R.E., Chaney, J.G., Morrall, S.W., and Lepoittevin, J.-P. (2004a). Development of a Peptide Reactivity Assay for Screening Contact Allergens. Toxicological Sciences *81*, 332-343.

Gerberick, G.F., Vassallo, J.D., Bailey, R.E., Chaney, J.G., Morrall, S.W., and Lepoittevin, J.P. (2004b). Development of a peptide reactivity assay for screening contact allergens. Toxicological sciences : an official journal of the Society of Toxicology *81*, 332-343.

Gonwa, T.A., Picker, L.J., Raff, H.V., Goyert, S.M., Silver, J., and Stobo, J.D. (1983). Antigen-presenting capabilities of human monocytes correlates with their expression

of HLA-DS, an Ia determinant distinct from HLA-DR. The Journal of Immunology *130*, 706-711.

Gonzaleznoriega, A., Grubb, J.H., Talkad, V., and Sly, W.S. (1980). Chloroquine Inhibits Lysosomal-Enzyme Pinocytosis and Enhances Lysosomal Enzyme-Secretion by Impairing Receptor Recycling. J Cell Biol *85*, 839-852.

Grakoui, A., Bromley, S.K., Sumen, C., Davis, M.M., Shaw, A.S., Allen, P.M., and Dustin, M.L. (1999). The Immunological Synapse: A Molecular Machine Controlling T Cell Activation. Science *285*, 221-227.

Gras, R., Müller, M., Gasteiger, E., Gay, S., Binz, P.-A., Bienvenut, W., Hoogland, C., Sanchez, J.-C., Bairoch, A., Hochstrasser, D.F.*, et al.* (1999). Improving protein identification from peptide mass fingerprinting through a parameterized multi-level scoring algorithm and an optimized peak detection. Electrophoresis *20*, 3535-3550.

Hagvall, L., Bäcktorp, C., Norrby, P.-O., Karlberg, A.-T., and Börje, A. (2011). Experimental and Theoretical Investigations of the Autoxidation of Geranial: A Dioxolane Hydroperoxide Identified as a Skin Sensitizer. Chemical Research in Toxicology *24*, 1507-1515.

Hanash, S.M. (2000). Biomedical applications of two-dimensional electrophoresis using immobilized pH gradients: Current status. Electrophoresis *21*, 1202-1209.

Harding, C.R. (2004). The stratum corneum: structure and function in health and disease. Dermatologic therapy *17 Suppl 1*, 6-15.

Hastings, K.T., and Cresswell, P. (2011). Disulfide reduction in the endocytic pathway: immunological functions of gamma-interferon-inducible lysosomal thiol reductase. Antioxid Redox Signal *15*, 657-668.

Hastings, K.T., Lackman, R.L., and Cresswell, P. (2006). Functional requirements for the lysosomal thiol reductase GILT in MHC class II-restricted antigen processing. J Immunol *177*, 8569-8577.

He, X.M., and Carter, D.C. (1992). Atomic-Structure and Chemistry of Human Serum-Albumin. Nature *358*, 209-215.

Heylings, J.R., Clowes, H.M., Cumberbatch, M., Dearman, R.J., Fielding, I., Hilton, J., and Kimber, I. (1996). Sensitization to 2,4-dinitrochlorobenzene: influence of vehicle on absorption and lymph node activation. Toxicology *109*, 57-65.

Hirai, A., Minamiyama, Y., Hamada, T., Ishii, M., and Inoue, M. (1997). Glutathione Metabolism in Mice Is Enhanced More With Hapten-Induced Allergic Contact Dermatitis Than With Irritant Contact Dermatitis. J Investig Dermatol *109*, 314-318.

Hirota, M., Suzuki, M., Hagino, S., Kagatani, S., Sasaki, Y., Aiba, S., and Itagaki, H. (2009). Modification of cell-surface thiols elicits activation of human monocytic cell line THP-1: Possible involvement in effect of haptens 2,4-dinitrochlorobenzene and nickel sulfate. The Journal of Toxicological Sciences *34*, 139-150.

Hoerth, P., Miller, C.A., Preckel, T., and Wenz, C. (2006). Efficient fractionation and improved protein identification by peptide OFFGEL electrophoresis. Molecular & Cellular Proteomics *5*, 1968-1974.

Hubner, N.C., Ren, S., and Mann, M. (2008). Peptide separation with immobilized pI strips is an attractive alternative to in-gel protein digestion for proteome analysis. Proteomics *8*, 4862-4872.

Ishikawa, T. (1992). The ATP-dependent glutathione S-conjugate export pump. Trends in Biochemical Sciences *17*, 463-468.

Jacob, S.E., and Steele, T. (2006). Contact Dermatitis and Workforce Economics. Seminars in Cutaneous Medicine and Surgery *25*, 105-109.

Jacobsen, C. (1972). Chemical modification of the high-affinity bilirubin-binding site of human-serum albumin. Eur J Biochem *27*, 513-519.

Jenkins, R.E., Yaseen, F.S., Monshi, M.M., Whitaker, P., Meng, X., Farrell, J., Hamlett, J., Sanderson, J.P., El-Ghaiesh, S., Peckham, D*., et al.* (2013). β-Lactam Antibiotics Form Distinct Haptenic Structures on Albumin and Activate Drug-Specific T-Lymphocyte Responses in Multiallergic Patients with Cystic Fibrosis. Chemical Research in Toxicology *26*, 963-975.

Jenkinson, C., Jenkins, R.E., Aleksic, M., Pirmohamed, M., Naisbitt, D.J., and Park, B.K. (2010). Characterization of p-phenylenediamine-albumin binding sites and T-cell responses to hapten-modified protein. The Journal of investigative dermatology *130*, 732-742.

Jewell, C., Heylings, J., Clowes, H.M., and Williams, F.M. (2000). Percutaneous absorption and metabolism of dinitrochlorobenzene in vitro. Arch Toxicol *74*, 356-365.

Johansson, H., Albrekt, A.S., Borrebaeck, C.A., and Lindstedt, M. (2013). The GARD assay for assessment of chemical skin sensitizers. Toxicology in vitro : an international journal published in association with BIBRA *27*, 1163-1169.

Kalinin, A.E., Kajava, A.V., and Steinert, P.M. (2002). Epithelial barrier function: assembly and structural features of the cornified cell envelope. BioEssays : news and reviews in molecular, cellular and developmental biology *24*, 789-800.

Kanitakis, J. (2002). Anatomy, histology and immunohistochemistry of normal human skin. European Journal of Dermatology *12*, 390-400.

Kaplan, D.H., Igyarto, B.Z., and Gaspari, A.A. (2012). Early immune events in the induction of allergic contact dermatitis. Nature reviews Immunology *12*, 114-124.

Kaplan, D.H., Jenison, M.C., Saeland, S., Shlomchik, W.D., and Shlomchik, M.J. (2006). Epidermal Langerhans cell deficient mice develop enhanced contact hypersensitivity. Journal of Investigative Dermatology *126*, 112-112.

Kehe, K., Abend, M., Kehe, K., Ridi, R., Peter, R.U., and van Beuningen, D. (1999). Tissue engineering with HaCaT cells and a fibroblast cell line. Archives of dermatological research *291*, 600-605.

Kidd, P. (2003). Th1/Th2 balance: the hypothesis, its limitations, and implications for health and disease. Alternative medicine review : a journal of clinical therapeutic *8*, 223-246.

Kimber, I., Basketter, D.A., Gerberick, G.F., and Dearman, R.J. (2002). Allergic contact dermatitis. International immunopharmacology *2*, 201-211.

Kimber, I., Quirke, S., and Beck, M.H. (1990). Attempts to identify the causative allergen in cases of allergic contact dermatitis using an in vitro lymphocyte transformation test. Toxicology in vitro : an international journal published in association with BIBRA *4*, 302-306.

Kimber, I., and Weisenberger, C. (1989). A Murine Local Lymph-Node Assay for the Identification of Contact Allergens - Assay Development and Results of an Initial Validation-Study. Arch Toxicol *63*, 274-282.

Kragh-Hansen, U., Chuang, V.T., and Otagiri, M. (2002). Practical aspects of the ligand-binding and enzymatic properties of human serum albumin. Biological & pharmaceutical bulletin *25*, 695-704.

Krishna, D.R., and Klotz, U. (1994). Extrahepatic metabolism of drugs in humans. Clinical pharmacokinetics *26*, 144-160.

Kupper, T.S., and Fuhlbrigge, R.C. (2004). Immune surveillance in the skin: mechanisms and clinical consequences. Nature reviews Immunology *4*, 211-222.

Lampe, M.A., Burlingame, A.L., Whitney, J., Williams, M.L., Brown, B.E., Roitman, E., and Elias, P.M. (1983). Human stratum corneum lipids: characterization and regional variations. Journal of Lipid Research *24*, 120-130.

Landsteiner, K., and Chase, M.W. (1937). Studies on the Sensitization of Animals with Simple Chemical Compounds : Iv. Anaphylaxis Induced by Picryl Chloride and 2:4 Dinitrochlorobenzene. J Exp Med *66*, 337-351.

Leavell, M.D., Novak, P., Behrens, C.R., Schoeniger, J.S., and Kruppa, G.H. (2004). Strategy for selective chemical cross-linking of tyrosine and lysine residues. J Am Soc Mass Spectr *15*, 1604-1611.

Leccia, M.T., Richard, M.J., Joanny-Crisci, F., and Beani, J.C. (1998). UV-A1 cytotoxicity and antioxidant defence in keratinocytes and fibroblasts. Eur J Dermatol *8*, 478-482.

Lee, H.Y., Cha, M.K., and Kim, I.H. (2000). Activation of thiol-dependent antioxidant activity of human serum albumin by alkaline pH is due to the B-like conformational change. Arch Biochem Biophys *380*, 309-318.

Lehmann, B. (1997). HaCaT cell line as a model system for vitamin D3 metabolism in human skin. The Journal of investigative dermatology *108*, 78-82.

Lemaître, G., Lamartine, J., Pitaval, A., Vaigot, P., Garin, J., Bouet, S., Petat, C., Soularue, P., Gidrol, X., Martin, M.T*., et al.* (2004). Expression profiling of genes and proteins in HaCaT keratinocytes: Proliferating versus differentiated state. J Cell Biochem *93*, 1048-1062.

Lepoittevin, J.P., and Leblond, I. (1997). Hapten-peptide-T cell receptor interactions: Molecular basis for the recognition of haptens by T lymphocytes. European Journal of Dermatology *7*, 151-154.

Liu, P.T., Stenger, S., Tang, D.H., and Modlin, R.L. (2007). Cutting edge: vitamin D-mediated human antimicrobial activity against Mycobacterium tuberculosis is dependent on the induction of cathelicidin. J Immunol *179*, 2060-2063.

Lu, J., Stewart, A.J., Sadler, P.J., Pinheiro, T.J.T., and Blindauer, C.A. (2008). Albumin as a zinc carrier: properties of its high-affinity zinc-binding site. Biochem Soc T *36*, 1317-1321.

Madison, K.C. (2003). Barrier function of the skin: "la raison d'etre" of the epidermis. The Journal of investigative dermatology *121*, 231-241.

Makarov, A. (2000). Electrostatic Axially Harmonic Orbital Trapping: A High-Performance Technique of Mass Analysis. Analytical chemistry *72*, 1156-1162.

Malten, K.E. (1981). Thoughts on irritant contact dermatitis. Contact Dermatitis *7*, 238-247.

Mansoor, M.A., Svardal, A.M., and Ueland, P.M. (1992). Determination of the in vivo redox status of cysteine, cysteinylglycine, homocysteine, and glutathione in human plasma. Analytical Biochemistry *200*, 218-229.

Maric, M., Arunachalam, B., Phan, U.T., Dong, C., Garrett, W.S., Cannon, K.S., Alfonso, C., Karlsson, L., Flavell, R.A., and Cresswell, P. (2001). Defective antigen processing in GILT-free mice. Science *294*, 1361-1365.

Martin, S., Ortmann, B., Pflugfelder, U., Birsner, U., and Weltzien, H.U. (1992). Role of Hapten-Anchoring Peptides in Defining Hapten-Epitopes for Mhc-Restricted Cytotoxic

T-Cells - Cross-Reactive Tnp-Determinants on Different Peptides. Journal of Immunology *149*, 2569-2575.

Martin, S., von Bonin, A., Fessler, C., Pflugfelder, U., and Weltzien, H.U. (1993). Structural complexity of antigenic determinants for class I MHC-restricted, hapten-specific T cells. Two qualitatively differing types of H-2Kb-restricted TNP epitopes. J Immunol *151*, 678-687.

Martin, S., and Weltzien, H.U. (1994). T-Cell Recognition of Haptens, a Molecular View. International Archives of Allergy and Immunology *104*, 10-16.

Martin, S.F. (2004). T Lymphocyte-Mediated Immune Responses to Chemical Haptens and Metal Ions: Implications for Allergic and Autoimmune Disease. International Archives of Allergy and Immunology *134*, 186-198.

Martin, S.F., Merfort, I., and Thierse, H.-J. (2006). Interactions of Chemicals and Metal Ions with Proteins and Role for Immune Responses. Mini Reviews in Medicinal Chemistry *6*, 247-255.

Mauri-Hellweg, D., Bettens, F., Mauri, D., Brander, C., Hunziker, T., and Pichler, W.J. (1995). Activation of drug-specific CD4+ and CD8+ T cells in individuals allergic to sulfonamides, phenytoin, and carbamazepine. The Journal of Immunology *155*, 462-472.

Megherbi, R., Kiorpelidou, E., Foster, B., Rowe, C., Naisbitt, D.J., Goldring, C.E., and Park, B.K. (2009). Role of protein haptenation in triggering maturation events in the dendritic cell surrogate cell line THP-1. Toxicology and Applied Pharmacology *238*, 120-132.

Meschkat, E., Barratt, M.D., and Lepoittevin, J.-P. (2000). Studies of the Chemical Selectivity of Hapten, Reactivity, and Skin Sensitization Potency. 2. NMR Studies of the Covalent Binding of the 13C-Labeled Skin Sensitizers 2-[13C]- and 3-[13C]Hex-1-ene-

and 3-[13C]Hexane-1,3-sultones to Human Serum Albumin. Chemical Research in Toxicology *14*, 118-126.

Morar, N., Willis-Owen, S.A.G., Moffatt, M.F., and Cookson, W.O.C.M. (2006). The genetics of atopic dermatitis. J Allergy Clin Immun *118*, 24-34.

Muszbek, L., Adany, R., and Mikkola, H. (1996). Novel Aspects of Blood Coagulation Factor XIII. I. Structure, Distribution, Activation, and Function. Critical Reviews in Clinical Laboratory Sciences *33*, 357-421.

Naik, S., Bouladoux, N., Wilhelm, C., Molloy, M.J., Salcedo, R., Kastenmuller, W., Deming, C., Quinones, M., Koo, L., Conlan, S.*, et al.* (2012). Compartmentalized control of skin immunity by resident commensals. Science *337*, 1115-1119.

Narazaki, R., Maruyama, T., and Otagiri, M. (1997). Probing the cysteine 34 residue in human serum albumin using fluorescence techniques. Biochimica et Biophysica Acta (BBA) - Protein Structure and Molecular Enzymology *1338*, 275-281.

Natsch, A., and Emter, R. (2008). Skin sensitizers induce antioxidant response element dependent genes: application to the in vitro testing of the sensitization potential of chemicals. Toxicological sciences : an official journal of the Society of Toxicology *102*, 110-119.

Natsch, A., Gfeller, H., Kuhn, F., Granier, T., and Roberts, D.W. (2010). Chemical Basis for the Extreme Skin Sensitization Potency of (E)-4-(Ethoxymethylene)-2-phenyloxazol-5(4H)-one. Chemical Research in Toxicology *23*, 1913-1920.

Natsch, A., Haupt, T., and Laue, H. (2011a). Relating Skin Sensitizing Potency to Chemical Reactivity: Reactive Michael Acceptors Inhibit NF-kappa B Signaling and Are Less Sensitizing than SNAr- and S(N)2-Reactive Chemicals. Chemical Research in Toxicology *24*, 2018-2027.

Natsch, A., Haupt, T., and Laue, H. (2011b). Relating skin sensitizing potency to chemical reactivity: reactive Michael acceptors inhibit NF-kappaB signaling and are less sensitizing than S(N)Ar- and S(N)2- reactive chemicals. Chem Res Toxicol *24*, 2018-2027.

Neefjes, J., Jongsma, M.L.M., Paul, P., and Bakke, O. (2011). Towards a systems understanding of MHC class I and MHC class II antigen presentation. Nat Rev Immunol *11*, 823-836.

Nicholas, B., Skipp, P., Mould, R., Rennard, S., Davies, D.E., O'Connor, D., and Djukanovic, R. (2006). Shotgun proteomic analysis of human induced sputum. Thorax *61*, Ii124-Ii124.

Niklasson, I.B., Ponting, D.J., Luthman, K., and Karlberg, A.T. (2014). Bioactivation of Cinnamic Alcohol Forms Several Strong Skin Sensitizers. Chemical Research in Toxicology *27*, 568-575.

Norlen, L., Nicander, I., Rozell, B.L., Ollmar, S., and Forslind, B. (1999). Inter- and intra-individual differences in human stratum corneum lipid content related to physical parameters of skin barrier function in vivo. Journal of Investigative Dermatology *112*, 72-77.

Nukada, Y., Ashikaga, T., Miyazawa, M., Hirota, M., Sakaguchi, H., Sasa, H., and Nishiyama, N. (2012). Prediction of skin sensitization potency of chemicals by human Cell Line Activation Test (h-CLAT) and an attempt at classifying skin sensitization potency. Toxicology in Vitro *26*, 1150-1160.

O'Farrell, P.H. (1975). High resolution two-dimensional electrophoresis of proteins. The Journal of biological chemistry *250*, 4007-4021.

Ohman, H., and Vahlquist, A. (1994). In vivo studies concerning a pH gradient in human stratum corneum and upper epidermis. Acta dermato-venereologica *74*, 375-379.

Olsen, J.V., Macek, B., Lange, O., Makarov, A., Horning, S., and Mann, M. (2007). Higher-energy C-trap dissociation for peptide modification analysis. Nat Meth *4*, 709-712.

Ortmann, B., Martin, S., von Bonin, A., Schiltz, E., Hoschutzky, H., and Weltzien, H.U. (1992). Synthetic peptides anchor T cell-specific TNP epitopes to MHC antigens. J Immunol *148*, 1445-1450.

Ouwehand, K., Scheper, R.J., de Gruijl, T.D., and Gibbs, S. (2010a). Epidermis-to-dermis migration of immature Langerhans cells upon topical irritant exposure is dependent on CCL2 and CCL5. European journal of immunology *40*, 2026-2034.

Ouwehand, K., Spiekstra, S.W., Reinders, J., Scheper, R.J., de Gruijl, T.D., and Gibbs, S. (2010b). Comparison of a novel CXCL12/CCL5 dependent migration assay with CXCL8 secretion and CD86 expression for distinguishing sensitizers from non-sensitizers using MUTZ-3 Langerhans cells. Toxicology in Vitro *24*, 578-585.

Padovan, E., Bauer, T., Tongio, M.M., Kalbacher, H., and Weltzien, H.U. (1997). Penicilloyl peptides are recognized as T cell antigenic determinants in penicillin allergy. Eur J Immunol *27*, 1303-1307.

Padovan, E., Mauri-Hellweg, D., Pichler, W.J., and Weltzien, H.U. (1996). T cell recognition of penicillin G: structural features determining antigenic specificity. Eur J Immunol *26*, 42-48.

Pedersen, A.O., and Jacobsen, J. (1980). Reactivity of the Thiol Group in Human and Bovine Albumin at pH 3–9, as Measured by Exchange with 2,2′ -Dithiodipyridine. Eur J Biochem *106*, 291-295.

Peiser, M., Tralau, T., Heidler, J., Api, A., Arts, J., Basketter, D., English, J., Diepgen, T., Fuhlbrigge, R., Gaspari, A*., et al.* (2012). Allergic contact dermatitis: epidemiology,

molecular mechanisms, in vitro methods and regulatory aspects. Cellular and Molecular Life Sciences *69*, 763-781.

Peng, L., Dasari, S., Tabb, D.L., and Turesky, R.J. (2012). Mapping Serum Albumin Adducts of the Food-Borne Carcinogen 2-Amino-1-methyl-6-phenylimidazo[4,5-b]pyridine by Data-Dependent Tandem Mass Spectrometry. Chemical Research in Toxicology *25*, 2179-2193.

Perkins, D.N., Pappin, D.J.C., Creasy, D.M., and Cottrell, J.S. (1999). Probability-based protein identification by searching sequence databases using mass spectrometry data. Electrophoresis *20*, 3551-3567.

Phan, U.T., Arunachalam, B., and Cresswell, P. (2000). Gamma-interferon-inducible lysosomal thiol reductase (GILT). Maturation, activity, and mechanism of action. The Journal of biological chemistry *275*, 25907-25914.

Pichler, W.J., and Tilch, J. (2004). The lymphocyte transformation test in the diagnosis of drug hypersensitivity. Allergy *59*, 809-820.

Pickard, C., Louafi, F., McGuire, C., Lowings, K., Kumar, P., Cooper, H., Dearman, R.J., Cumberbatch, M., Kimber, I., Healy, E.*, et al.* (2009). The cutaneous biochemical redox barrier: a component of the innate immune defenses against sensitization by highly reactive environmental xenobiotics. J Immunol *183*, 7576-7584.

Pickard, C., Smith, A.M., Cooper, H., Strickland, I., Jackson, J., Healy, E., and Friedmann, P.S. (2007). Investigation of mechanisms underlying the T-cell response to the hapten 2,4-dinitrochlorobenzene. The Journal of investigative dermatology *127*, 630-637.

Proksch, E., Brandner, J.M., and Jensen, J.-M. (2008). The skin: an indispensable barrier. Experimental dermatology *17*, 1063-1072.

Rabilloud, T., Chevallet, M., Luche, S., and Lelong, C. (2010). Two-dimensional gel electrophoresis in proteomics: Past, present and future. J Proteomics *73*, 2064-2077.

Rammensee, H.G., Bachmann, J., Emmerich, N.P.N., Bachor, O.A., and Stevanovic, S. (1999). SYFPEITHI: database for MHC ligands and peptide motifs. Immunogenetics *50*, 213-219.

Rees, J.L., Friedmann, P.S., and Matthews, J.N.S. (1990). The influence of area of application on sensitization by dinitrochlorobenzene. Brit J Dermatol *122*, 29-31.

Ritter, U., Meissner, A., Scheidig, C., and Korner, H. (2004). CD8 alpha- and Langerin-negative dendritic cells, but not Langerhans cells, act as principal antigen-presenting cells in leishmaniasis. European journal of immunology *34*, 1542-1550.

Saint-Mezard, P., Berard, F., Dubois, B., Kaiserlian, D., and Nicolas, J.F. (2004). The role of CD4+ and CD8+ T cells in contact hypersensitivity and allergic contact dermatitis. European journal of dermatology : EJD *14*, 131-138.

Saint-Mezard, P., Krasteva, M., Chavagnac, C., Bosset, S., Akiba, H., Kehren, J., Kanitakis, J., Kaiserlian, D., Nicolas, J.F., and Berard, F. (2003). Afferent and efferent phases of allergic contact dermatitis (ACD) can be induced after a single skin contact with haptens: evidence using a mouse model of primary ACD. The Journal of investigative dermatology *120*, 641-647.

Samuelsson, K., Bergstrom, M.A., Jonsson, C.A., Westman, G., and Karlberg, A.T. (2011). Diphenylthiourea, a Common Rubber Chemical, Is Bioactivated to Potent Skin Sensitizers. Chemical Research in Toxicology *24*, 35-44.

Sarin, A., Adams, D.H., and Henkart, P.A. (1993). Protease inhibitors selectively block T cell receptor-triggered programmed cell death in a murine T cell hybridoma and activated peripheral T cells. The Journal of Experimental Medicine *178*, 1693-1700.

Schmidt, M., Raghavan, B., Muller, V., Vogl, T., Fejer, G., Tchaptchet, S., Keck, S., Kalis, C., Nielsen, P.J., Galanos, C.*, et al.* (2010). Crucial role for human Toll-like receptor 4 in the development of contact allergy to nickel. Nature immunology *11*, 814-819.

Schmidt, R.J., and Chung, L.Y. (1992). Biochemical responses of skin to allergenic and non-allergenic nitrohalobenzenes. Archives of Dermatological Research *284*, 400-408.

Schmidt, R.J., and Chung, L.Y. (1993). Perturbation of glutathione status and generation of oxidative stress in mouse skin following application of contact allergenic sesquiterpene lactones and isothiocyanates. Xenobiotica *23*, 889-897.

Schnyder, B., Burkhart, C., Schnyder-Frutig, K., von Greyerz, S., Naisbitt, D.J., Pirmohamed, M., Park, B.K., and Pichler, W.J. (2000). Recognition of Sulfamethoxazole and Its Reactive Metabolites by Drug-Specific CD4+ T Cells from Allergic Individuals. The Journal of Immunology *164*, 6647-6654.

Schoop, V.M., Mirancea, N., and Fusenig, N.E. (1999). Epidermal Organization and Differentiation of HaCaT Keratinocytes in Organotypic Coculture with Human Dermal Fibroblasts. *112*, 343-353.

Schuler, M., Nastke, M.-D., and Stevanović, S. (2007). SYFPEITHI. In Immunoinformatics, D. Flower, ed. (Humana Press), pp. 75-93.

Seglen, P.O., Grinde, B., and Solheim, A.E. (1979). Inhibition of the Lysosomal Pathway of Protein Degradation in Isolated Rat Hepatocytes by Ammonia, Methylamine, Chloroquine and Leupeptin. European Journal of Biochemistry *95*, 215-225.

Sette, A., Fleri, W., Peters, B., Sathiamurthy, M., Bui, H.-H., and Wilson, S. (2005). A Roadmap for the Immunomics of Category A–C Pathogens. Immunity *22*, 155-161.

Shaltiel, S. (1967). Thiolysis of some dinitrophenyl derivatives of amino acids. Biochemical and biophysical research communications *29*, 178-183.

Sieling, P.A., Chatterjee, D., Porcelli, S.A., Prigozy, T.I., Mazzaccaro, R.J., Soriano, T., Bloom, B.R., Brenner, M.B., Kronenberg, M., Brennan, P.J.*, et al.* (1995). CD1-restricted T cell recognition of microbial lipoglycan antigens. Science *269*, 227-230.

Silva, J.C., Denny, R., Dorschel, C.A., Gorenstein, M., Kass, I.J., Li, G.-Z., McKenna, T., Nold, M.J., Richardson, K., Young, P.*, et al.* (2005). Quantitative Proteomic Analysis by Accurate Mass Retention Time Pairs. Analytical chemistry *77*, 2187-2200.

Simonsson, C., Andersson, S.I., Stenfeldt, A.L., Bergstrom, J., Bauer, B., Jonsson, C.A., Ericson, M.B., and Broo, K.S. (2011). Caged Fluorescent Haptens Reveal the Generation of Cryptic Epitopes in Allergic Contact Dermatitis. Journal of Investigative Dermatology *131*, 1486-1493.

Sirisattha, S., Momose, Y., Kitagawa, E., and Iwahashi, H. (2004). Toxicity of anionic detergents determined by Saccharomyces cerevisiae microarray analysis. Water Research *38*, 61-70.

Skoet, R., Zachariae, R., and Agner, T. (2003). Contact dermatitis and quality of life: a structured review of the literature. Brit J Dermatol *149*, 452-456.

Skold, M., Borje, A., Matura, M., and Karlberg, A.T. (2002). Studies on the autoxidation and sensitizing capacity of the fragrance chemical linalool, identifying a linalool hydroperoxide. Contact Dermatitis *46*, 267-272.

Smith, C.K., Moore, C.A., Elahi, E.N., Smart, A.T., and Hotchkiss, S.A. (2000). Human skin absorption and metabolism of the contact allergens, cinnamic aldehyde, and cinnamic alcohol. Toxicol Appl Pharmacol *168*, 189-199.

Smith Pease, C.K., White, I.R., and Basketter, D.A. (2002). Skin as a route of exposure to protein allergens. Clin Exp Dermatol *27*, 296-300.

Stamler, J.S., Jaraki, O., Osborne, J., Simon, D.I., Keaney, J., Vita, J., Singel, D., Valeri, C.R., and Loscalzo, J. (1992). Nitric oxide circulates in mammalian plasma primarily as an S-nitroso adduct of serum albumin. Proceedings of the National Academy of Sciences *89*, 7674-7677.

Steinman, L. (2007). A brief history of TH17, the first major revision in the TH1/TH2 hypothesis of T cell-mediated tissue damage. Nat Med *13*, 139-145.

SUDLOW, G., BIRKETT, D.J., and WADE, D.N. (1975). The Characterization of Two Specific Drug Binding Sites on Human Serum Albumin. Molecular Pharmacology *11*, 824-832.

Sugio, S., Kashima, A., Mochizuki, S., Noda, M., and Kobayashi, K. (1999). Crystal structure of human serum albumin at 2.5 A resolution. Protein engineering *12*, 439-446.

Swartz, M.E. (2005). UPLC™: An Introduction and Review. Journal of Liquid Chromatography & Related Technologies *28*, 1253-1263.

Theodore Peters, J. (1995). All about Albumin – Biochemistry Genetics and Medical Applications (San Diego: Academic Press).

Thyssen, J.P., Linneberg, A., Menné, T., and Johansen, J.D. (2007). The epidemiology of contact allergy in the general population – prevalence and main findings. Contact Dermatitis *57*, 287-299.

Toebak, M.J., Pohlmann, P.R., Sampat-Sardjoepersad, S.C., von Blomberg, B.M.E., Bruynzeel, D.P., Scheper, R.J., Rustemeyer, T., and Gibbs, S. (2006). CXCL8 secretion by dendritic cells predicts contact allergens from irritants. Toxicology in Vitro *20*, 117-124.

Trombetta, E.S., and Mellman, I. (2005). Cell biology of antigen processing in vitro and in vivo. Annual review of immunology *23*, 975-1028.

Valladeau, J., Ravel, O., Dezutter-Dambuyant, C., Moore, K., Kleijmeer, M., Liu, Y., Duvert-Frances, V., Vincent, C., Schmitt, D., Davoust, J*., et al.* (2000). Langerin, a novel C-type lectin specific to Langerhans cells, is an endocytic receptor that induces the formation of Birbeck granules. Immunity *12*, 71-81.

van der Veen, J.W., Pronk, T.E., van Loveren, H., and Ezendam, J. (2013). Applicability of a keratinocyte gene signature to predict skin sensitizing potential. Toxicology in Vitro *27*, 314-322.

Vocanson, M., Hennino, A., Rozières, A., Poyet, G., and Nicolas, J.F. (2009). Effector and regulatory mechanisms in allergic contact dermatitis. Allergy *64*, 1699-1714.

Vocanson, M., Nicolas, J.-F., and Basketter, D. (2013). In vitro approaches to the identification and characterization of skin sensitizers. Expert Review of Dermatology *8*, 395-405.

von Andrian, U.H., and Mackay, C.R. (2000). T-Cell Function and Migration — Two Sides of the Same Coin. New England Journal of Medicine *343*, 1020-1034.

Vyas, J.M., Van der Veen, A.G., and Ploegh, H.L. (2008). The known unknowns of antigen processing and presentation. Nat Rev Immunol *8*, 607-618.

Wang, H., Chang-Wong, T., Tang, H.-Y., and Speicher, D.W. (2009). Comparison of Extensive Protein Fractionation and Repetitive LC-MS/MS Analyses on Depth of Analysis for Complex Proteomes. Journal of proteome research *9*, 1032-1040.

Wardell, M., Wang, Z., Ho, J.X., Robert, J., Ruker, F., Ruble, J., and Carter, D.C. (2002). The Atomic Structure of Human Methemalbumin at 1.9 Å. Biochemical and biophysical research communications *291*, 813-819.

Watt, F.M., and Fujiwara, H. (2011). Cell-extracellular matrix interactions in normal and diseased skin. Cold Spring Harbor perspectives in biology *3*.

Watts, C. (1997). Capture and processing of exogenous antigens for presentation on MHC molecules. Annual review of immunology *15*, 821-850.

Weber, L.W., Zesch, A., and Rozman, K. (1991). Penetration, distribution and kinetics of 2,3,7,8-tetrachlorodibenzo-p-dioxin in human skin in vitro. Arch Toxicol *65*, 421-428.

Weltzien, H.U., Moulon, C., Martin, S., Padovan, E., Hartmann, U., and Kohler, J. (1996). T cell immune responses to haptens. Structural models for allergic and autoimmune reactions. Toxicology *107*, 141-151.

Wetzel, R., Becker, M., Behlke, J., Billwitz, H., BöHm, S., Ebert, B., Hamann, H., Krumbiegel, J., and Lassmann, G. (1980). Temperature Behaviour of Human Serum Albumin. Eur J Biochem *104*, 469-478.

White, S.I., Friedmann, P.S., Moss, C., and Simpson, J.M. (1986). The Effect of Altering Area of Application and Dose Per Unit Area on Sensitization by Dncb. Brit J Dermatol *115*, 663-668.

Williams, H., and Flohr, C. (2006). How epidemiology has challenged 3 prevailing concepts about atopic dermatitis. The Journal of allergy and clinical immunology *118*, 209-213.

Zhang, W., and Chait, B.T. (2000). ProFound: An Expert System for Protein Identification Using Mass Spectrometric Peptide Mapping Information. Analytical chemistry *72*, 2482-2489.

Ziegler, H.K., and Unaue, E.R. (1982). Inhibition of Antigen Presentation by Lysosomotropic Agents. Fed Proc *41*, 379-379.